



University  
of Glasgow

<https://theses.gla.ac.uk/>

Theses Digitisation:

<https://www.gla.ac.uk/myglasgow/research/enlighten/theses/digitisation/>

This is a digitised version of the original print thesis.

Copyright and moral rights for this work are retained by the author

A copy can be downloaded for personal non-commercial research or study, without prior permission or charge

This work cannot be reproduced or quoted extensively from without first obtaining permission in writing from the author

The content must not be changed in any way or sold commercially in any format or medium without the formal permission of the author

When referring to this work, full bibliographic details including the author, title, awarding institution and date of the thesis must be given

Enlighten: Theses

<https://theses.gla.ac.uk/>  
[research-enlighten@glasgow.ac.uk](mailto:research-enlighten@glasgow.ac.uk)

ELECTRON SPIN RESONANCE IN AROMATIC HYDROCARBONS

by

T.D.S. Hamilton, M.Sc.

Thesis presented for the Degree of

Doctor of Philosophy

at

The University of Glasgow.

December 1962

ProQuest Number: 10646816

All rights reserved

INFORMATION TO ALL USERS

The quality of this reproduction is dependent upon the quality of the copy submitted.

In the unlikely event that the author did not send a complete manuscript and there are missing pages, these will be noted. Also, if material had to be removed, a note will indicate the deletion.



ProQuest 10646816

Published by ProQuest LLC (2017). Copyright of the Dissertation is held by the Author.

All rights reserved.

This work is protected against unauthorized copying under Title 17, United States Code  
Microform Edition © ProQuest LLC.

ProQuest LLC.  
789 East Eisenhower Parkway  
P.O. Box 1346  
Ann Arbor, MI 48106 – 1346

TO MY WIFE



CONTENTS.

	Page
<u>PART I: Introduction.</u>	
1.1 Introduction	1
1.2 Energy Levels and Resonance Conditions for Electron Spin Resonance	2
1.3 Triplet States in Aromatic Hydrocarbons	4
1.4 Aromatic Ions	6
1.5 Hyperfine Splitting and Configuration Interaction	8
1.6 Molecular Orbital Theory	10
 <u>PART II: Electron Spin Resonance in Triplet States.</u>	
2.1 Introduction	12
2.2 Light Intensity	13
2.3 Light Source	14
2.4 Specimens and Resonance Detector	16
2.5 Operation of Equipment	17
2.6 Conclusion	18
 <u>PART III: Microwave Spectrometer.</u>	
3.1 Introduction	20
3.2 Sensitivity Considerations	21
3.3 Microwave System	23
3.4 I.F.-Lock System	25

3.5	Cavity-Lock System	25
3.6	Signal Preamplifier	26
3.7	Main Signal Amplifier and I.F. Phase Sensitive Detector	26
3.8	I.F.-Lock Amplifier and Discriminator	28
3.9	Klystron Reflector Control	28
3.10	Klystrons and Klystron Power Supply	29
3.11	Operation and Adjustment of Locking Systems	31
3.12	Spectrometer Sensitivity	32
3.13	Spectrometer Improvements	33

#### PART IV: Magnet Stabilizers.

4.1	Introduction	35
4.2	Current Stabilizer No.1	37
4.3	Magnet Impedance	39
4.4	Reference Elements	40
4.5	Magnet Stabilizer No.2	41
4.6	Magnetic Field Sweep	42
4.7	Pound Spectrometer	43
4.8	Magnetic Field and Sweep Calibration	44
4.9	Audio Phase Sensitive Detector	44

#### PART V: Aromatic Hydrocarbon Ions

5.1	Theory of Configuration Interaction	46
-----	-------------------------------------	----

5.2	Spin Density in Aromatic Ions	49
5.3	Positive Ions	52
5.4	Ions in Rigid Media	54

PART VI: Results and Discussion.

6.1	Check Results	56
6.2	Compounds Studied: Preparation of Samples	57
6.3	Results: Coronene	58
6.4	Results: 1,12 Benzperylene	60
6.5	Results: Pyrene, 1,2 Benzpyrene, 3,4 Benzpyrene	61
6.6	Non-Planar Molecules: 9,10 Diphenylanthracene	63
6.7	Rigid Glasses	73
6.8	Fluorescence of Ionized Molecules	77
6.9	Conclusion	79

<u>References.</u>	81
--------------------	----

Figures.

2a	Pulsed Light Source	15
3a	Microwave Spectrometer	21
3b	Microwave System	23
3c	Signal Preamplifier	26

3d	Signal Amplifier and R.F. Phase Detector	26
3e	I.F.-Lock Amplifier	28
3f	Klystron Reflector Control	28
3g	Klystron Power Supply: Cathode Supply	30
3h	Klystron Power Supply: Reflector Supply	30
3i	Stabilized Filament Supply	30
4a	Degenerative Current Stabilizers	36
4b	Magnet Current Stabilizer	37
4c	Amplifiers A2 and A3 of Fig.4b	37
4d	Magnet Current Stabilizer No.2	42
4e	Pound Spectrometer	43
4f	Audio Phase Sensitive Detector: Oscillator and Phase Shifters	44
4g	Phase Sensitive Detector: Audio Amplifier, Narrow Band Amplifier, and Phase Detector	44
4h	Magnetic Field Sweep Calibration	44
6a	Molecular Structures	57
6b	ESR Spectra of Perylene	57
6c	ESR Spectrum of Tetracene	57
6d	ESR Spectrum of Coronene	59
6e	ESR Spectrum of 1,12 Benzperylene	61
6f	ESR Spectrum of 1,2 Benzpyrene	62

6g	ESR Spectrum of 3,4 Benzpyrene	62
6h	Impurity Resonances	62
6i	ESR Spectrum of 9,10 Diphenylanthracene	67
6j	ESR Spectrum of 9,10 Diphenylanthracene:	
	Ends of Spectrum	67
6k	Variation of $\Delta H$ with $\theta$ for	
	9,10 Diphenylanthracene	67
6m	Calculated Spectra for 9,10 Diphenylanthracene	
	for $Q = 34.4$	69
6n	Calculated Spectra for 9,10 Diphenylanthracene	
	for $Q = 31.8$	69
6p	ESR Spectrum of Triphenylene in Boric Acid	
	Glass	75

TABLE 6.5.1:	HMO Electron Densities for	
	9,10 Diphenylanthracene	67

Preface.

The work reported in this thesis was started in 1956 under the supervision of Dr. G.A.P.Wyllie. Previous work by the author on fluorescence in organic phosphors, in particular on the lifetime of excited states, had already brought contact with the work of G.N.Lewis and others on long lived excited states of aromatic hydrocarbons. These were supposed to be triplet states, having unpaired electrons, and should therefore be paramagnetic. The static paramagnetism had been demonstrated by Lewis and Calvin (1945), but this paramagnetism should also be detectable by the techniques of electron spin resonance (ESR), which would give added information not obtainable by the static techniques and definitely establish whether the excited states were in fact triplet states.

At the time the present work was undertaken there were no published results of work on the problem of detecting this paramagnetism by ESR. As it was of considerable importance from the fluorescence point of view to establish the multiplicity of this excited state, an investigation of the possibility of detecting this paramagnetism and determining the multiplicity by means of ESR was undertaken.

The author's attempts to detect ESR in the triplet state were unsuccessful up to the time of publication by Hutchison and Mangum (1958) of the first successful attempt, using the triplet state of naphthalene. Although the immediate interest had been in the success of the ESR technique, the long term interest was in the organic phosphors themselves, so that now the application had been proved further efforts in this direction were abandoned. By this time a high sensitivity superheterodyne ESR spectrometer had been developed by the author, and following the interest in organic phosphors, my attention turned to other possibilities of applying ESR to these materials. Positive and negative ions of aromatic hydrocarbons had been shown to give electron resonance spectra (Lipkin et al 1953, Yokozawa and Miyashita, 1956), and later workers found considerable hyperfine structure in the spectra. It was shown by Weissman (1956) and McConnell (1956) that this structure could be correlated with the distribution of the unpaired electron around the molecule, and the author's work on this application forms the second part of this thesis. The results of the work on ions have been combined with luminescence measurements to provide possible explanations of a number of luminescence and chemical

phenomena.

For several reasons this work has taken rather longer than might be expected. To start work on a new line without the benefit of association with an established group means that little equipment was immediately available. As suitable commercial equipment was generally unavailable, almost all the equipment required had to be constructed. The various units have been described in sufficient detail to be of use to others as there is little published information. At the beginning of 1961 most of the ESR spectrometer was transferred to the Physics Department, Manchester University, and this necessitated the construction of a certain amount of new equipment. Apart from the few machining jobs required, almost all of the equipment has been constructed by the author. All experimental work and interpretation of results has been done without collaboration.

I should like to thank the following for their assistance, financial, technical or otherwise:

Dr. G.A.P.Wyllie, for his help and encouragement.

Mr. P.Carmichael, for my introduction to ESR spectroscopy and for information relating to his spectrometer.

Mr. E.J.G.Beeson, of the BTH Research Laboratory, Rugby,



for his assistance with the xenon light source.

Mr. A. Trotter and Miss K. Irvine, for their technical assistance.

Mr. J.L. Williams of the Scientific Apparatus Department, AEI Ltd., Manchester, for arranging the loan of a magnet.

Professor B.H..Flowers and Dr. J.B. Birks, of the Physics Department, Manchester University, for facilities to complete this work and encouragement to do so.

The Shell Petroleum Co. and Rhodes University, for scholarships during the first part of this work, and the University of Glasgow for a research studentship during part of this work, and for facilitating the transfer of the ESR spectrometer to Manchester.

Unless otherwise stated the work described in this thesis is claimed to be original.

December, 1962.

## PART I.

### 1.1 Introduction.

Since the postulation of spin and magnetic moment for nuclei by Pauli (1924) and for electrons by Uhlenbeck and Goudsmit (1925), efforts have been made to detect and measure these properties by methods more direct than the effects observed in atomic spectra i.e. hyperfine structure. Direct detection of atomic magnetism was first observed in the classic experiments of Stern and Gerlach (Stern 1921) who demonstrated the space quantization of an atomic magnetic moment in a magnetic field and later measured the magnetic moment of the proton. Gorter (1936), through an unfortunate choice of materials, was unable to demonstrate experimentally the absorption of radio frequency radiation by nuclei in a suitable magnetic field. Lasherew and Schubnikow (1937) measured the magnetic moment of the proton by measurement of the static paramagnetism of solid hydrogen. The molecular beam technique was improved by Rabi et al (1939) by the introduction of a resonance method. Transitions of the atom in the magnetic field were produced by an applied radio frequency field at the Larmor frequency. This technique resulted in a considerable increase in the precision of measurement of magnetic moments.

The first nuclear resonance experiments on matter in bulk were performed by Bloch, Hansen and Packard (1946) and by Purcell, Torrey and Pound (1946), using protons in water or in solid paraffin respectively. The first electron resonance experiments were carried out by Zavoisky (1945) and Cummerow and Halliday (1946). Both nuclear magnetic resonance (NMR) and electron spin resonance (ESR) were rapidly developed and are now standard analytical tools available commercially, although at considerable expense. The development of NMR and ESR has produced a wealth of new information and has resulted in many techniques and experiments of great elegance.

Since the primary interest in this work is in ESR rather than NMR, attention will be confined to this, although there is much in common between this and NMR.

## 1.2 Energy Levels and Resonance Conditions for ESR.

Paramagnetism, excluding that due to nuclei, is produced by unpaired electrons. As a consequence of the exclusion principle, the electrons of any system are as far as possible paired, i.e. the spins of each pair are always in opposite directions, and whatever is done to one, the other does the opposite to maintain the pairing. Most cases of electron paramagnetism are found in systems with an odd number of electrons, although there are some

with an even number, as for example those discussed in the next section.

An electron, with spin  $S = \frac{1}{2}$ , has two possible orientations in a magnetic field  $H_0$  i.e. aligned with the field or opposite to it. Thus an electronic level of some atomic or molecular system that is normally degenerate in the spin quantum number 'm', will be split into two levels in the magnetic field. Since, for an electron, the spin  $S$  and the magnetic moment  $\mu$  are oppositely directed, the  $m = +\frac{1}{2}$  level will increase in energy and the  $m = -\frac{1}{2}$  level will decrease. Each level will be shifted by an amount  $\mu H_0$ , or in terms of the splitting or g-factor ( $g = \mu/\beta S$  where the Bohr magneton  $\beta = e\hbar/2M_e c$  and  $M_e$  = electronic mass,  $c$  = velocity of light,  $h$  = Planck's constant), by an amount  $\frac{1}{2}g\beta H_0$ . Thus the separation between levels is  $g\beta H_0$ . When the system is irradiated with radiation of frequency  $\nu$  such that  $h\nu = g\beta H_0$ , then resonance occurs and transitions between the levels are induced. Since according to the Einstein theory, the probabilities of absorption ( $m = -\frac{1}{2}$  to  $+\frac{1}{2}$ ) and stimulated emission ( $m = +\frac{1}{2}$  to  $-\frac{1}{2}$ ) are equal, and the probability of spontaneous emission is normally negligible (Purcell 1946), there will be no net effect unless the populations of the two energy levels are

different. Due to thermal motions both levels are normally populated and at thermal equilibrium at temperature  $T$  the difference in population is given by

$$\frac{N(-\frac{1}{2})}{N(+\frac{1}{2})} = \exp(g\beta H_0/kT) \quad 1.2.1.$$

i.e. an excess in the lower level. There will therefore be a nett absorption of the incident radiation.

In an isolated system this difference in population will decrease to zero when the population of the two levels will be equal. When this occurs the system is said to be saturated. If interactions with the surroundings or 'lattice' are considered, various relaxation mechanisms are possible whereby the downward transition probability is increased and saturation thus avoided.

### 1.3 Triplet States in Aromatic Hydrocarbons.

The luminescence from organic phosphors may be divided into two parts on the basis of the excited state from which it originates and on the lifetime of the state. In general the predominant part originates from the first excited singlet state ( $S = 0$ ), the ground state being also a singlet state ( $S = 0$ ). The transition, being between two states of the same multiplicity, is 'allowed' and the lifetime of the excited state is thus short.

In general the lifetimes fall in the range 1 - 100nsec. The other part originates from the first excited triplet state ( $S = 1$ ) and, due to the different multiplicity, the transition to the ground state is 'forbidden'. The lifetime is therefore long, and may be of the order of several seconds. The original suggestion as to the origin of this long lifetime component, commonly called phosphorescence, (fluorescence being reserved for the fast component), was made by Lewis and Kasha (1944). They suggested that a triplet state was possible and that it should be slightly lower in energy than the singlet state (Hund's rule). This state could then be populated from the first excited singlet state, assuming there was some mechanism to cause the necessary spin transition. Since this state has  $S = 1$ , it should be paramagnetic. This was demonstrated by Lewis and Calvin (1945) who detected the static paramagnetism of fluorescein in boric acid glass when illuminated by intense light of suitable wavelength. (See also Lewis, Calvin and Kasha, 1949). Later Evans (1955), using a more sensitive susceptibility balance, measured the paramagnetism of triphenylene and showed that the decay time on removal of the exciting light was the same as the phosphorescence decay, thus confirming that the identical

level was involved in both phenomena.

It was now well established that the excited states involved were paramagnetic, but conclusive evidence that they were triplet levels could be given by ESR investigations. If a resonance absorption was found, further information concerning the interaction between the two spins and between them and their environment could be obtained. Efforts to achieve this are discussed in part II.

#### 1.4 Aromatic Ions.

The reaction between alkali metals and aromatic hydrocarbons has been known for a considerable time, but it was not until the work of Scott et al (1936), who showed the importance of the solvent, that significant progress was made. The resultant solutions are intensely coloured and have good electrical conductivity. It was supposed that the alkali metal donates one or two electrons to the hydrocarbon molecule, the reaction being facilitated by good electron transfer solvents such as tetrahydrofuran or 1, 2 dimethoxyethane.

If only one electron is transferred, the product should be paramagnetic, whereas two would result in a diamagnetic product unless a triplet state was formed. The product of the reactions between sodium and a number

of aromatic compounds were examined by means of ESR by Lipkin et al (1953), who found that they exhibited strong paramagnetic resonance absorption. Since the reaction had been shown to involve one aromatic molecule per atom of sodium and that the g-factor was equal to the free-electron value, it was concluded that a free radical ion was formed by the transfer of one electron. This electron will be in the lowest unoccupied  $\pi$  orbital of the molecule and will therefore move around the whole molecule. Soon after this, Weissman et al (1953) detected hyperfine splitting in the naphthalene negative ion, and suggested that this must be due to the magnetic moments of the protons.

There are two modes of interaction possible to produce the hyperfine splitting: dipole-dipole and the Fermi 'contact' interaction (Abragam and Pryce 1951). The first is averaged out due to the rapid tumbling motions of the molecules in the solution, but the second, due to the finite value of the electron wave function at the proton, is independent of orientation. However, for  $\pi$  electrons the plane of the molecule is generally a nodal plane so that this interaction should also be absent. A resolution of this difficulty by invocation of 'configuration interaction' is discussed in section 1.5.



Some time later, it was reported by Yokozawa and Miyashita (1956) that a solution of perylene in sulphuric acid showed a strong ESR absorption. Weissman, de Boer and Conradi (1957) showed that hyperfine structure was also present and that the spectrum was very similar to that obtained with the negative ion, and considered that positive ions were probably formed. Further work (de Boer 1956, Weissman, Tuttle and de Boer 1957, Kon and Blois 1958) improved the hyperfine structure resolution and it became possible to correlate the splittings with the electron spin densities as calculated by Hückel molecular orbital theory. This correlation is discussed in 1.6.

### 1.5 Hyperfine Splitting and Configuration Interaction.

As mentioned above the supposition that the hyperfine splitting is due to interaction of the electron with the protons presents some difficulty.

The Hamiltonian describing the isotropic interaction between the magnetic moment of an electron and a nucleus may be written: (Fermi 1930)

$$H = \frac{32\pi^3}{3h^2} g_e g_n \mu_e \mu_n S_e \cdot I_n \delta(r_e - r_n) \quad 1.5.1.$$

where (with subscripts e for electron, n for nucleus)

$g$  = gyromagnetic ratio.

$\mu$  = Bohr or nuclear magneton.

$S$  = electron spin operator.

$I$  = nuclear spin operator.

$\delta(r_e - r_n)$  = delta function for electron-nuclear distance.

It is the delta function which causes the interaction to be zero unless the electron wave function is finite at the position of the nucleus. The  $\pi$  electron wavefunctions are normally zero in the plane of the molecule, but if interaction between excited  $\sigma$  states and  $\pi$  states, known as configuration interaction, is considered, it is found that there is a finite unpaired  $\pi$  electron density at the protons. It can be shown (sec. 5.1) that the splitting  $\Delta H$  due to the proton 'i' is proportional to the unpaired electron density  $\rho$  at carbon  $C_i$  to which the proton is bonded i.e.

$$\Delta H = Q\rho \qquad 1.5.2$$

where  $Q$  is approximately constant, and has been estimated theoretically to be about 28 gauss. If the values of  $\rho$  calculated by molecular orbital theory are taken as correct, then the values of  $Q$  resulting from the experimental values of  $\Delta H$  are found to vary over a small range about 28 gauss. It should be noted that if any of

the carbon atoms (which have no magnetic moment and therefore produce no splitting) are replaced by an atom with a magnetic moment, e.g.  $C^{13}$  or  $N^{14}$ , there will be an added interaction to that of the protons. A useful technique for elucidating spectra is the substitution of a deuteron for a proton, which will considerably reduce the splitting at this position due to its smaller magnetic moment (see e.g. Venkateraman and Fraenkel 1956).

#### 1.6 Molecular Orbital Theory.

Molecular orbital theory, based on the linear combination of atomic orbitals and applying the approximations due to Hückel (1931), has been applied to many molecular systems to calculate energy levels and wavefunctions with a fair degree of success (see e.g. Daudel et al 1959). Applying even this simplified theory to aromatic molecules results in considerable numerical calculation, although this can be somewhat reduced in the case of molecules with some symmetry by the application of simple group theory (see e.g. Roberts 1961). As noted above, the unpaired electron in the negative ion is in the lowest normally unoccupied level. The squares of the coefficients  $C_i$  of the atomic orbitals in the linear combination forming this molecular orbital give the unpaired electron density at each respective

carbon atom 'i'. These are the values for  $\rho$  in 1.5.2, and using an average value for Q the splitting  $\Delta H$  is found for each proton.

The agreement found with experimental values is generally very good for such a sensitive test of the wave function. Measurements of hyperfine splittings are thus a useful test of molecular orbital calculations, although the information only applies to the lowest unoccupied orbital for negative ions or the highest occupied orbital for positive ions. This is not a serious limitation, as these are the levels normally involved in any molecular process.

It is thus seen that ESR measurements on aromatic ions give useful information about important molecular orbitals, and, once the spectrum of a given ion is known, the technique can be used to identify its presence in other more complex situations.

## PART II: Electron Spin Resonance in Triplet States.

### 2.1 Introduction.

At the time the present investigation was undertaken there were no published reports of any work on attempts to detect ESR in triplet states, so that there was no indication of conditions suitable for observing this.

The first consideration in the attempt to detect electron resonance in the triplet state was the maximum concentration of molecules that would be required in this state for a given detection system. The latter was limited by the equipment available to a system that did not have the very highest sensitivity possible. It was found that a very intense light source would be required, and in order to be able to use a large sample to improve sensitivity and light collection, and make use of available equipment, it was necessary to operate at a frequency of about 300Mc/s with magnetic fields of about 100gauss.

Direct transitions from the ground singlet state ( $S_0$ ) to a triplet state (T) are forbidden so that the absorption spectrum of an aromatic hydrocarbon is due almost entirely to transitions to excited singlet states ( $S_1$ ,  $S_2$  etc). However, in the excited state

due to the comparable energy of the two states  $S_1$  and  $T_1$ , intersystem crossing in higher vibrational levels of  $S_1$  and spin-orbital coupling can produce quite efficient transfer from  $S_1$  to  $T_1$  (Kasha and McGlynn 1956). An estimate of the transfer rate  $k$  can be made from a knowledge of the  $S_1 \rightarrow S_0$  fluorescence lifetime  $\tau$  and the relative quantum yield  $R$  of  $S_1 \rightarrow S_0$  and  $T_1 \rightarrow S_0$ , assuming that the only quenching process operating is  $S_1 \rightarrow T_1$ . If  $p$  is the  $S_1 \rightarrow S_0$  transition probability and  $k$  the  $S_1 \rightarrow T_1$  transition probability:

$$\tau = \frac{1}{p+k} \quad 2.1.1.$$

$$R = \frac{p}{k} \quad 2.1.2.$$

For anthracene for example,  $\tau \approx 10^{-8}$ ,  $R \approx 9$  so that  $k \approx 10^7/\text{sec}$  and  $p \approx 10^8/\text{sec}$ . The triplet state can therefore be fairly efficiently and rapidly populated by excitation to the singlet state.

## 2.2 Light Intensity.

The light source caused considerable difficulty. A consideration of the required intensity indicated that a lamp with a power input of the order of kilowatts would be required. The absorption spectra of the materials to be examined extend from about 4000Å downwards, so that a

quartz envelope tube would be required. After a considerable search a possible light source was discovered at the B.T.H. research laboratory, Rugby. This was a  $2\frac{1}{2}$  Kw quartz envelope Xenon arc lamp. With a light output of 35lumens/watt, the light energy output is (1 lumen = 0.0016 watt at about 6000A):

$$\text{Light output} = 35 \times 2500 \times 0.0016 = 1.4 \times 10^9 \text{ erg/sec.}$$

From the spectral distribution of the emitted light it was found that about 0.05 of the energy was emitted in the region below 4000A (the emission extended from 2000 - 30,000A). The equivalent number of quanta is then about  $10^{19}$  quanta/sec. Light collection efficiency would be about 1% so that the number of quanta reaching the specimen  $\approx 10^{17}$  quanta/sec. In order to achieve higher intensities it is necessary to pulse the light source, keeping the average power the same. It was decided to do this to achieve the maximum possible concentration in the triplet state as an increase of the order of  $10^3$  in intensity should be possible.

### 2.3 Light Source.

The light source outlined above was chosen because of its high power rating although the useful output in the UV region is somewhat less than an equivalent mercury arc. The important point was that the arc size

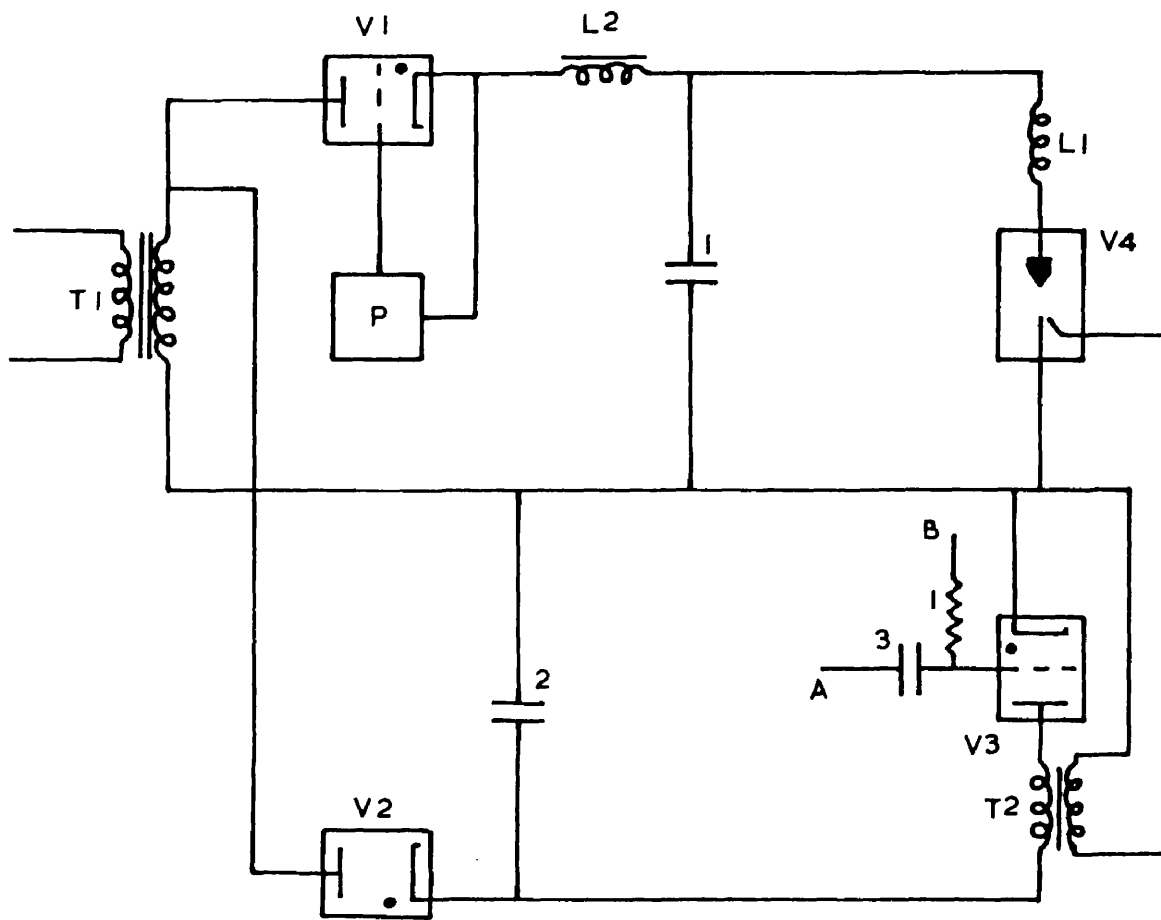




Figure 2a: Pulsed Light Source.

$T_1$  Transformer, 3KV RMS.  
 $T_2$  Pulse transformer.  
 $C_1$  150uf, 3000V variable.  
 $C_2$  8uf, 4000V.  
 $C_3$  0.01uf, 6000V.  
 $L_1$  100uH.  
 $L_2$  0 to 1H, variable.  
 $R_1$  50K.  
 $V_1$  CV1145/BT9.  
 $V_2$  CV5/GU21.  
 $V_3$  BT45.  
 $V_4$  Xenon lamp.  
B Negative bias.  
A Positive trigger pulse.  
P Variable phase control voltage.

was about  $1 \times 0.5\text{cm}$ . so that light collection and focusing were much easier.

The lamp had not been used as a flash tube before so that some research was needed into suitable operating conditions. It was found that an anode voltage of about 3KV was suitable. To obtain the maximum peak power with a maximum pulse rate of 10pps required a capacity of about 150 $\mu\text{f}$ . The trigger anode voltage was about 4-5KV and a momentary trigger-cathode current of greater than 5A was required to ionize the main gap. These requirements represented a considerable engineering problem. An outline of the final arrangement is shown in fig. 2a.

A large mercury thyatron  $V_1$  was used as the main rectifier as it was possible to control the d.c. output voltage by controlling the conduction period, and because it has a high P.I.V.(10KV) and peak current (75A). A choke was found necessary to limit the charging current surges and so spread the charging over a longer period, and even then the surges were large enough to cause trouble from flash-over in the choke. The main capacitor was made up of several sections ( $4 \times 30\mu\text{f} + 3 \times 10\mu\text{f}$ ) to allow further adjustment of the energy per pulse, and were specially constructed to withstand the repeated short

circuiting. A small choke was included in series with the lamp to limit the peak discharge current.

The trigger circuit used a thyatron to discharge a capacitor through the primary of a pulse transformer. The latter was wound on a large C-core with a few turns of heavy insulated wire so that a large secondary current could be obtained as required to ionize the main lamp gap. The positive trigger input to the trigger thyatron was obtained by dividing down from the mains frequency.

#### 2.4 Specimens and Resonance Detector.

There were a number of aromatic hydrocarbons that had a strong phosphorescence emission and were suitable from the point of view of lifetime. Of these naphthalene, which was available as large single crystals, and solutions of aromatic hydrocarbons in rigid glasses (see e.g. Pringsheim, 1949, p453) appeared to be most suitable. A cylindrical crystal of naphthalene 1cm dia. x 1cm long was obtained from Nash and Thomson Ltd., and the rigid glasses were made up according to the directions of Kasha (1948). The specimen size was about the size of the lamp arc so that a simple quartz condensing lens could be used for light collection and focusing.

The resonance detector consisted of a high frequency marginal oscillator with self-detection

followed by a high gain audio amplifier (see e.g. Ingram 1955, p103). This was a simple arrangement that could be operated at the required high frequency ( $\approx 300\text{Mc/s}$ ). The magnetic field was provided by a pair of Helmholtz coils fed by a stabilized current supply. This provided a uniform field over a large volume as required for the large specimen.

## 2.5 Operation of Equipment.

When the flash lamp was operated some difficulty was experienced from self triggering after a normal flash. It was difficult to examine the discharge because of its intensity, but by using a very dense filter it was possible to see small luminous globules circulating inside the bulb after a pulse causing the gap to break down. The origin of these globules is not clear and the effect could only be eliminated by reducing the pulse power. This was not investigated further as a much more serious drawback was found when the detector was tried with the lamp. When the lamp was pulsed the interference produced either by direct pickup or by mains transients due to the capacitors being recharged was so great as to make the observation of any resonance effects quite impossible. This meant that it would only be possible to operate the lamp as a steady light source which would require a

detector of considerably greater sensitivity.

In order to achieve greater sensitivity a microwave spectrometer was required. Construction of such an instrument was started, but before it could be completed the first announcement of the detection of triplet state electron resonance was made by Hutchison and Mangum (1958), who found a highly anisotropic spectrum of four lines in a suitably oriented crystal of a solid solution of naphthalene in durene (tetramethylbenzene) at liquid air temperatures.

## 2.6 Conclusion.

The work of Hutchison and Mangum showed why all previous work had been unsuccessful. Spin-spin interaction between the two unpaired electrons produces a large anisotropic zero field splitting which widened the resonance lines in a randomly oriented specimen beyond the limit of detection. Oriented specimens were therefore required, but these had to be dilute because of the self-quenching processes in a pure crystal. Anisotropic hyperfine structure was also observed due to interaction with the protons (Hutchison and Mangum, 1961). Thus even if our equipment had operated successfully we would not have detected a resonance in the single crystal of naphthalene, nor in the rigid glass unless

low temperatures had been used.

Soon after this van der Waals and de Groot (1959, de Groot and van der Waals, 1960), showed that it was possible to observe a resonance in a randomly oriented phosphor in a rigid glass at liquid nitrogen temperatures. This resonance is due to  $\Delta m = 2$  transitions and the r.f. field is parallel to the constant magnetic field. This has opened up new possibilities, and recently energy transfer between triplet states of different molecules has been detected by ESR in such systems (Farmer et al 1961). However, as we were not equipped at the time to produce crystals even if suitable host materials were known, or to operate at low temperatures, it was decided to abandon work on this line.

The high sensitivity and versatility of the microwave spectrometer that was now completed (described in part 3) provided new possibilities for the application of ESR to aromatic hydrocarbons. In particular, a study of the ions of these molecules promised to give useful information. Work on this line is described in parts 5 and 6.

### PART III.    Microwave Spectrometer.

#### 3.1    Introduction.

It has been shown by Feher (1957) that the superheterodyne type of spectrometer has the highest sensitivity. Although it is somewhat more complex to construct and operate than the high modulation frequency type, it is the most generally useful. A superheterodyne spectrometer has therefore been constructed, including i.f. lock and signal frequency/cavity lock systems. The spectrometer is in general similar to that of Hirshon and Fraenkel (1955) and operates at a frequency of 9350Mc/s. i.e. the centre of X-Band. This was chosen to obtain optimum performance from the microwave components.

The frequency stability of klystrons is in general not good enough to remain tuned to a high Q cavity or to maintain the difference between two klystrons within the bandwidth of the following i.f. amplifiers. It is therefore necessary to provide means of increasing the long term frequency stability. If the control systems have adequate bandwidth they will also reduce any frequency modulation which, because of the frequency characteristics of the sample cavity in the microwave bridge, appears as amplitude modulation at

the signal output and thus reduces the signal to noise ratio. Two control systems are therefore included. The first maintains the frequency difference between the two klystrons equal to the required i.f., and the second locks the frequency of the signal klystron to the resonant frequency of the bridge cavity. One important effect of the latter is that the output signal will be due to absorption only, as the accompanying dispersion is manifested as a change of frequency of the sample cavity which is compensated for by the locking system. The dispersion signal can however be observed by monitoring the cavity lock error signal (see section 6.3 and fig.6d for an example). These systems are shown in outline in fig.3a and described more fully below.

### 3.2 Sensitivity Considerations.

A full treatment of spectrometer sensitivity has been given by Feher (1957). The average power  $P$  absorbed per unit volume of a paramagnetic sample is ( $\omega$  = angular frequency,  $\chi''$  = magnetic susceptibility)

$$P = \frac{1}{2} \omega H_1^2 \chi'' \quad 3.2.1.$$

If the sample is placed in a resonant cavity to obtain the maximum volume of  $H_1$ , then the resultant change of cavity  $Q$  is given by:



$$\Delta Q = 4 \pi \chi'' \eta Q_0^2 \quad 3.2.2.$$

where  $Q_0$  = unloaded Q,  $\eta$  = filling factor.

If this cavity is used in a balanced bridge and the detector output is proportional to the input voltage (e.g. for a crystal diode), then the relative change in voltage  $V$  for a reflection cavity is given by:

$$\frac{\Delta V}{V} = \mp \sqrt{2} \pi \chi'' \eta Q_0 \quad 3.2.3.$$

This has a maximum value when the cavity is matched to the guide but it also changes sign here, so that it is necessary to work enough off match so that the absorption signal will not carry the cavity through the match condition when sweeping through a resonance.

If the random noise voltage is considered then the minimum detectable value of  $\chi''$  is found to be:

$$\chi''_{\text{minimum}} = \frac{1}{Q_0 \eta \pi} \left( \frac{k T \Delta \nu}{2 P_0} \right)^{1/2} \quad 3.2.4.$$

where  $k$  = Boltzman's constant,  $\Delta \nu$  = detector bandwidth.

Thus the maximum sensitivity is achieved with the maximum possible values of  $Q_0$  and power  $P_0$  for a given filling factor  $\eta$ , temperature  $T$  and detector bandwidth  $\Delta \nu$ . The maximum value of  $Q_0$  is limited by the magnet gap which limits the cavity size, and  $P_0$  by the stability of the bridge balance.

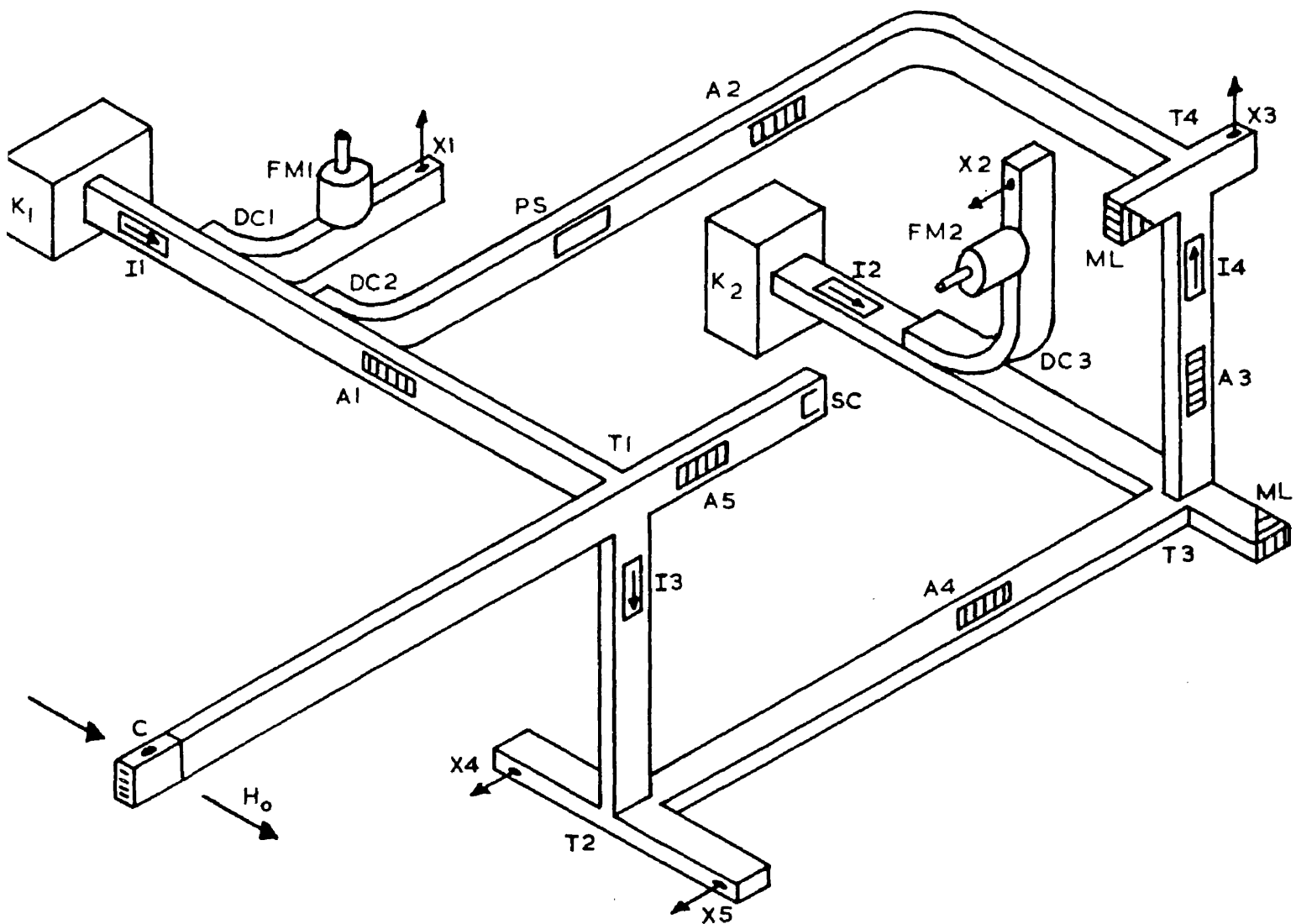


Figure 3b: Microwave System.

A Attenuator  
C Resonance cavity  
DC Directional coupler  
FM Frequency meter (absorption cavity)  
I Ferrite isolator  
 $K_1$  Signal klystron  
 $K_2$  Local oscillator klystron  
ML Matched load  
PS Dielectric phase shifter  
SC Variable short circuit  
T Magic tee  
X Crystal detector

### 3.3 Microwave System.

An isometric schematic diagram of the microwave system is shown in fig.3b. Microwave power from the signal Klystron  $K_1$  passes through isolator  $I_1$  and attenuator  $A_1$  to the bridge tee  $T_1$ . One balance arm of the bridge is terminated by the resonant cavity  $C$  and the opposite arm is balanced against this by means of an attenuator  $A_5$  and movable short circuit  $SC$ . The unbalance power in the output arm passes through isolator  $I_3$  to tee  $T_2$  and thence to crystals  $X_4$  and  $X_5$  which form a balanced mixer. A balanced mixer has a considerable advantage over the standard single crystal in that the noise due to the local oscillator is completely eliminated for a perfectly balanced arrangement. A full treatment of balanced mixers has been given by Pound (1948, chapter 6).

A small amount of signal power is taken by way of a 20db directional coupler  $DC_2$ , a phase shifter  $PS$  and attenuator  $A_2$  to tee  $T_4$  and thence to crystal  $X_3$ . Power from the local oscillator klystron  $K_2$  passes through isolator  $I_2$  to tee  $T_3$ . This power is divided equally between the two adjacent arms, half going via attenuator  $A_4$  to  $T_2$  to mix with the unbalance signal from the bridge in  $X_4$  and  $X_5$ , and the other half going via attenuator  $A_3$

and isolator  $I_4$  to  $T_4$  to mix with the power from  $K_1$  in  $X_3$ . The i.f. signal from this crystal is used for the i.f.-lock system. Directional couplers  $DC_1$  and  $DC_3$  (20db) feed power to detector crystals  $X_1$  and  $X_2$  via cavity wavemeters  $FM_1$  and  $FM_2$ . These sections are used to monitor the power output and frequency of the two klystrons. The cavity mostly used is a rectangular  $H_{012}$  mode cavity with slots cut in the end wall to allow irradiation of samples. A small screw is inserted through the centre of the broad face of the guide just outside the coupling iris. This serves to adjust the matching of the cavity to the guide ( see e.g. Varian Associates, 1960, p197). High Q cavities have little advantage when investigating lossy samples which reduce the Q considerably. They are also of larger size than low Q cavities and therefore require larger magnet gaps with consequent loss of field homogeneity.

The complete microwave system is supported by four Barrymount anti-vibration mountings to reduce the effects of external vibration. Due to the very high sensitivity of the spectrometer this was not completely effective and large disturbances produced jumps in the recorded spectra.

### 3.4 I.F.-Lock System.

This system controls the frequency of the local oscillator (L.O.) klystron and maintains it at a fixed distance from the signal klystron frequency. As explained above, signals from the two klystrons are mixed in  $X_3$ . The resulting beat frequency signal which is produced in the crystal mixer is amplified by a tuned i.f. amplifier with a bandwidth of about 2Mc/s at 42Mc/s (the i.f. frequency). The output is limited and fed to a frequency discriminator with a centre frequency of 42Mc/s. The D.C. output from the discriminator controls the reflector voltage of the L.O. klystron and hence its frequency. The details are described more fully in section 3.8.

### 3.5 Cavity-Lock System.

This system controls the frequency of the signal klystron and locks it to the resonant frequency of the sample cavity. The phase of the microwave signal reflected from the sample cavity changes by  $180^\circ$  on passing from one side of resonance to the other. This phase change is preserved in the i.f. signal obtained from the balanced mixer. If the i.f. signal at the output of the i.f.-lock amplifier is used as a reference phase signal, the variable phase signal from the sample

cavity may be fed to a phase sensitive detector and the output used to control the frequency of the signal klystron by means of its reflector characteristic.

### 3.6 Signal Preamplifier.

This is shown in fig.3c. It is a conventional cascode circuit (Valley and Wallman 1948, p656-664) based on a circuit published by the General Electric Company.

The circuit has been arranged for use with a balanced mixer, and since opposite polarity crystals are now available (e.g. SIM 2 and 5), the more complex input circuit described by Pound (1948, p272) is no longer necessary. The preamplifier is fixed directly on to the crystal mounts to obtain optimum performance, and has a low impedance output to feed the main signal amplifier by 70ohm cable. All interconnecting coaxial cables in the spectrometer had two seperate screens to reduce pickup and interactions as far as possible.

### 3.7 Main Signal Amplifier and I.F. Phase Sensitive Detector.

This is shown in fig.3d. The first two stages amplify the signal which is then detected by  $D_1$ . The output is filtered and fed to an audio amplifier and oscilloscope for presentation of the resonance absorption.

$V_2$  also feeds the limiter stages  $V_3$  and  $V_4$  and thus a driver stage  $V_5$ . This signal is the cavity-lock error signal and is fed to the phase sensitive detector. The reference phase signal is supplied from the i.f.-lock amplifier (see 3.8) by way of  $V_6$ , and its phase relative to the cavity error signal can be varied by means of the microwave phase shifter PS(fig.3b). The phase sensitive detector (PSD) is a balanced hybrid transformer arrangement with detectors  $D_2$  and  $D_3$ , and gives no output if either signal is applied alone. The limiters ensure that no change in output occurs due to changes in amplitude, as these can only be corrected at the klystron by changes of frequency. The PSD is insulated from earth and fed through high voltage capacitors, since it has to be connected directly to the input of the reflector control which is at approximately -650V. The cavity-lock system has a bandwidth of 2-3Mc/s, so that small changes in i.f. frequency have a negligible effect. With limiters operating, the d.c. voltage across half the output of the PSD is about 15V for the reference signal and 1.3V for the error signal. The current in  $D_1$  from the rectified carrier is monitored to indicate the balance of the microwave bridge.



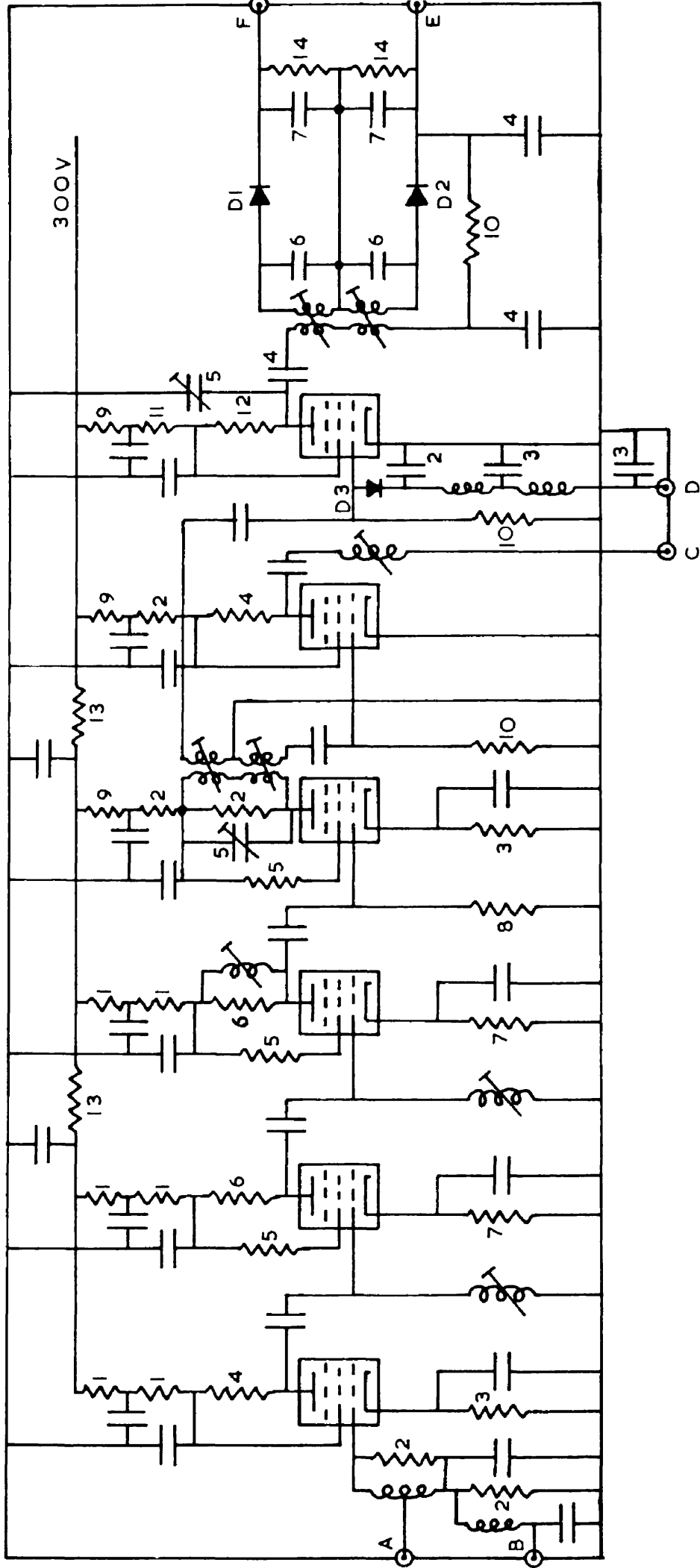


Figure 3e: I.F.-Lock Amplifier

R1	270ohm	C1	1000pf Ce (all capacitors
2	1K		not otherwise marked)
3	330ohm	2	60pf Ce
4	4.7K	3	0.01uf Ce
5	100ohm	4	1000pf 4000V Ce
6	3.3K	5	1.4-20pf trimmer
7	680ohm	6	10pf Ce
8	10K	7	100pf Ce
9	33K		
10	22K		All valves CV4014
11	15K 1w		All diodes GEX34
12	2.2K		
13	68ohm		
14	100K		

- A Signal input.
- B To crystal current meter.
- C Reference phase signal output to D of fig.3d.
- D Monitor output.
- E I.f.-lock signal output to F of fig.3f.
- F I.f.-lock signal output to E of fig.3f.

All resistors 1/4w and carbon unless otherwise specified  
Ce = ceramic

### 3.8 I.F.-Lock Amplifier and Discriminator.

This is shown in fig.3e. The amplifier is fed directly from crystal  $X_3$  (fig.3b) and has four stages of gain up to  $V_4$ , which feeds limiters  $V_5$  and  $V_6$  in parallel. The output from  $V_5$  is the reference signal for the phase sensitive detector of section 3.7.  $V_6$  drives a frequency discriminator of the Travis type with a peak to peak separation of  $2Mc/s$  and a centre frequency of  $42Mc/s$ . The discriminator is isolated from earth so that it may be directly connected to the reflector control circuit.

### 3.9 Klystron Reflector Control.

The reflector control circuits are shown in fig.3f. The output of the phase sensitive detector and i.f.-lock discriminator are connected directly to the points shown. For the signal klystron, the feedback gain is controlled by  $RV_1$  and the reflector voltage set by  $RV_2$ . The centre-zero meter  $M_1$  driven by  $V_1$  indicates the amplitude and phase of the correction signal.  $RV_3$  sets the meter zero. For the L.O. klystron, the error signal is amplified by  $V_4$  and the reflector voltage set by  $RV_5$ . The correction signal is indicated on the centre zero meter  $M_2$  driven by  $V_2$ .  $V_3$  is included to eliminate changes in  $M_2$  while setting the

reflector voltage by  $RV_5$ . This is only effective in so far as  $V_3$  and  $V_4$  are equivalent. By selection from a small number, suitable valves were easily found.

$RV_4$  sets the zero of the meter. This circuit operates between the -350V (klystron cathode) line and a -850V line to give the necessary reflector voltages.

### 3.10 Klystrons and Klystron Power Supply.

To obtain the required klystron performance as regards power output, frequency stability and minimum frequency modulation, a highly stable power supply and high quality klystrons are required. The most suitable klystron available was found to be the English Electric type K324/CV2304. The important specifications are as follows:

Resonator voltage	350V
Resonator current	35ma
Reflector voltage	-260 to -390V
Power output	45mw
Frequency drift on warm-up	3Mc/s (after 4min.)
Mechanical tuning rate	7Mc/s per turn
Electronic tuning range	30Mc/s

The small frequency drift on warm-up and long term stability has meant that the i.f.-lock system once set will lock in repeatedly for indefinite periods without

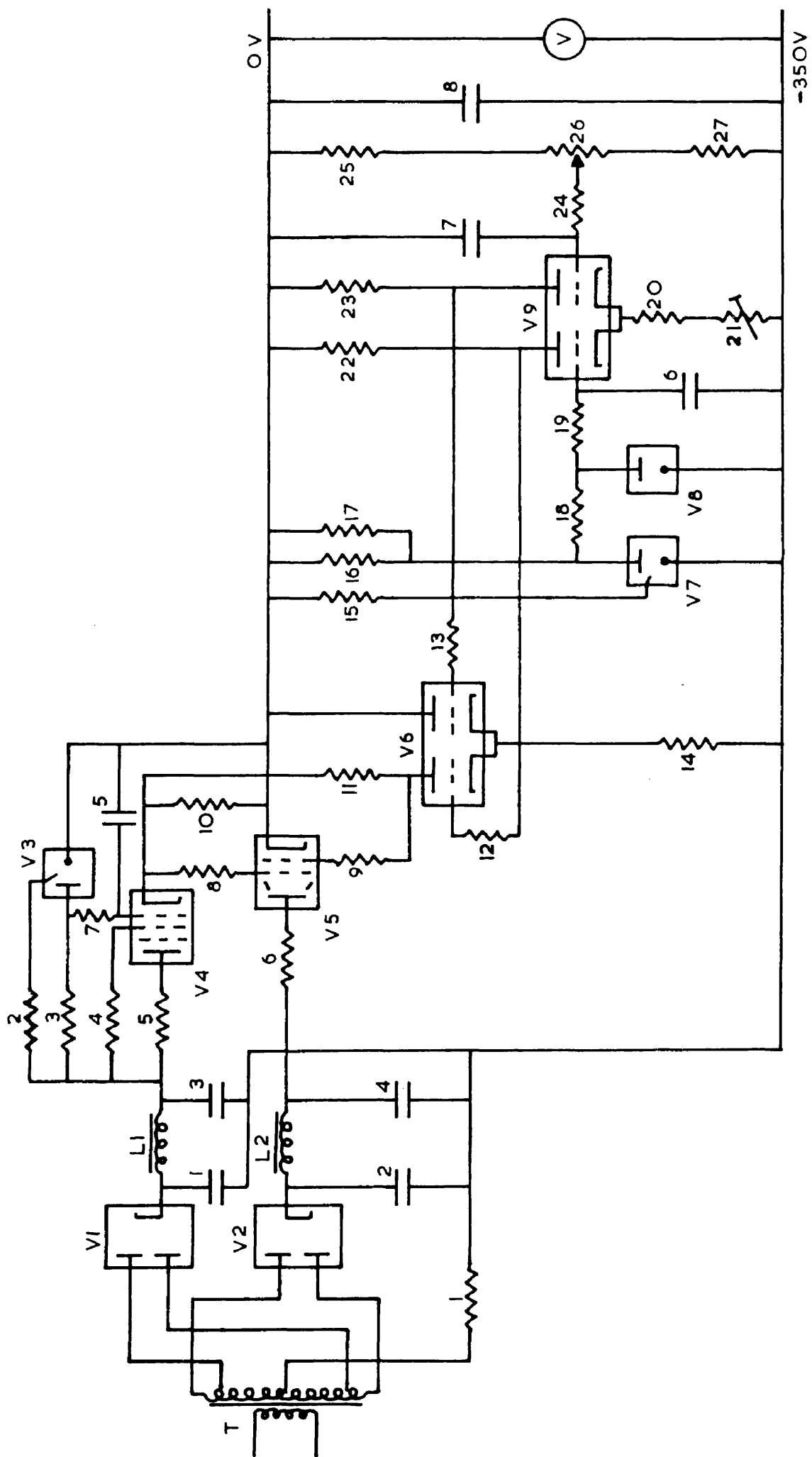


Figure 3g: Klystron Power Supply: Cathode Supply.

R1	47ohm 1w	C1-4	8uf 800V P
2	680K 1w	5-7	1uf 600V P
3	56K ww	8	8uf 600V P
4	100ohm		
5	100ohm	V1	CV4005
6	100ohm 3w ww	2	CV378
7	100K	3	CV287
8	100ohm	4	CV4055
9	1K	5	KT88
10	56K ww	6	CV4004
11	1M	7	CV287
12	1K	8	CV449
13	1K	9	CV4004
14	330K 2w		
15	560K 1w	T	Transformer, Gardners RS3206, 550/500/0/500/550V, 175ma
16	33K ww	L1	20H, 50ma, Gardners CS5083.
17	33K ww	L2	10H, 175ma, Gardners CS5142.
18	15K 3w ww		
19	1M		
20	330K 1w		
21	100K preset		
22	1.2M HS		
23	1.2M HS		
24	100K		
25	82K ww		
26	10K ww pot.		
27	27K ww		
All resistors 1/4w and carbon unless otherwise noted.			
ww = wire wound 6w		HS = high stability 2%	
P = paper			

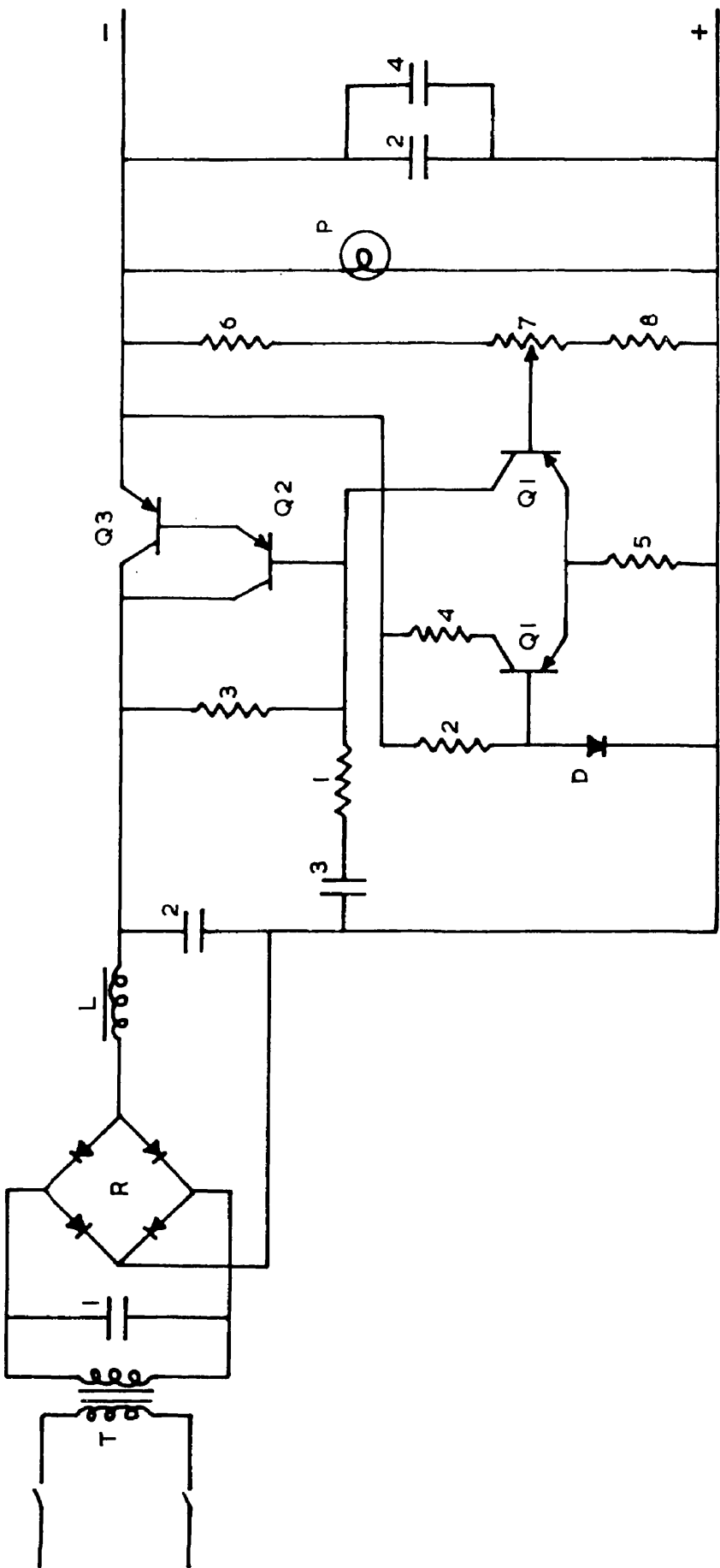


Figure 3i: Stabilised Filament Supply.

R1	47ohm	C1	0.01uf
2	120ohm	2	5000uf, 25V E1
3	1.2K HS	3	0.1uf P
4	100ohm	4	1uf P
5	680ohm HS		
6	100ohm HS	P	Pilot lamp, 8V, 150ma
7	100ohm ww pot.		
8	470ohm HS		

	1A Supply	3.5A Supply
Q1	GET114	GET114
Q2	GET114	OC16
Q3	OC16	2N277
D	SX51	SX51
R	SX631BLPLF	GEX541B1P1F
L	0.05H, 1A	0.05H, 4A
T	13V, 1.2A RMS	15.6V, 5.25A RMS Gardners BS6104

All resistors 1/4w and carbon unless otherwise noted.

ww = wire wound

HS = high stability 2%

E1 = electrolytic

P = paper



further adjustment. The small tuning rate makes tuning to the resonant frequency of high Q cavities much easier. The tuning arrangement, a threaded plunger with worm and gear drive, and robust cavity make it far superior to the older klystrons which were tuned by mechanical distortion of the cavity.

The power supply is shown in figs.3g and 3h. The two high voltage supplies were well underrated, isolated from earth and carefully insulated to eliminate the possibility of any leakage. Both klystrons are operated from the same supply so that any variations affect both, although possible drifts are probably negligible. The stability is good as the reference source is of the cascade neon type which has a stability of better than 1 part in  $10^4$  (Rogers 1957).

In order to eliminate any frequency modulation due to hum voltages from the klystron filament, a d.c. heater supply was included. The circuit is shown in fig.3i, and will supply up to 1A at 6-8V. Since the heater is internally connected to the cathode and the cathode currents were to be monitored individually, two separate supplies were required. The supplies are isolated from earth and the ripple at full load was a few millivolts.

With the spectrometer operating at the higher power levels some residual modulation is present in the output, but this is eliminated when the cavity lock system is in operation. It would appear that a locking system of this kind, using a cavity other than the bridge cavity if necessary, is a more satisfactory way of removing modulation than attempts to improve the stability of the power supplies.

### 3.11 Operation and Adjustment of Locking Systems.

Assuming the bridge cavity resonant frequency is known to within say 10Mc/s, the signal klystron frequency is set to this value with the aid of the frequency meter  $FM_1$  which is accurate to a few Mc/s. The cavity-lock gain control  $RV_1$  (fig.3f) is turned to zero. The local oscillator frequency is set 42Mc/s above the signal frequency with the aid of  $FM_2$  and then varied until the i.f.-lock system locks in as indicated by the tuning meter  $M_2$  (fig.3f). A reading should also be seen on the carrier level monitor (see section 3.7). To set the signal klystron to the cavity resonant frequency, a large amplitude 50c/s modulating signal is applied to its reflector, and the klystron mode is then displayed on the monitoring oscilloscope connected to the output of the signal amplifier. If the mode covers

the cavity frequency a large dip will be seen on the mode trace. The dip is brought to the centre of the mode by tuning the klystron, and the reflector voltage set for maximum power output. The cavity matching screw is now adjusted until the dip extends down to the base line, indicating that the cavity is matched to the guide as all the incident power is being absorbed. The modulation is now removed but the cavity lock is not applied until the bridge has been balanced and the incident power set by attenuator  $A_1$  (fig.3b). This is so that the phase and amplitude balance of the bridge can be achieved and because the attenuator  $A_1$  causes a large variable phase change.

### 3.12 Spectrometer Sensitivity.

The spectrometer sensitivity has been determined in a manner similar to that used by Henning (1961), except that the positive-ion spectrum of perylene was used instead of a solution of diphenylpicrylhydrazyl. Taking the outermost line of the perylene spectrum shown in fig.6b(iii), and assuming that all molecules have been ionised, we have the following conditions:

$$\text{Total number of spins in sample} = 6 \times 10^{16}$$

$$\text{Proportion contributing to outer line} = 1/4136$$

Line width = 0.5gauss

Microwave power  $\leq$  10mw approx.

Signal/noise ratio = 5 approx.

In order to compare the sensitivity with the results of Feher (1957), the sensitivity has been computed for the same conditions i.e. modulation  $\approx$  line width, detector bandwidth = 0.03c/s and power level 1mw. The cavity Q is probably somewhat less than for Feher's cavity, but has been assumed to be the same. For a signal/noise ratio of 1 the number of spins is found to be about  $6 \times 10^{11}$ , which agrees well with the results of Feher.

### 3.13 Spectrometer Improvements.

When the spectrometer was operated at higher power levels it was found that the bridge balance was liable to drift. This is probably due mainly to variations in temperature as a similar effect was noted by Feher. Temperature stabilisation of the room would be the most suitable means of reducing this effect. Insulation of the bridge, cavity etc., would be rather awkward and prbbably not as effective.

An examination of the variation of noise factor with frequency for a detector crystal-i.f. amplifier system shows that the minimum is quite broad,

and that it occurs at lower frequencies for better crystals (see e.g. Strum, 1953). This means that it would be possible to change the i.f. frequency from the present 42Mc/s to a somewhat lower value, say 20Mc/s or even less, without any deterioration in spectrometer sensitivity. Such a change would have a number of advantages. Regeneration in i.f. amplifiers would be reduced, and the passband stability of the i.f. amplifiers would be improved as at the high i.f. frequency the tuning relies on valve and stray capacity only. The i.f. discriminator cross-over frequency stability would be improved and the i.f. PSD would be much easier to construct and balance.

## PART IV. Magnet Stabilizers.

### 4.1 Introduction.

To achieve the necessary field stability with electromagnets for observing narrow resonance lines, precision current stabilizers are required. The stability of the magnetic field is primarily dependent on the current stability, but can also be affected by temperature variations which cause mechanical changes in the magnet yoke. Current variations are due to variations in the supply voltage and the load resistance. The relations between the various variables are given by Jervis (1955) for a degenerative type stabilizer (fig.4a):

$$\frac{\delta I}{I} = \frac{R_L}{AR} \cdot \frac{\delta V}{V}$$

and 
$$\frac{\delta I}{I} = \frac{R_L}{AR} \cdot \frac{1+\mu}{\mu} \cdot \frac{\delta R_L}{R_L}$$

where  $I$  = load current

$R_L$  = load resistance.

$R$  = reference resistance.

$V$  = load voltage.

$A$  = amplifier gain.

$\mu$  = series element amplification factor.

For a stability of 1 part in  $10^5$  with 5% variations in

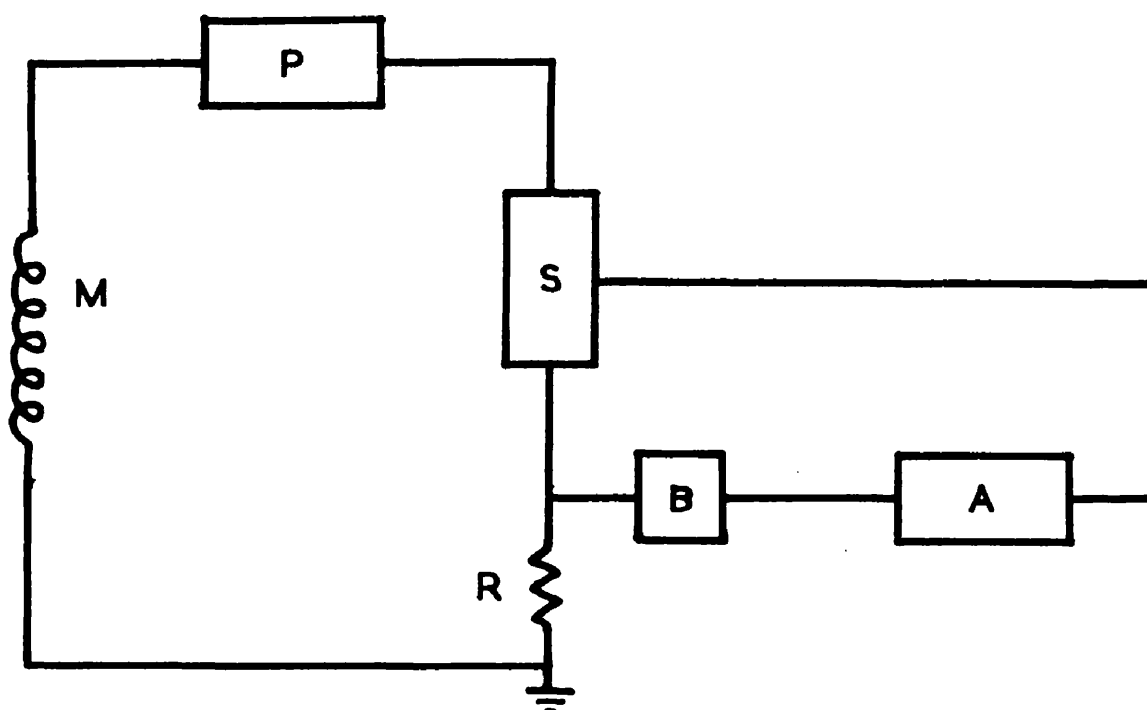
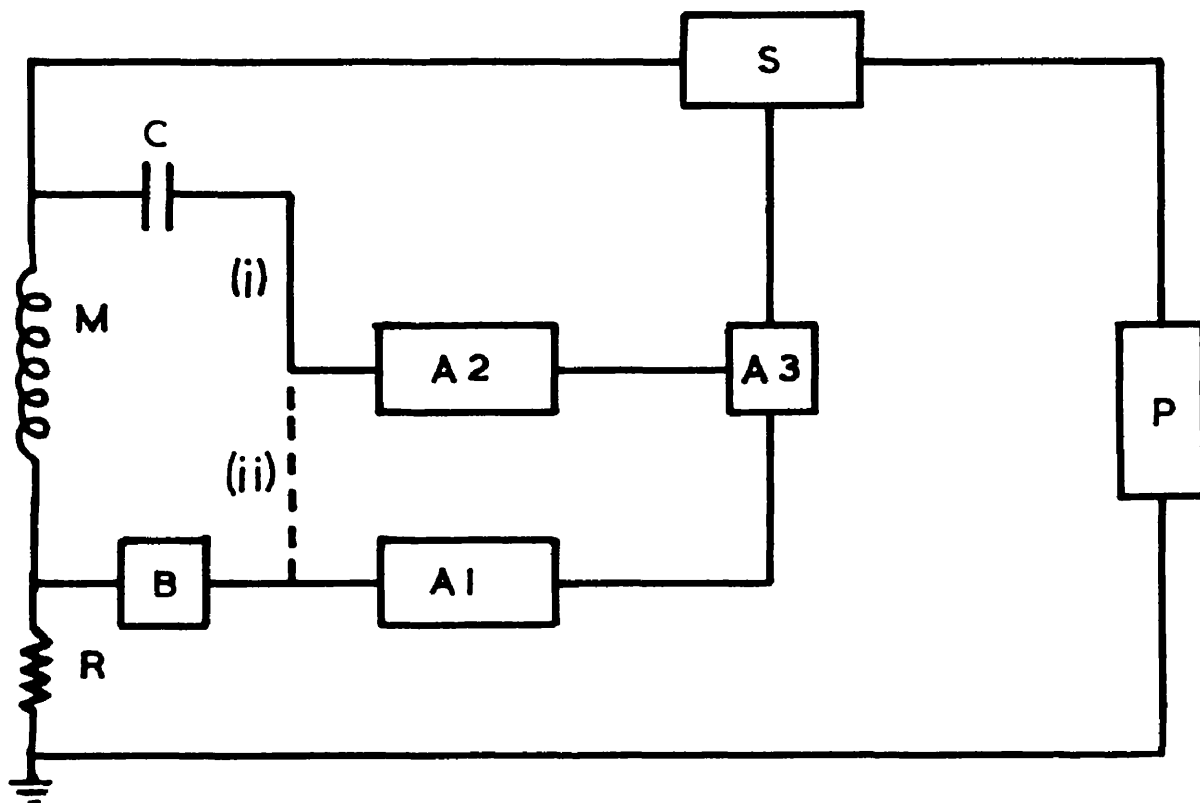


Figure 4a: Degenerative Current Stabilizers.

(i) and (ii)

M	Magnet
P	Power supply
S	Series element
R	Reference resistor
B	Reference voltage
A	Feedback amplifier
A1	d.c. Amplifier
A2	a.c. Amplifier
A3	Combining amplifier

(iii)

Alternative arrangement, components as above.



V or  $R_L$ , with  $R_L = 38\text{ohms}$ ,  $R = 2\text{ohms}$ ,  $\mu = 5$ , we find  $A = 10^5$ . The value of  $R_L$  corresponds to the Newport type A magnet used at first with the ESR spectrometer. With reference voltages of the order of 1V this requires a d.c. amplifier with an input stability of the order of  $1\mu\text{v}$ . This can be achieved by means of a 'chopper' type amplifier, but as these only have a small bandwidth (0-1c/s in this case) they have to be supplemented by a parallel a.c. amplifier of equal gain. The technique for doing this has been described by Buckerfield (1952). Since high frequency variations are not expected in the load it is possible to use a lower gain a.c. amplifier by connecting it to the top of the load rather than to the reference resistor (fig.4a(i)). This arrangement has been found to have a serious drawback. The magnet current is changed by varying the reference voltage. Unless this change is made very slowly so that the a.c. amplifier cannot sense the change, it will tend to oppose the change. This causes overloading of the a.c. amplifier which may lead to oscillation in the feedback loop. This drawback is not serious if the current is seldom changed but for the present work frequent changes were required. Equal gain amplifiers

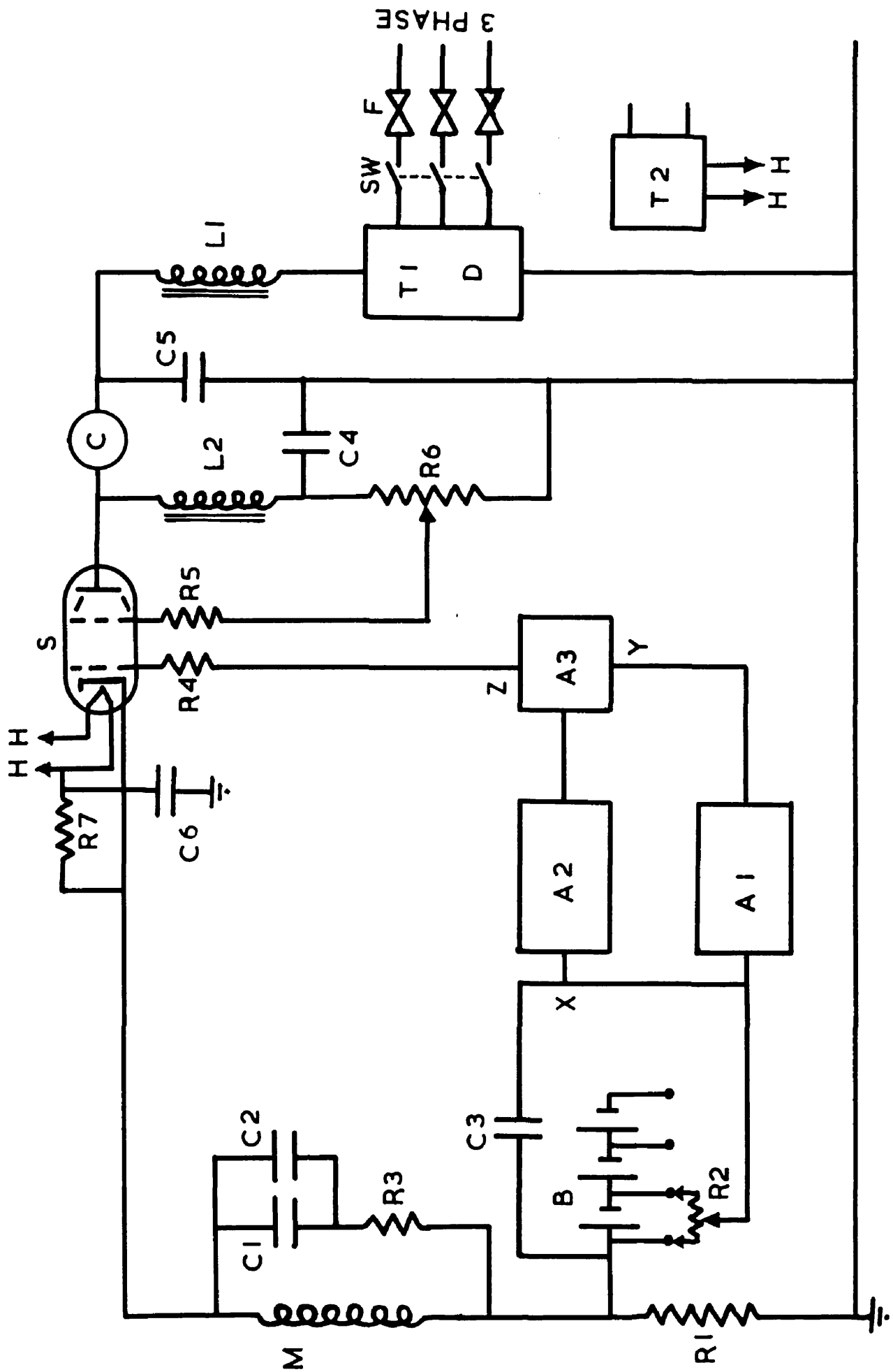


Figure 4b: Magnet Current Stabilizer.

R1	2ohm(see sec.4.4)	C1	120uf 600V P
2	1K Helipot	2	0.1uf 500V P
	Beckman type A	3	0.1uf 250V P
3	39ohm	4	8*32uf 450V El
4	1K	5	12*32uf 450V El
5	1K	6	0.01uf 500V Ce
6	18K 30w ww pot.		
7	10K		

L1 1.5H, 3A  
L2 10H, 250ma  
SW Three phase starter, MEM 84ADS  
C Meter, 0-4A  
D Three phase rectifier, SX754NB1P1F  
T1 Three phase delta/star transformer with  
electrostatic screen. Secondary 130V phase  
to neutral, 3.5A d.c.  
T2 Filament transformer, 3 off Gardners LS4093  
S Series valves, 30 off CV345 in parallel  
M Magnet, Newport type A, coils in series = 39ohm  
B Reference cells, Mallory type RM12  
F Fuses, 5A  
A1 Sunvic d.c. amplifier type DCA1  
A2 Amplifiers shown in fig.4c  
A3

Points X,Y,Z, correspond to points in fig.4c

All resistors 1/4w and carbon unless otherwise noted.

ww = wire wound 6w                      HS = high stability 2%

Ce = ceramic              P = paper              El = electrolytic

300V

-300V

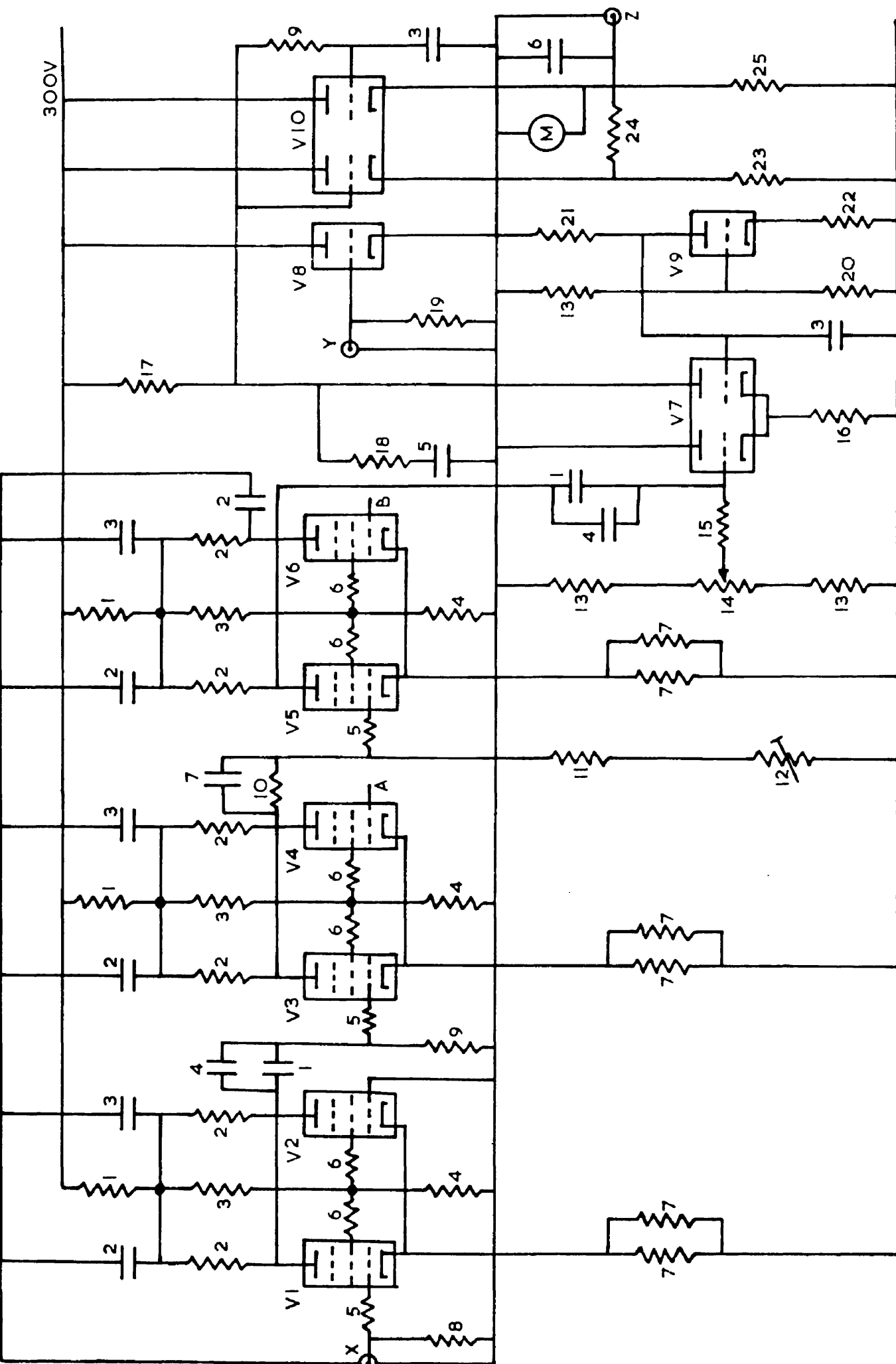


Figure 4c: Amplifiers A2 and A3 of Figure 4b.

R1	2.2K 2w	C1	1.0uf 350V Terecap
2	6.8K 2w	2	0.1uf P
3	8.2K 2w	3	0.01uf Ce
4	47K ww	4	100pf Ce
5	47ohm	5	0.005uf Ce
6	100ohm	6	0.02uf Ce
7	47K ww	7	10pf Ce
8	180K		
9	1M	V1-6	CV4014
10	1.5M HS	7,10	CV4003
11	1.8M HS	8,9	CV4004
12	250K preset		
13	470K HS	M	Voltmeter, 150/0/150V
14	100K ww	A}	Grids connected as are other
15	820K	B}	grids of respective pair.
16	39K 2w	X,Y,Z	Corresponding points in
17	150K 2w		fig.4b
18	680ohm		
19	100K		
20	100K HS		
21	150K HS		
22	56K HS		
23	56K ww		
24	100K 1w		
25	150K ww		

All resistors 1/4w and carbon unless otherwise noted.

ww = wirewound 6w      HS = high stability 2%

Ce = ceramic              P = paper

were therefore required with connection as shown in fig.4a.(ii).

As a high gain is required at ripple frequencies the high frequency cut-off of the feedback loop cannot be started at very low frequencies. The passband of the a.c. amplifier must therefore extend from about 1c/s to several hundred kc/s to ensure loop stability.

#### 4.2 Current stabilizer No.1.

The circuit is shown in fig.4b. The d.c. amplifier A was a Sunvic type DCA1. This was used at a gain of  $2.5 \times 10^4$ . Although not stated in his paper, this is the same amplifier used by Jervis and the frequency response is therefore as shown in his fig.3. The a.c. amplifier was a balanced pentode arrangement as shown in fig.4c. Points XYZ indicate corresponding points on fig.4b. Since the output of the d.c. amplifier is a virtual earth the input of the a.c. amplifier may be directly coupled to this point, which eliminates one coupling capacitor. This makes the required low frequency response easier to achieve.

The output stage has a gain of 11 and is designed to add the signals from the preceeding amplifiers and to provide the required output voltage swing

(about -100V to +100V). This feeds the series valves by way of a cathode follower. Two frequency controlling networks are used: the R24/C6 filter at the output and the R18/C5 phase shift network at the output amplifier anode. The overall d.c. gain is thus about  $3 \times 10^5$ , which gives a field stability of about 10 milligauss in 3000gauss for a 5% change in  $V$  or  $R_L$ . The stability was checked by tapping off part of the voltage across the reference resistor, backing this off with a standard cell and measuring the fluctuations with a Pye scalamp galvanometer. After the initial warmup drift the short term stability was found to be better than 1 part in  $10^6$ . It may be noted that slow steady drifts are not generally as serious as more rapid fluctuations, since resonances are usually traced out by sweeping the field and the drifts will just add to the sweep. This emphasises the need to maintain as high a loop gain at ripple frequencies as possible. The residual ripple across the magnet was found to be about 1mV at a frequency of 300c/s. Due to the increased magnet impedance at this frequency this corresponds to a ripple current of about 1 $\mu$ amp through the magnet.

### 4.3 Magnet Impedance.

The impedance of the magnet varies with current and frequency. The variation with current will be reduced by the large inherent air gap and in any case there is not much that can be done about it. The variation with frequency is, however, more serious. The feedback ratio  $Z_L/R$  will increase and thus the loop gain decrease with increase of frequency, and phase shifts will be introduced. It was found that the magnet inductance resonated with its stray capacity at about 6-7Kc/s and it was possible to get the system to oscillate at this frequency. It would be desirable if  $Z_L/R$  could be made constant and equal to the d.c. value  $R_L/R$  in the interest of stability. This can be achieved by shunting the magnet with a resistor and capacitor in series as shown in fig.4b ( $C_1$  and  $R_3$ ).  $R_3$  is made equal to  $R_L$  and  $C_1$  is chosen such that  $L/C_1 = R_L^2$ . The parallel network,  $L+R_L$  and  $C_1 + R_3$ , is then resistive at all frequencies. This disregards the stray capacity of the magnet, but this is only about 0.001uf and can therefore be neglected. For the given values of  $L$  and  $R_L$  the value of  $C_1$  comes out to be inconveniently large. Electrolytic capacitors cannot be used due to the leakage current, which will flow through  $R$ .



In practice, however, it is only necessary to produce a resultant resonant frequency of a few cycles per second for satisfactory operation, as the resonant peak is then small and has a negligible effect on the loop response. Since the resonance is at 6-7Kc/s with 0.001uf it should be at about 6-7.c/s with 100uf: in fact the peak was at 9-10c/s. The curves given by Terman (1950, p.147) illustrate this, although one resistor is missing. High frequency currents will now flow through  $C_1$  rather than L and thus will not affect the magnetic field. A somewhat similar arrangement is used by Garwin et al (1959): it may be noted that the condenser leakage problem is not as serious as would appear from their figures, as only the variations in the leakage would affect the stability.

#### 4.4 Reference Elements.

The reference resistor ( $R_1$  fig.4b) consisted of four ordinary 2ohm, 20watt wire-wound resistors connected in series/parallel to give an effective resistance of 2ohm. They were cooled in a large oil bath (Shell Diala Oil B) but no temperature control was used. The reference voltage (6 volts) was provided by 5 Mallory mercury cells type RM12. These have a temperature coefficient of about 20 parts in  $10^6/^{\circ}\text{C}$ . These may be efficiently insulated from rapid temperature fluctuations by insulating with one

of the expanded plastics.

The magnet current can be varied from zero upwards. For small output currents, it would normally be necessary to use large negative control grid voltages on the series valves, which complicates the output stage of the feedback amplifier and would exceed the valve rating. To limit the swing required, the screen voltage may be reduced by means of a potentiometer. For currents up to about 0.5A the screen control is used to limit the control grid voltage to a maximum negative value of about 80V.

For high current power supplies it is a considerable advantage to use a three phase supply, as the ripple in the rectified output is only 1/10th of that of a single phase rectifier of the same type, so that smaller smoothing chokes can be used.

#### 4.5 Magnet Stabilizer No. 2.

During the course of this work it became necessary to use another magnet in place of the Newport type A. This new magnet was of high impedance and so required a different current stabilizer. The general considerations regarding the design are the same as those described previously and the circuit is shown in fig.4d. It is in general similar to the previous stabilizer, but

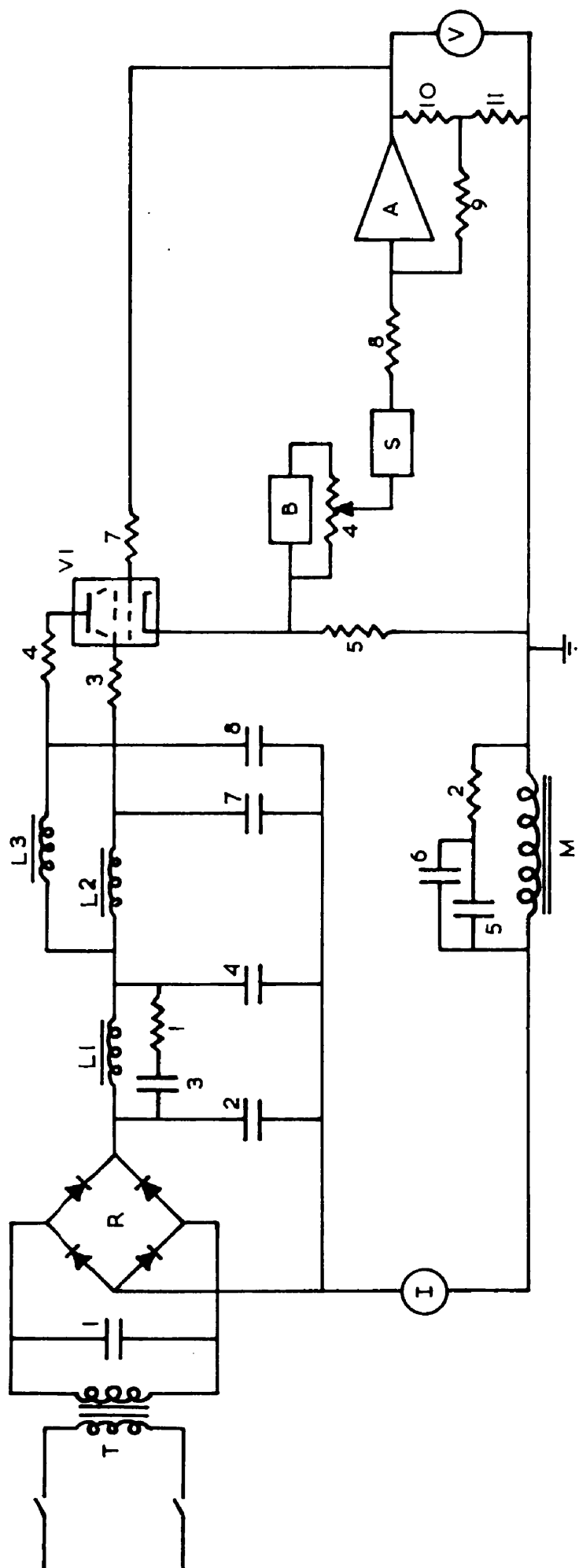


Figure 4d: Magnet Current Stabilizer No.2.

R1	10K 1w	C1	0.03uf 1500V P
2	1.8K	2	0.1uf 2000V P
3	1K	3	0.1uf P
4	47ohm 1w	4	50uf 900V El
5	100ohm ww	5	1uf P
6	20K Helipot	6	0.01uf Ce
	Beckman type A	7	150uf 900V El
7	1K	8	100uf 900V El
8	100K HS		
9	10M HS		
10	22K HS		
11	220ohm HS		

R Bridge rectifier, 4\*80BS

T Transformer, 650V 250ma RMS, Gardners BS6050

L1 } 10H, 250ma, Gardners CS5147  
L2 }

L3 100H, 25ma, Gardners CS5037

I Meter, 250ma

M Magnet, resistance 1.8K

V1 Series valves, 2\*KT88 in parallel

B Reference voltage, 12 RM12 Mallory mercury cells

V Voltmeter, 0-100V

S Field sweep

A Solartron amplifier type AA621.2

All resistors 1/4w and carbon unless otherwise noted

ww = wire wound 6w HS = high stability 2%

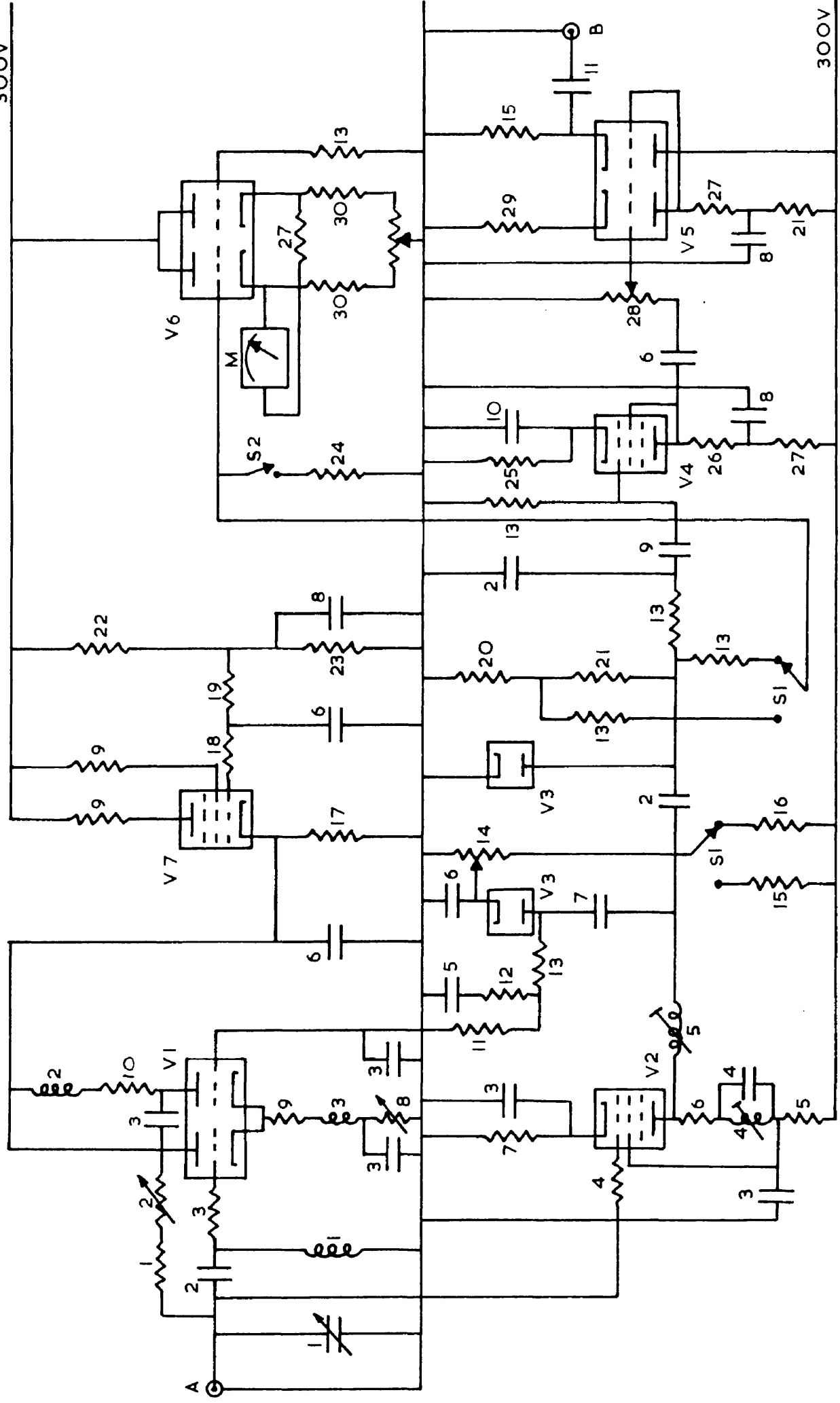
Ce = ceramic P = paper El = electrolytic

but the circuit has been rearranged so that the output voltage from the feedback amplifier does not have to compensate for the voltage across the magnet winding (fig.4a(iii)). The amplifier is a Solartron AA621.2 'chopper stabilized' type, of the kind normally used in analog computers, and it is fed back to have a gain of  $10^4$ . A large reference resistor (100ohm) and reference voltage (15V) are used. With a magnet impedance of 1800ohms this results in a stability of 2 parts in  $10^5$  for a 1% change of input voltage (i.e. 60milligauss in 3000gauss).

#### 4.6 Magnetic Field Sweep.

The most efficient method of providing magnetic field sweeps is to vary the reference voltage of the current stabilizer. Electronic sweeps have the advantage of smoothness and simple variation of sweep rate. However with the stabilizers used the reference voltage is isolated from earth so that electronic sweeps are difficult to use. A mechanical sweep (a motor driven helipot with reference cell) is easily inserted in the circuit, the sweep rate being altered by means of a set of gears. A few fixed ratios can cover most requirements and the discrete ratio can be more easily calibrated. A small synchronous motor with reduction gears

300V



300V

Figure 4e: Pound Spectrometer.

R1	330ohm	C1	70pf(Oscr. frequency)
2	10K(Oscr. feedback)	2	1000pf Ce
3	47ohm	3	0.01uf Ce
4	18ohm	4	1.4-20pf trimmer
5	2K ww	5	1.0uf P
6	1.2K 1w	6	0.1uf P
7	82ohm	7	60pf Ce
8	1K Helipot(Oscr. bias)	8	8uf 450V E1
	Beckman type C	9	0.22uf P
9	100ohm	10	250uf 12V E1
10	680ohm	11	0.47uf P
11	470ohm		
12	10K	V1	E88CC
13	1M	2	Z759
14	10K ww(Oscn. level)	3	CV140
15	150K 1w	4	EF86
16	560K 1w	5	CV4003
17	270K 1w	6	CV4024
18	1K	7	CV4055
19	560K		
20	15K	L1	R.F. choke
21	33K	2	1uH
22	560K 1w	3	50uH
23	220K 1w	4	6.2uH
24	470K	5	8uH
25	3.3K HS		
26	220K	M	Meter, 0-25uA(Oscn. level)
27	47K	SW1	Oscn. level Hi/Lo
28	1M(Audio gain)	SW2	Meter range Hi/Lo
29	3.9K	A	Probe coil
30	5.6K	B	Signal output
31	5K ww(Meter zero)		

(Everett Edgecumbe Synlock) drives a Beckman model A 10-turn Helipot of good linearity ( $\pm 0.25\%$ ) connected through switched resistors to a mercury cell. The amplitude of the sweep is then altered by the switched series resistors.

#### 4.7 Pound Spectrometer.

In order to measure magnetic fields and to detect nuclear resonances when required, a Pound type marginal oscillator spectrometer was built (see e.g. Mays et al, 1958). The circuit is shown in fig.4e. The signal from the marginal oscillator V1 is amplified in V2 which has a gain of 20 from 1 to 20Mc/s. The output is detected in V3 to control the oscillation level and to give the audio output signal, which is amplified in V4 and V5. The filament of V3 is under-run to minimise spurious automatic level control bias due to electron emission (Blume, 1958). The high pass filter in the input to the oscillator reduces modulation pickup, which modulates the oscillator and so produces spurious signals when using phase sensitive detection (Robinson and Geiger, 1958). A stabilized low voltage d.c. supply using transistors was designed and constructed to run the valve filaments to eliminate hum. This was similar to those shown in the klystron power supply in fig.3i, but



300V

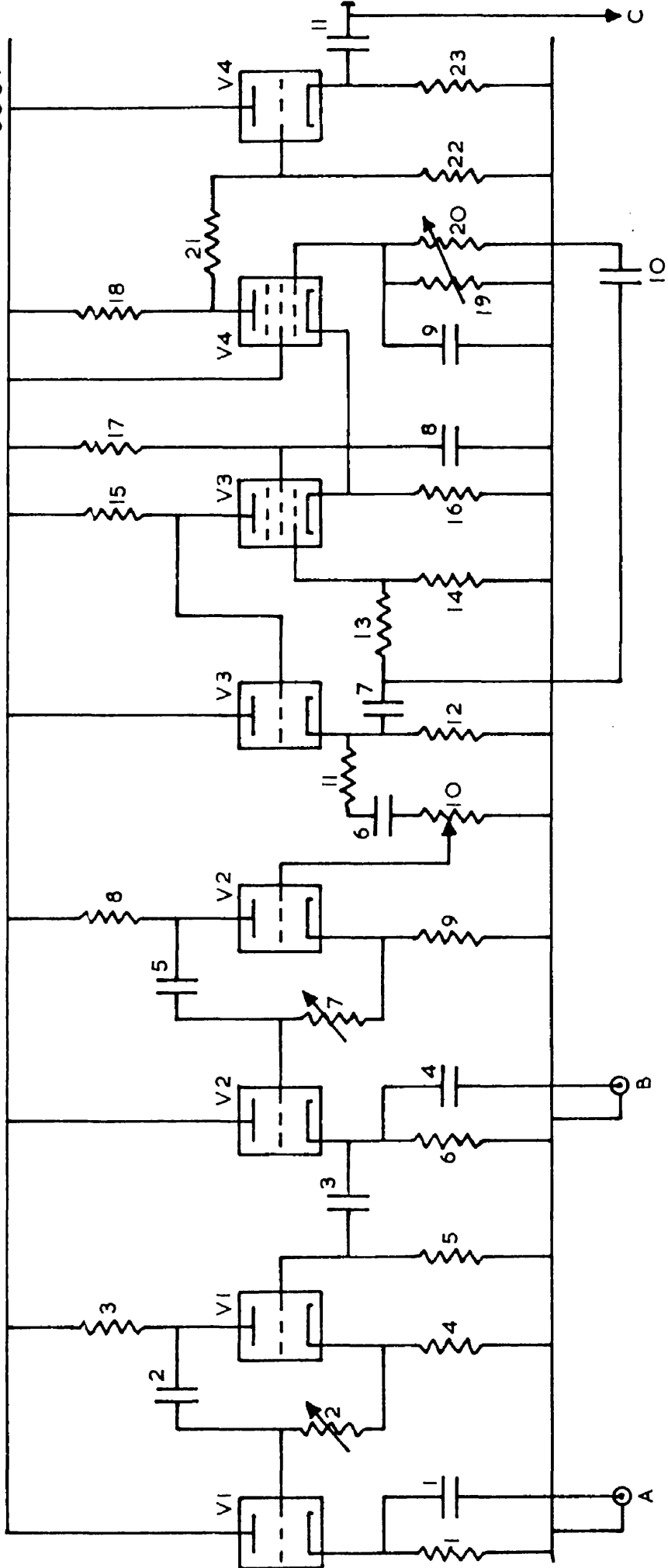


Figure 4f: Audio Phase Sensitive Detector; Oscillator  
and Phase Shifters.

R1	10K	C1	0.22uf P
2	100K ww	2	0.1uf P
3	4.7K HS	3	0.1uf P
4	4.7K HS	4	0.22uf P
5	1M	5	0.1uf P
6	10K	6	0.22uf P
7	100K ww	7	8uf 450V E1
8	4.7K HS	8	0.1uf P
9	4.7K HS	9	0.005uf matched
10	100K(Modn.Amplitude)	10	
11	180K	11	0.22uf P
12	22K		
13	Thermistor type	V1,2	CV4003
	R15 (STC)	3,4	ECF80
14	2.7K HS		
15	150K 1w	A }	Modulation outputs
16	1K	B }	
17	100K	C	To monitor switch fig.4g
18	22K	D	Switching volts to D in
19 }	18K HS + 50K ww pot.		fig.4g
20 }	ganged(Oscr,frequency)		
21	560K		
22	560K		
23	33K 1w		

All resistors 1/4w and carbon unless otherwise noted

ww = wire wound

HS = high stability 2%

E1 = electrolytic

P = paper

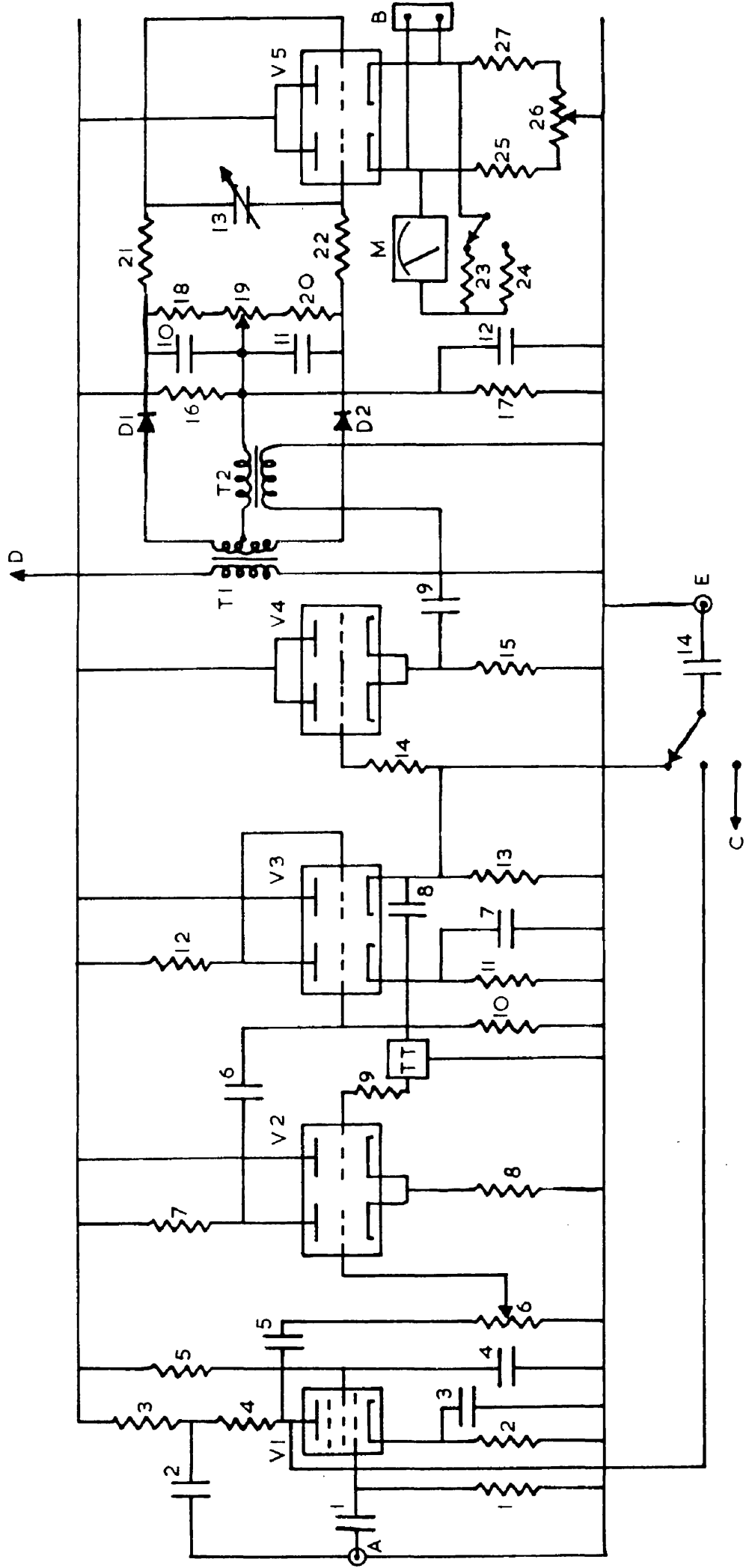


Figure 4g: Phase Sensitive Detector; Audio Amplifier,  
Narrow Band Amplifier and Phase Detector.

R1	1M	C1	0.1uf P
2	2.2K HS	2	8uf 450V EL
3	100K HS	3	250uf 12V E1
4	100K HS	4	0.1uf P
5	1M	5	0.05uf P
6	1M(Audio gain)	6	0.01uf P
7	220K	7	250uf 12V E1
8	1K	8	0.47uf P
9	1.5K	9	0.47uf P
10	1M	10	1.0uf 125V P
11	1.2K	11	1.0uf 125V P
12	56K 1w	12	0.1uf P
13	39K 1w	13	0-8uf switched(Time const)
14	10K	14	0.1uf
15	22K 2w	V1	EF86
16	560K	2	CV4004
17	39K	3,5	CV4003
18	330K	4	CV4024
19	100K ww preset (Detector balance)	D1,2	CV448
20	330K	T1	Fortiphone MM2A
21	1.2M	T2	Ardente D3008
22	1.2M	TT	Twin-tee network(R=82K HS 1%, C=0.01uf matched)
23	22K	M	Meter, 50/0/50uA
24	100K	A	Signal input
25	3.9K	B	External Recording meter 0.5/0/0.5mA
26	2.5K ww(Meter zero)	C	To C of fig.4g
27	3.9K	D	Switching volts input from D of fig.4g
E	Monitor scope		

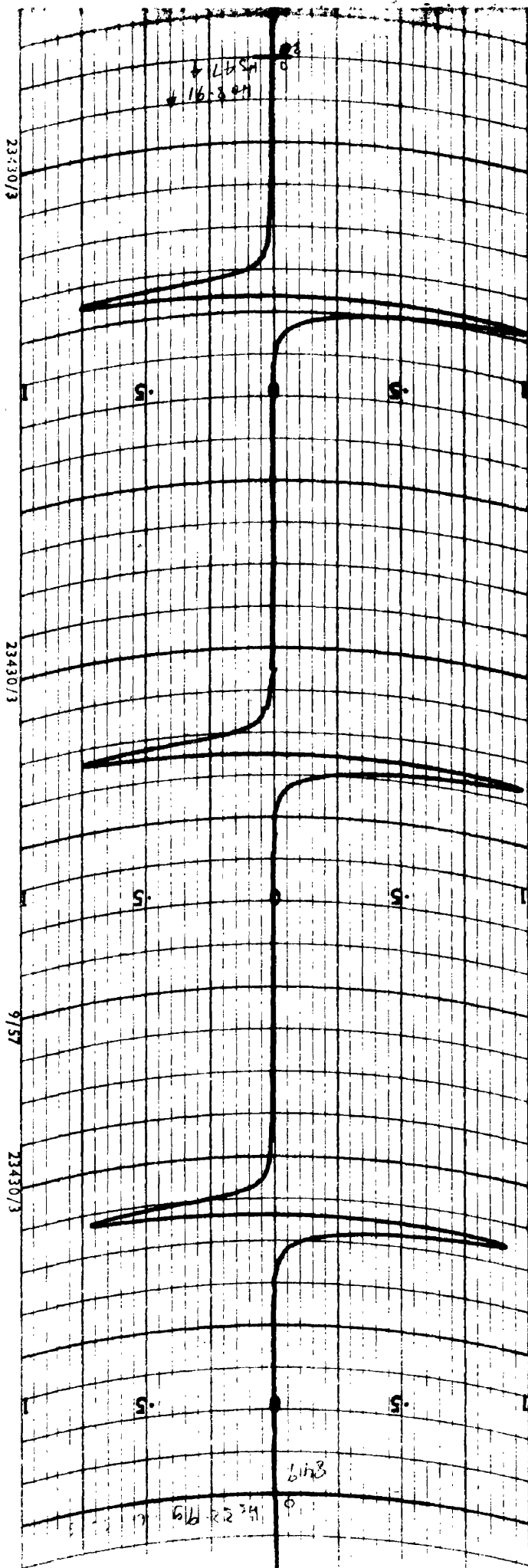


Figure 4h: Magnetic Field Sweep Calibration.

ESR in Peroxylamine Disulphonate

Fixed field approx. 3314gauss

Operating frequency approx. 9350Mc/s

Modulation 0.5gauss peak to peak

Detector bandwidth 0.4c/s

Chart speed 1/5" per min.

Specimen: 0.02ml of 0.02M solution in 0.1N Sodium  
Carbonate

Recorded 2 weeks after making up

Resultant sweep rate = 47.4gauss in 50min, or

1" on chart = 4.74gauss.

has a larger output of 3.5A.

#### 4.8 Magnetic Field and Sweep Calibrations.

The magnetic field was calibrated against the proton nuclear resonance in water (frequency = 4.26 Mc/s per gauss, Ingram 1958, p.64), and the diphenylpicrylhydrazyl ( $g = 2.0036$ , Ingram 1958, p.136) and peroxyamine disulphonate (Freymy's salt,  $g = 2.0054$ , Pake et al 1952) electron resonances. The accuracy was limited to about 1% by the accuracy of the signal generator in the NMR case and the cavity wavemeters in the ESR cases. This was quite adequate for the present work as  $g$  values were not being measured.

The magnetic field sweeps were calibrated against the electron resonance in Freymy's salt, which has three equally spaced lines (due to  $N^{14}$  hyperfine splitting) separated by 13gauss. The solution in water is unstable and decays in a few minutes, but Townsend et al (1953) have found that a solution in 0.1N sodium carbonate is stable for several days. This solution was used but it was found that a strong resonance was still obtained after at least six weeks. A derivative trace of the resonance is shown in fig.4h.

#### 4.9 Audio Phase Sensitive Detector.

The phase sensitive detector is shown in

figures 3f (oscillator and phase shifters) and 3g (audio amplifier, narrow band amplifier and phase detector). The oscillator is of the Wien bridge type and can be tuned over a small range around 170c/s. One output, by way of the phase shifters, feeds a power amplifier of the 'Williamson' type (G.E.C. 1957, p.40-43) which provides magnetic field modulation by means of an auxiliary field coil. The other oscillator output provides a reference signal for the phase sensitive detector.

The input signal is amplified in the audio amplifier (fig.3g) and a twin-T narrow band amplifier, and then fed to one input of a balanced hybrid phase detector. The detector output time constant can be varied to give bandwidths down to 0.01c/s. The balanced cathode follower output drives a 0.5/0/0.5ma recording meter (Record Electrical Co.).



## PART V. Aromatic Hydrocarbon Ions.

### 5.1 Theory of Configuration Interaction.

A theory of configuration interaction has been given by Weissman (1956). An alternative treatment has been given by McConnell (1956) and extended by others. The following outline of the theory follows Weissman.

If the bond between a carbon atom and its associated proton is represented by a bonding orbital  $\sigma_B$ , then the electronic configuration of the ground state of the negative ion can be written:

$$(\text{filled orbitals}) \cdot \sigma_B^2 \cdot \pi \quad 5.1.1.$$

and an excited state that can interact with the ground state may be written:

$$(\text{filled orbitals}) \cdot \sigma_B \cdot \pi \cdot \sigma_A \quad 5.1.2.$$

where  $\sigma_A$  represents an electron in an antibonding orbital. Since the spins of the filled orbitals remain paired, only the two parts  $\sigma_B^2 \cdot \pi$  and  $\sigma_B \cdot \pi \cdot \sigma_A$  need be considered. Including the spin functions  $\alpha, \beta$ , the ground state 5.1.1. can be written as a Slater determinant:

$$\phi_0 = \frac{1}{\sqrt{6}} \begin{vmatrix} \alpha_1 \sigma_B(1) & \alpha_2 \sigma_B(2) & \alpha_3 \sigma_B(3) \\ \beta_1 \sigma_B(1) & \beta_2 \sigma_B(2) & \beta_3 \sigma_B(3) \\ \alpha_1 \pi(1) & \alpha_2 \pi(2) & \alpha_3 \pi(3) \end{vmatrix} \quad 5.1.3.$$

There are three possible configurations for the

excited state, which have the same value of  $S_z$  (i.e.  $+1/2$ ) as 5.1.3. Written in short form, but representing determinants similar to 5.1.3:

$$\begin{aligned}\phi_1 &= 1/\sqrt{6} \cdot | \alpha_1 \sigma_B(1) & \beta_2 \sigma_A(2) & \alpha_3 \pi(3) | \\ \phi_2 &= 1/\sqrt{6} \cdot | \beta_1 \sigma_B(1) & \alpha_2 \sigma_A(2) & \alpha_3 \pi(3) | \\ \phi_3 &= 1/\sqrt{6} \cdot | \alpha_1 \sigma_B(1) & \alpha_2 \sigma_A(2) & \beta_3 \pi(3) |\end{aligned} \quad 5.1.4.$$

Acceptable excited state functions must also be eigenfunctions of  $S^2$  since this commutes with the Hamiltonian. Suitable linear combinations of 5.1.4. must be taken and are found to be (see e.g. Daudel et al 1959, p.433):

$$\begin{aligned}\phi_A &= 1/\sqrt{2}(\phi_1 - \phi_2) \text{ eigenvalue } \frac{3}{4} \hbar^2 \text{ or } S=\frac{1}{2} \text{ (doublet)} \\ \phi_B &= 1/\sqrt{6}(\phi_1 + \phi_2 - 2\phi_3) \quad " \quad \frac{3}{4} \hbar^2 \text{ or } S=\frac{1}{2} \text{ (doublet)} \\ \phi_C &= 1/\sqrt{3}(\phi_1 + \phi_2 + \phi_3) \quad " \quad \frac{15}{4} \hbar^2 \text{ or } S=\frac{3}{2} \text{ (quartet)}\end{aligned} \quad 5.1.5.$$

$\phi_C$  may be eliminated since it has different multiplicity (quartet) to the ground state (doublet) so that no interaction is possible.  $\phi_A$  may also be eliminated since, as a combination of  $\phi_1$  and  $\phi_2$ , it has the two spins in the  $\sigma$  states paired, and it is unpaired spin in the  $\pi$  states that is required for hyperfine interaction. The configurational mixture representing the system may now be written:

$$\psi_0 = \phi_0 + \lambda_B \phi_B \quad 5.1.6.$$

if the perturbation  $\lambda_B$  is small. First order perturbation theory gives:

$$\lambda_B = \frac{(\phi_B | H' | \phi_0)}{W_B - W_0} = \text{Const.} \int_{\tau} \frac{\sigma_A(1) \pi(2) \left| \frac{e^2}{r_{12}} \right| \pi(1) \sigma_B(2) d\tau}{W_B - W_0} \quad 5.1.7.$$

where  $H'$  is the Hamiltonian for the electrostatic repulsion energy of the three electrons i.e.  $e^2/r_{ij}$ . The  $\pi$  orbital is formed by a linear combination of atomic orbitals  $\phi_n$ :

$$\pi = \sum_n c_n \phi_n \quad 5.1.8.$$

If this is substituted in 5.1.7. and only the interaction due to the proton attached to carbon i considered, then:

$$\lambda_B = K \rho_i \int_{\tau} \frac{\sigma_A(1) \phi_i(2) \left| \frac{e^2}{r_{12}} \right| \phi_i(1) \sigma_B(2) d\tau}{W_B - W_0} \quad 5.1.9.$$

where  $\rho_i = c_i^2$ , the spin density at carbon i.

The first order interaction energy  $\Delta E$  is given by the expectation value of  $H$  (given by 1.5.1.):

$$\begin{aligned}\Delta E &= (\psi_0 | H | \psi_0) = 2 \lambda_B (\phi_0 | H | \phi_B) \\ &= \text{Const. } \lambda_B \sigma_B(0) \sigma_A(0)\end{aligned}\quad 5.1.10.$$

where  $\sigma_B(0)$ ,  $\sigma_A(0)$ , are the values of the functions at the position of the nucleus. This may be written in terms of the field splitting  $\Delta H$ :

$$\Delta H = Q \rho_i \quad 5.1.11.$$

where  $Q$  is a constant.

## 5.2 Spin Density in Aromatic Ions.

It has been estimated by Jarrett (1956) that the value of  $Q$  in equation 5.1.11. should be about 28gauss, and this has been found to be true for many hydrocarbons (see e.g. Ingram 1958, p.111). However, for some molecules a considerably larger value was required to fit experimental results, which led to a further examination of the problem. An analysis using valance-bond theory by Brovetto and Ferroni (1957) and McConnell and Chestnut (1957) showed the possibility of 'negative spin density'. This is caused by the effect of the unpaired spin density on the spins of the paired electrons in the filled orbitals. This may be regarded as a spin polarization effect or as a form of spin repulsion. The normal unpaired spin density (taken as positive) causes a partial antiparallel spin

polarization in the filled orbitals (which is therefore reckoned as negative). The positive density is also increased to keep the total density equal to 1. The total  $\Delta H$  splitting is independent of the sign of the spin density so that  $\Delta H = Q \sum |\rho_i|$ , in which the sum may now be larger than 1. Simple HMO theory cannot give negative densities, but it is found that the positions predicted to have zero spin density are the most likely to have negative densities, with values of about  $1/2$  to  $1/3$  of the adjacent positive density.

The theory so far has applied to negative ions, which are formed in alternant hydrocarbons by the addition of an electron. Since positive ion spectra differ only in total splitting, (being somewhat larger), from the negative ion spectra, it appears that the above theory should also hold for positive ions. In simple HMO theory for alternant hydrocarbons, the coefficients of the atomic orbitals in the highest occupied and lowest unoccupied molecular orbitals differ only in sign, and hence the same spin density will result from the removal of an electron from the highest molecular orbital (positive ion) as for the addition of an electron to the lowest unoccupied orbital (negative ion) (see e.g. McLachlan 1959).

The positive ions may also be considered from the point of view of the 'positive hole' left when an electron is removed which leads to the same conclusions (see e.g. McLachlan 1961). The equivalence of the orbital coefficients does not hold for non-alternant hydrocarbons, so that different spectra are to be expected. This has been demonstrated for acepleiadiene by de Boer and Weissman (1958).

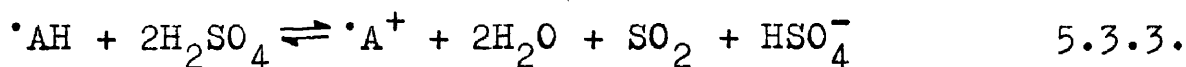
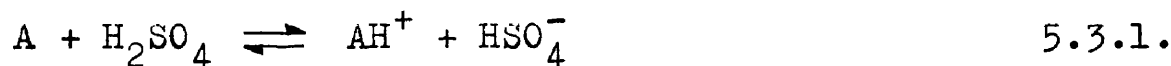
The total splitting for any molecule will be proportional only to that fraction of the total spin density at carbon positions to which protons are bonded. The fraction on the other carbons does not contribute and accounts for the smaller total splitting (i.e. less than 28gauss) found in some molecules containing such 'carbons'. Because of the possibility of negative density such a reduction is not always obtained.

The hyperfine pattern obtained for each group of  $N$  equivalent protons follows the normal binomial distribution for spin  $1/2$  particles i.e.  $N$  protons produce a pattern of  $N + 1$  lines with intensities proportional to the binomial coefficients  $N!/(N-n)!n!$  where  $n$  is the number of the line and runs from 0 to  $N$  (see Ingram 1958, p.22-28).

In the present work the resolution obtained in the ESR spectra has in general been insufficient for the purposes of the experiments. Negative ions have therefore not been used as the resolution for these is less than for the corresponding positive ions.

### 5.3 Positive Ions.

Positive ions of aromatic hydrocarbons may be formed by reaction with concentrated sulphuric acid. The reaction has been suggested by Carrington et al (1959) to be (A = Aromatic Hydrocarbon):



The first step involves the transfer of a proton, the second the transfer of an electron and the third, one of a number of possible reactions, the transfer of an H atom and an electron. The positive ions  $\cdot A^+$  in 5.3.2. and 5.3.3. are the paramagnetic ions although not indicated in the paper. Kon and Blois (1958) held that the solubility of different hydrocarbons in  $H_2SO_4$  could only be explained on the basis of their proton affinity or atom localisation energy. However Weijland (1958) shows that a better correlation exists between

solubility and oxidation potential as measured by Lund (1957). Electrochemical oxidation involves the loss of an electron from the highest occupied orbital to the anode to form a positive ion, and a good correlation has been found between the oxidation potentials and the energy coefficients of these orbitals for a number of molecules (Hoijtink 1958).

Positive ions may also be formed by reaction with other strong proton donors such as mixture of trifluoroacetic acid and  $\text{BF}_3 \cdot \text{H}_2\text{O}$  (Aalbersberg et al 1959a) and by reactions with strong Lewis acids such as antimony pentachloride (Aalbersberg et al 1959b).

Solutions of positive ions are in general intensely coloured and this may be used as a quick but not necessarily certain test. Molecules which form dipositive ions (non paramagnetic) also give coloured solutions but usually the colour is very much less intense. New sharp absorption bands responsible for the strong coloration are found in the optical spectra, although discrimination must be made against the new peaks due to the formation of proton complexes (Aalbersberg et al 1959b).

The lifetime of the positive ions is found to vary widely. For ions in sulphuric acid the times are



found to range from seconds to several months. The reasons for the decay are not known. We have found however, that the addition of water to the solutions produces a precipitate and the solutions become colourless. The precipitate is not paramagnetic. This may be a clue to one possible cause of the decay since water is one of the products of the reaction as shown in 5.3.3. On extraction with benzene from the diluted solution the original hydrocarbons can be recovered (Aalbersberg et al 1959a).

#### 5.4 Ions in Rigid Media.

Evans (1955), during his investigation of the paramagnetism of triplet states in rigid media, found that a solution of triphenylene in boric acid glass becomes blue on exposure to ultra-violet radiation and retained a residual paramagnetism on removal of the radiation. The colour and paramagnetism were found to disappear on heating. He suggested that the radiation ejected electrons from the triphenylene molecules to form positive ions, the electrons being trapped in the rigid glass. The disappearance of colour and paramagnetism on heating can then be explained by the diffusion of the electrons back to the ionized molecules. A similar effect has been found for 3,4 benzpyrene by Muel and Hubart-

Habart (1958). Bennema et al (1959) have demonstrated the equivalence of the ions formed in the boric acid glass and those obtained by the methods described in section 5.3, by comparison of the optical absorption spectra. They also mention that the glasses show electron spin resonance but do not give any results. It is unlikely that well resolved hyperfine spectra would be obtained since the non-isotropic interaction (section 5.1) will no longer be averaged out and the molecules will be randomly oriented. However, if aligned ions could be obtained this could provide a means of studying the non-isotropic interactions.

## PART VI. Results and Discussion.

### 6.1 Check Results.

In order to test the operation of the spectrometer, the preparation of specimens, resolution and sensitivity, the spectra of the positive ions of several molecules with known spectra were recorded. These were perylene (fig.6a-7), anthracene (fig.6a-1) and tetracene (fig.6a-3), which have been investigated by Carrington et al (1959). The spectra of perylene and tetracene are shown in figs.6b and 6c, and show that the resolution is not as good as that obtained in the published spectra. This is due to poor field homogeneity even though specimens of about 0.01ml were used.

Perylene is particularly useful as a reference as the lifetime of the positive ion is of the order of 6 months or more. In the perylene spectrum shown in fig.6b(i) the two outer groups are just visible. Fig.6b(ii) shows one of the outer groups (5 lines) at higher gain, and fig.6b(iii) shows the whole spectrum of a smaller sample at higher gain than (i), showing some further lines just resolved between the groups. The spectrum, which has 59 lines, agrees with the theoretical spectrum computed using the splitting values given by Carrington et al. The anthracene and tetracene also agree, although the resolution is relatively worse than for perylene.



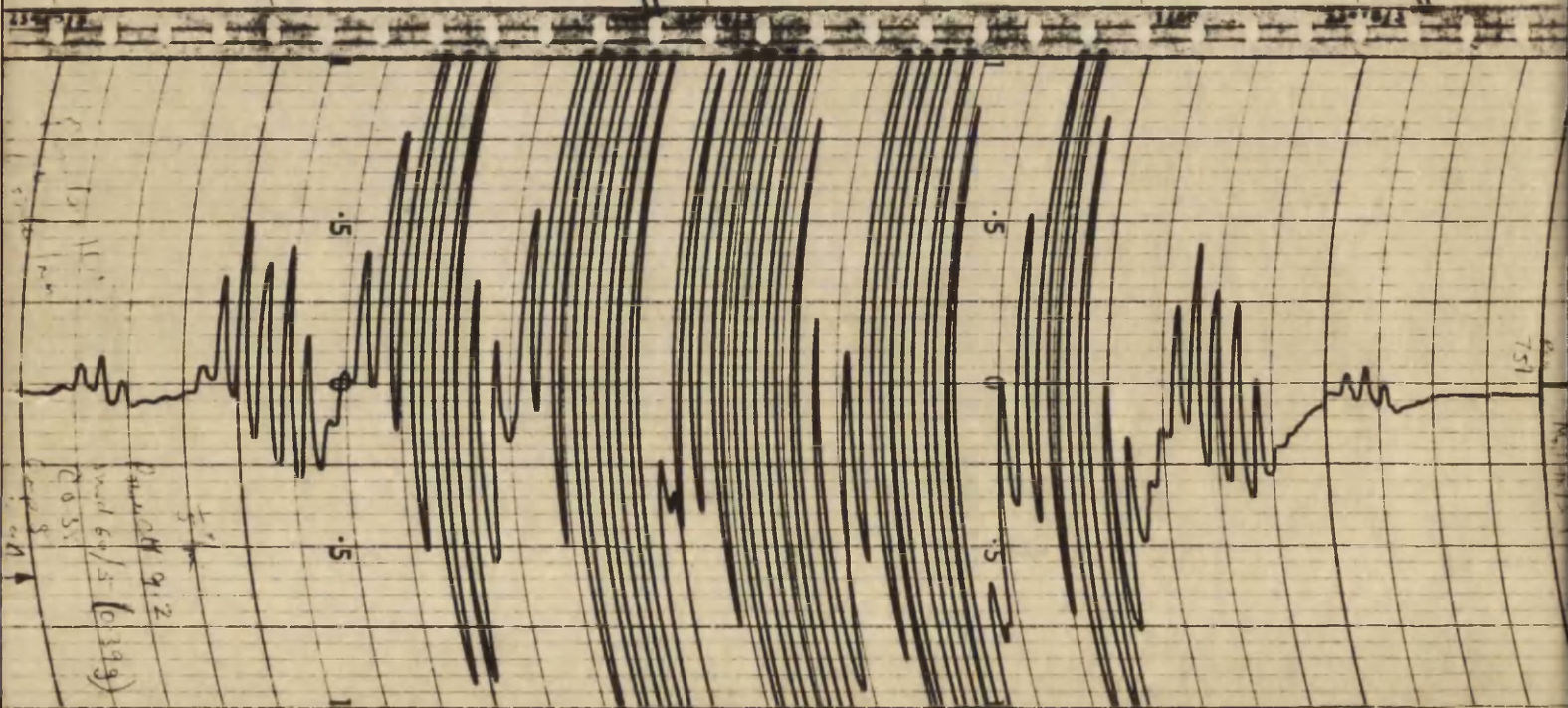


Figure 6b: ESR Spectra of Perylene.

(i) Field sweep: 140.5gauss/50min

Chart scale: 1" = 5.62gauss

Gain : 5

Bandwidth : 0.42c/s

Sample : Approx. 0.03ml at 0.02M

Source : Rutgerswerke

Colour : Purple

Lifetime : 6 months or more

(ii) Field sweep: 14.5gauss/50min

Chart scale: 1" = 1.45gauss

Modulation : 0.5gauss

Gain : 10

Sample : Approx. 0.03ml at 0.02M

Source : Rutgerswerke

(iii) Field sweep: 47.4gauss/50min

Chart scale: 1" = 4.74gauss

Modulation : 0.39gauss

Gain : 5

Bandwidth : 0.42c/s

Sample : Approx. 0.005ml at 0.02M

Source : ICI

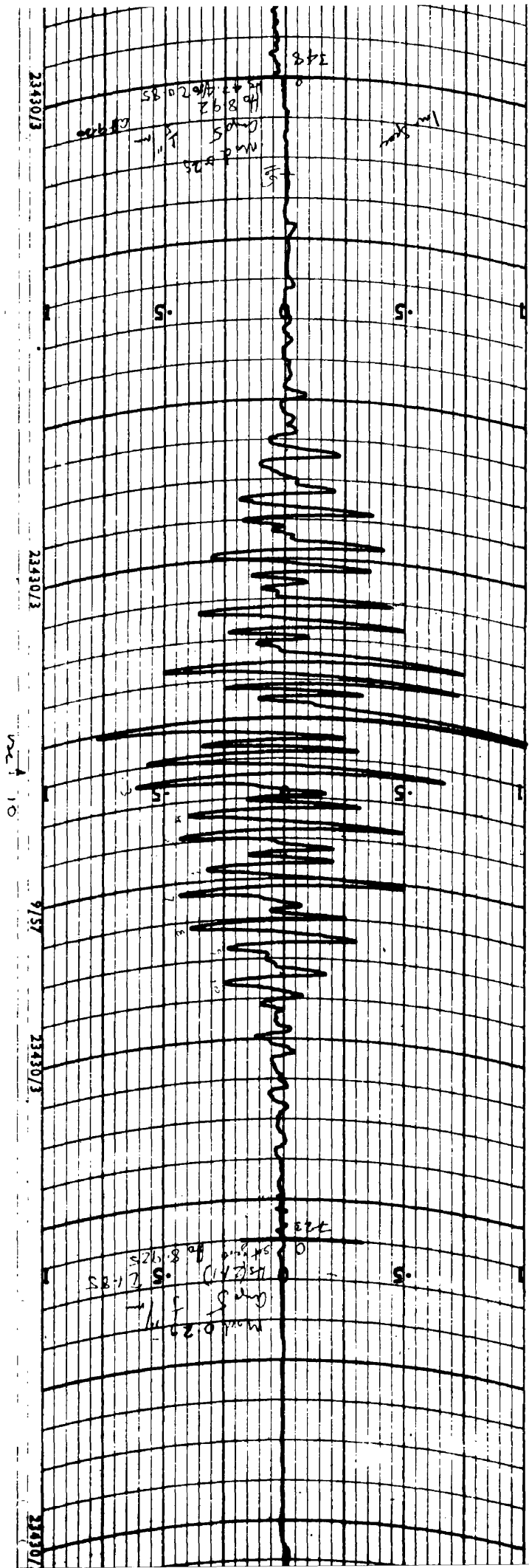




Figure 6c: ESR Spectrum of Tetracene.

Field sweep: 47.4gauss/50min

Chart scale: 1" = 4.74gauss

Modulation : 0.2gauss

Gain ; 5

Bandwidth : 0.17c/s

Sample : Approx. 0.005ml at 0.018M

Source : ICI

Colour : Deep green

Lifetime : Several weeks

Amplifier gain values quoted are arbitrary, but an increase of 1 represents a factor 2 of gain. Sweep times were typically 50mins... The only limit on increasing the sweep time was the field stability: the sweep rate is preferably rather higher than the field fluctuations, but runs of up to 2.5hr. have been made.

## 6.2 Compounds Studied: Preparation of Samples.

A large number of compounds have been tested for formation of positive ions in sulphuric acid. These are listed in three sections according to the results.

### (1) Form positive ions of reasonable lifetime:

Perylene	1,2 Benzpyrene	Coronene
Tetracene	3,4 Benzpyrene	1,12 Benzperylene
Anthracene	9,10 Diphenylanthracene	

### (2) Form positive ions of short lifetime:

Pyrene	1,2 Benzanthracene	Pentacene
--------	--------------------	-----------

### (3) Do not form positive ions:

Anthrone	Fluoranthene
Anthanthrene	Ferrocene
Acenaphthene	Naphthalene
Azulene	Picene
Acridone	Phenanthrene
Chrysene	Phthalocyanine
Carbazole	trans-Stilbene



9,9' Dianthryl	Triphenylene
Diphenylhexatriene	Tetrabenzonaphthalene
Tetraphenylbutadiene	p-Terphenyl
4,5 Methylenephenanthrene	

Two compounds, 1,2:5,6 and 1,2:7,8 dibenzanthracene appeared to form ions, judging from the colour of the solution, but gave very weak resonances. During a search among available compounds for larger condensed ring systems, a number of dyes similar to violanthrene were examined. Of these the following were found to be normally paramagnetic:

Indanthrene	Pyranthrone
Isoviolanthrone(Isodibenzanthrone)	

The positive ions were made up by adding Analar 98% sulphuric acid to weighed amounts of the hydrocarbon to give concentrations of about 0.1 to 0.2M, which had been found to be suitable by Carrington et al (1959). No attempt was made to deoxygenate the solutions as this had been variously reported to have no effect. The samples were contained in flattened glass tubes (1mm by 5mm) to obtain a good filling factor while keeping the lossy solution out of the electric field in the cavity.

### 6.3 Results: Coronene.

This molecule (fig.6a-9) is of interest as the

23430/3

23430/3

23430/3

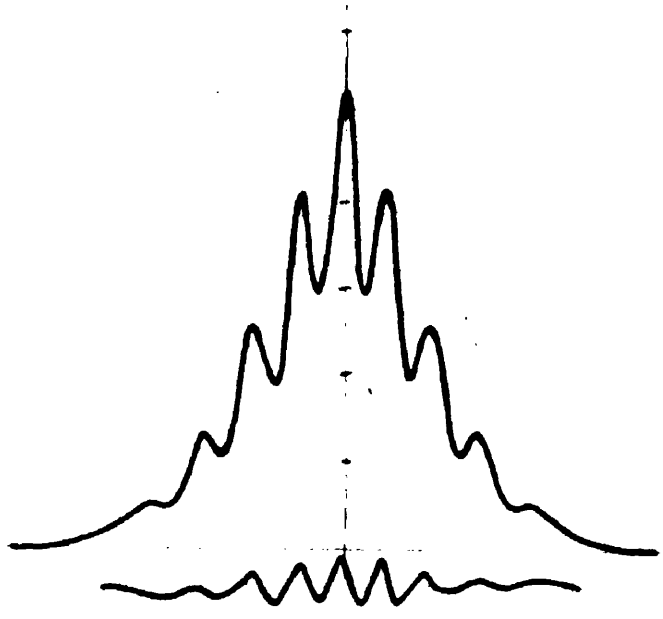
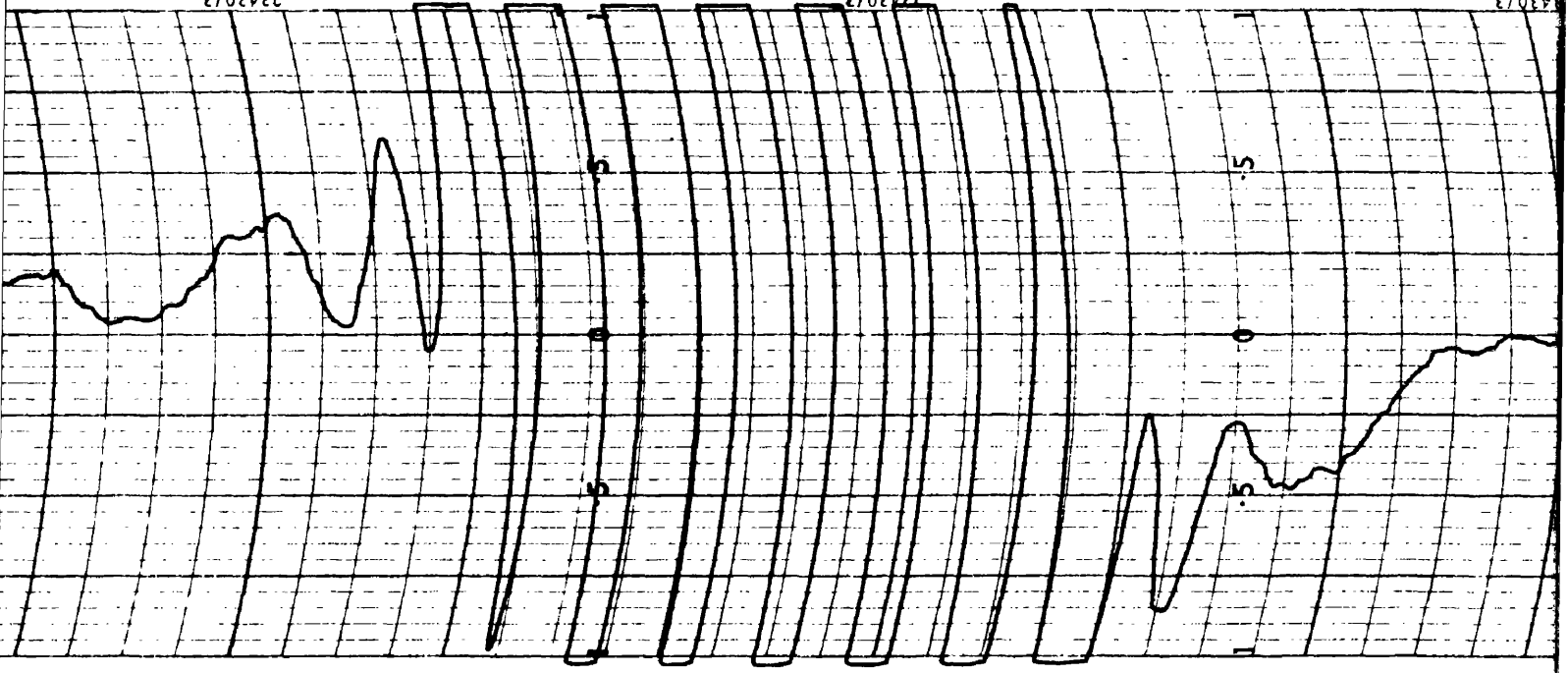


Figure 6d: ESR Spectrum of Coronene.

Field sweep: 33.3gauss/50min

Chart scale: 1" = 3.33gauss

Modulation : 0.7gauss

Gain : 8

Bandwidth : 0.02c/s

Sample : Approx. 0.01ml at 0.01M

Source : Rutgerswerke

Colour : Green

Lifetime : About 36hr

Oscilloscope presentation of ESR absorption and  
dispersion in coronene.

next completely symmetrical condensed ring molecule after benzene, all the twelve protons being equivalent. The spectrum of the negative ion has been recorded by Townsend and Weissman (1960), and the spectrum of the positive ion has recently been reported by Bolton and Carrington (1961), but both resolved only 11 of the 13 possible lines. The positive ion has therefore been further investigated to see if the missing lines could be detected. The solution formed in sulphuric acid is a strong green colour, and the ions have a lifetime of about 36hr. The spectrum obtained is shown in fig.6d. The large intensity ratio (12:1) between the outer and adjacent line, and the greater line width in coronene compared with other positive ions (Bolton and Carrington 1961), make the outer lines difficult to detect as they are largely lost in the skirts of the adjacent lines. The spectrum shows a small bump on the outside of the two outer recorded lines. These appear to be reproducible, but occur slightly closer to the centre of the spectrum than calculated for equally spaced lines. A shift of this sort is, however, expected for a small peak close to a much larger peak.

To indicate the resolution of the spectrometer a tracing of the resonance absorption of the positive ion,

with 50c/s field sweep, is shown in fig.6d(ii). The lower trace shows the dispersion signal obtained at the output of the signal-klystron-cavity-lock system (see section 3.1) with the loop gain somewhat reduced. The noise has been removed in tracing and is about 0.2mm on the same scale. There is also a small instrumental phase shift between the absorption and dispersion signal.

#### 6.4 Results: 1,12 Benzperylene.

1,12 Benzperylene (fig.6a-8) forms a dark green solution in sulphuric acid and the ions have a lifetime of several months. The results of the molecular orbital calculation for 1,12 benzperylene have been supplied by Streitwieser (1962). The coefficients  $C_i$  times  $10^3$ , spin densities  $C_i^2$  times  $10^3$  and splittings  $\Delta H$  for the highest filled level are shown in the table.

Position

	1	2	3	4	5	6	18	15	14	13	16
$C_i$	218	203	308	344	83	307	152	218	6	147	68
$C_i^2$	48	41	95	118	7	94	23	48	0	22	5
$\Delta H_c$	-	1.4	3.26	4.05	0.24	3.23	0.79	-	-	-	-
$\Delta H_e$	-	1.34	3.37	4.37	0.4	3.37	0.66	-	-	-	-

$\Delta H_c$  is the calculated splitting using a value of  $Q=34.4$



Figure 6e: ESR Spectrum of 1,12 Benzperylene.

Field sweep: 33.3gauss/50min

Chart scale: 1" = 3.33gauss

Modulation : 0.26gauss

Gain : 7

Bandwidth : 0.08c/s

Sample : Approx. 0.02ml at 0.02M

Source : Rutgerswerke

Colour : Dark green

Lifetime : Several weeks



in equation 5.1.11. This is an average value obtained from the known splittings of perylene, anthracene and tetracene (Carrington et al 1959).  $\Delta H_e$  are the experimental values derived by trial from the recorded spectrum. The reconstructed spectrum is shown with the derivative trace in fig.6e. As the recorded spectrum is just resolved, measurement of relative amplitudes is not possible. The calculated spectrum has therefore been worked out for position only and the smallest splitting has been omitted from the figure, as its value is uncertain. The agreement as to position is good, but the apparent amplitudes do not always agree for the reason given above, and because the direct addition of amplitudes of lines that do not exactly coincide contributes some error.

#### 6.5 Results: Pyrene, 1,2 Benzpyrene, 3,4 Benzpyrene.

These compounds formed strongly coloured solutions in sulphuric acid:

	Colour	Trace	Molecule fig.6a.
Pyrene	Dark Green	6h(i)	4
1,2 Benzpyrene	Dark Green	6f	6
3 ,4 Benzpyrene	Blood Red	6g	5

The lifetime of the pyrene ion was too short to be recorded, although a small signal without structure



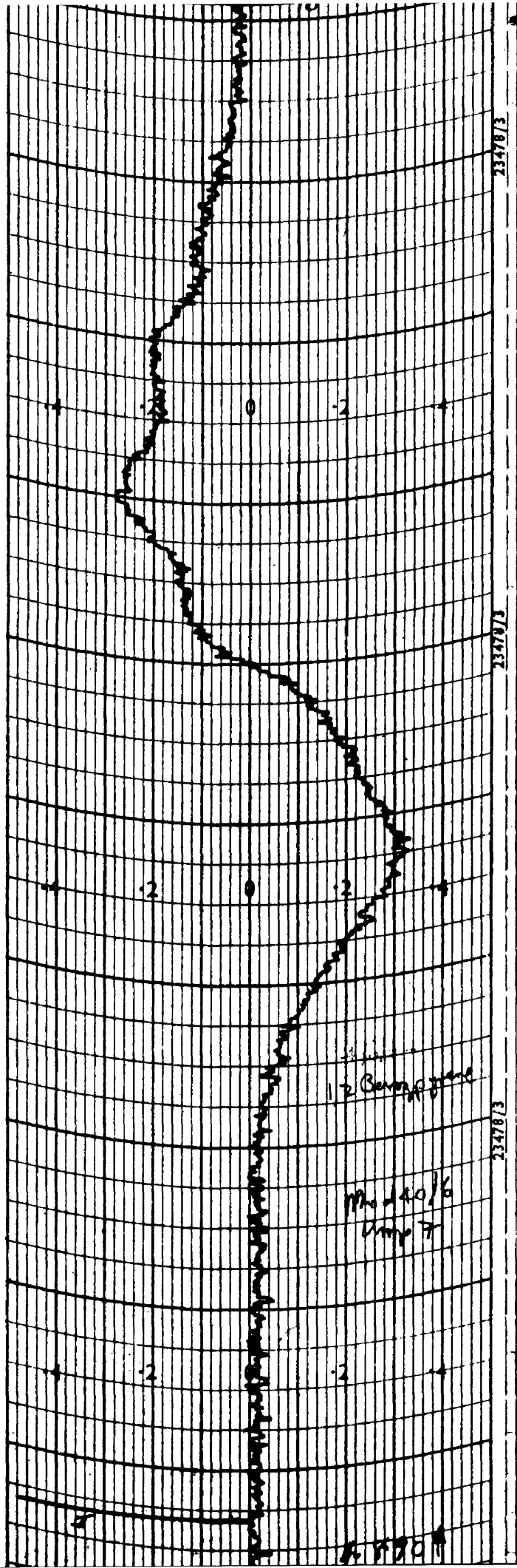


Figure 6f: ESR Spectrum of 1,2 Benzopyrene.

Field sweep: 33.3gauss/50min

Chart scale: 1" = 3.33gauss

Modulation : 1.6gauss

Gain ; 7

Bandwidth : 0.42c/s

Sample : Approx. 0.05ml at 0.01M

Source : Rutgerswerke

Colour : Dark green

Lifetime : Several months

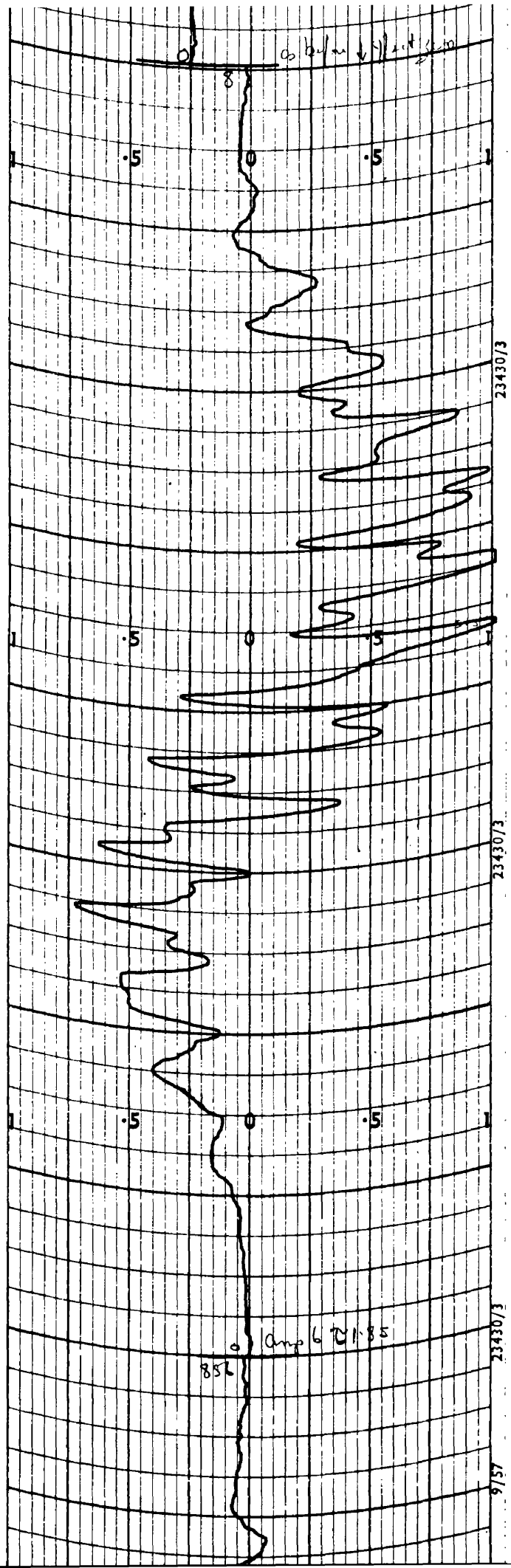


Figure 6g: ESR Spectrum of 3,4 Benzpyrene.

Field sweep: 47.4gauss/50min

Chart scale: 1" = 4.74gauss

Modulation : 0.5gauss

Gain : 6

Bandwidth : 0.08c/s

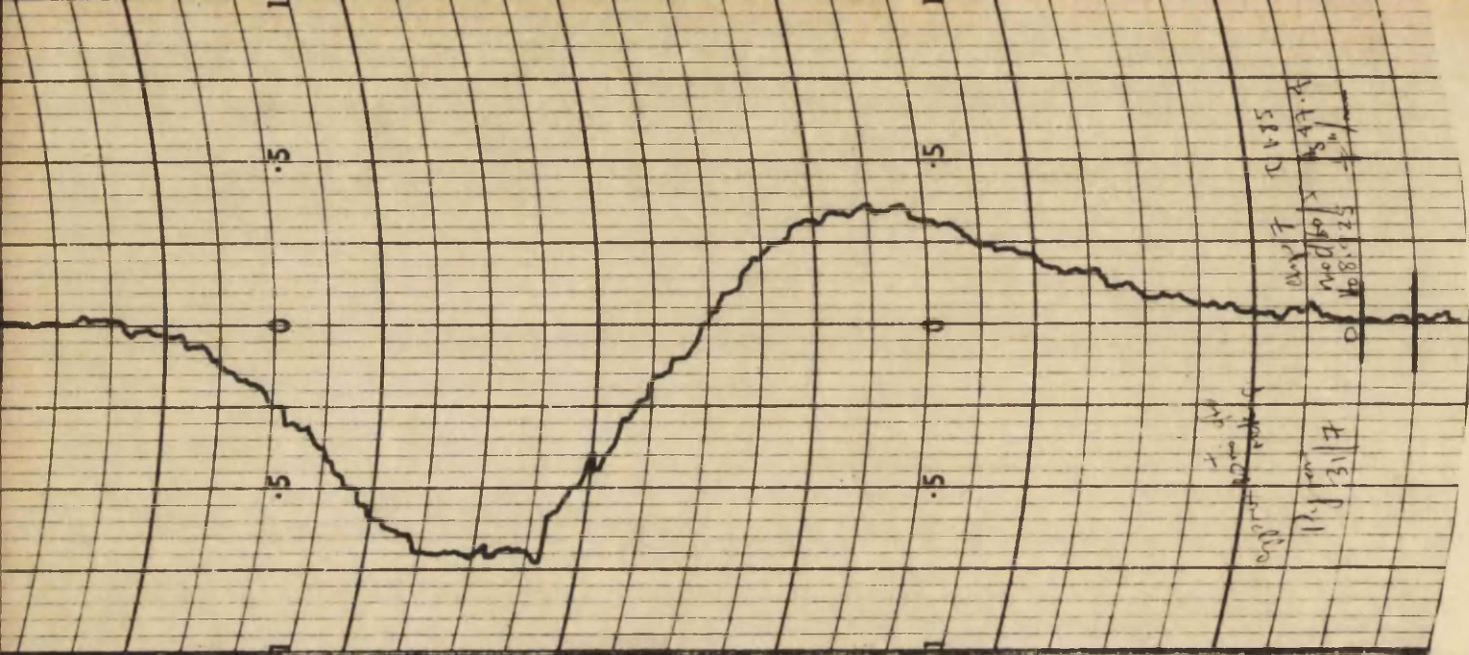
Sample : Approx. 0.025ml at 0.02M

Source : Rutgerswerke

Colour : Blood red

Lifetime : 12 to 24hr





11.1 31.7  
 10.8.25  
 10.47.4  
 10.4.5

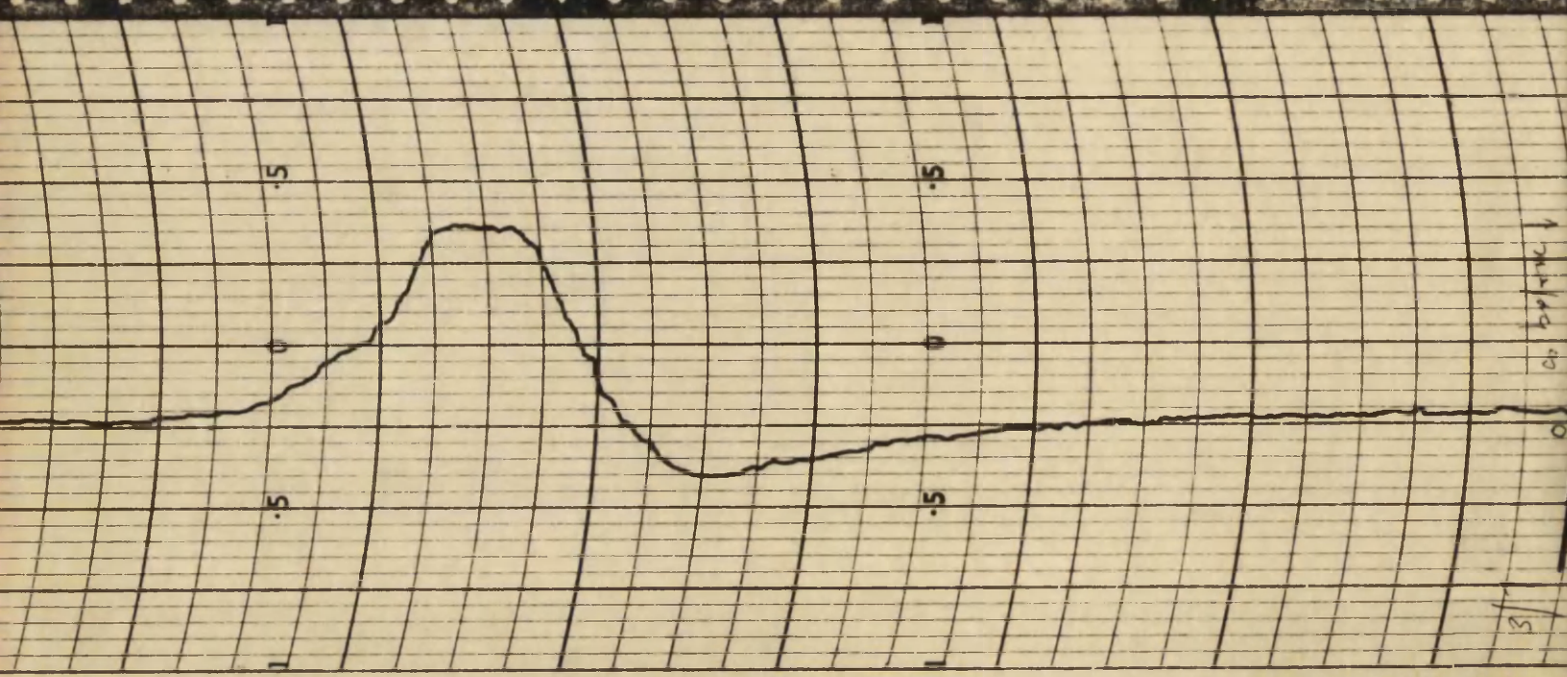
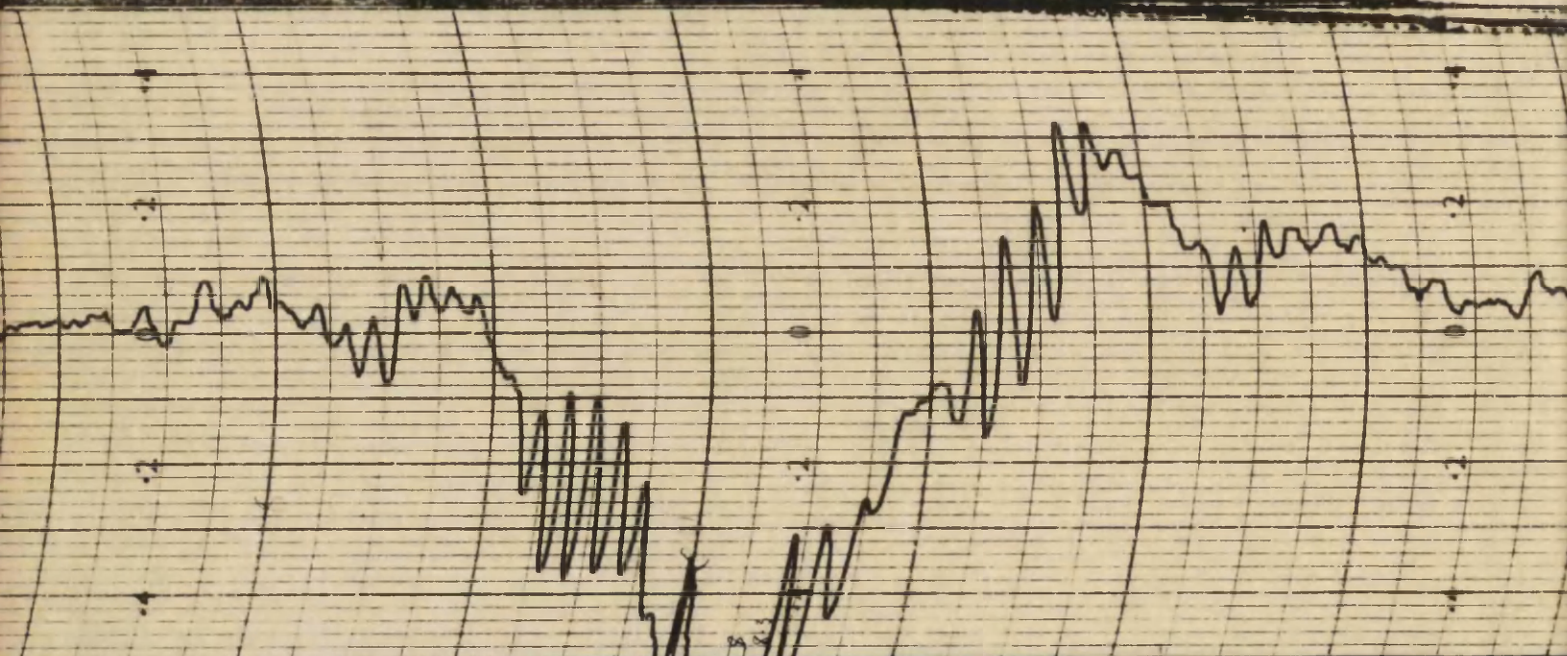


Figure 6h: Impurity Resonances.

(i) Perylene + Unknown in 3,4 Benzpyrene

Field sweep: 33.3gauss/50min

Chart scale: 1" = 3.33gauss

Modulation : 0.7gauss

Gain : 8

Bandwidth : 0.04c/s

(ii) Unknown in 3,4 Benzpyrene

As for fig.6g but 24hr later

(iii) Unknown in Pyrene

Field sweep: 47.4gauss/50min

Chart scale: 1"= 4.74gauss

Modulation : 0.39gauss

Gain : 7

Bandwidth : 0.08c/s

was recorded even after several days (fig.6h(i)). This is probably due to some impurity although well purified material was used. The impurity is evidently difficult to remove and may be the source of the weak signal detected by Kon and Blois (1958).

The resonance signal from 1,2 benzpyrene (fig.6f), shows some sign of structure, but was unexpectedly weak considering the strong colour of the solution. A possible explanation is that mainly dipositive ions are formed, which are not paramagnetic (van der Meij, 1958):

The spectrum of 3,4 benzpyrene (fig.6g) is strong, but due to the low resolution and lack of symmetry of the molecule, the spectrum is not well resolved. After 24hrs. a completely different spectrum was obtained as shown in fig.6h(ii). This was identified as the spectrum of perylene. Even with a purified specimen there was still a signal due to a further impurity (fig.6h(iii)). This trace was taken with the same specimen and under the same conditions as fig.6g and is responsible for the assymetry of this trace. No attempt to analyse the 3,4 benzpyrene spectrum has been made as previous cases of such poorly resolved spectra have given substantially wrong values. For example, in the case of the pyrene negative ion, de Boer and Weissman (1958) give the value of the largest



splitting as 5.8gauss, which led McLachlan (1960) to an incorrect interpretation of the spectrum. The latest value, as obtained by Hoijtink et al (1961) from a completely resolved spectrum, is 4.75gauss.

#### 6.6 Non-Planar Molecules: 9,10 Diphenylanthracene.

This compound (fig.6a.10) is of particular interest because of the possible affect of the non-planarity of the molecule on its properties. It has a very high fluorescence quantum yield in solution and does not form photo-dimers (Bowen and Tanner, 1955). Jones (1947) has found that the optical absorption spectrum of 9,10 diphenylanthracene is almost identical with that of anthracene. He suggested that the two phenyl groups were twisted out of the plane of the anthracene nucleus due to steric interaction between the pairs of hydrogen atoms at the 4-16 and equivalent positions (see fig.6a-10), and from models obtained a minimum angle of twist of  $57^{\circ}$  (Jones, 1945). The interaction of the  $\pi$  electrons on the anthracene and phenyl parts would then be much reduced, so that the absorption spectrum would be primarily due to anthracene as the phenyl groups, now acting independently, absorb at much shorter wavelengths. (9,10 Diphenylanthracene will be abbreviated to 9,10 DPA).



The similarity of spectra would also be expected to hold for the fluorescence spectra, but when they were examined they were found to be different (Cherkasov, 1959). It was suggested that the difference in this case could be due to increased planarity of the 9,10 DPA molecule in the excited state (from which the fluorescence originates) as compared with the molecule in the ground state (from which the absorption originates). Coulson (1958) has discussed the shift of energy levels with variation of the angle of twist, but it appears to be difficult to predict effects with any certainty.

There is no published data on any direct measurement of the shape of the 9,10 DPA molecule, but there are a number of other molecules in which similar twisting effects occur, and for which measurements have been made. The simplest case is that of diphenyl. The steric hindrance is less in this molecule, so that this should give a lower limit for the angle of twist  $\theta$ . The first investigation of this molecule, by X-ray diffraction, was carried out by Dhar (1932, 1949), who found that the molecule was flat! This result is contradicted by the results of Bastiansen (1949), following the work of Karle and Brockway (1944), who studied the electron diffraction of diphenyl vapour, and

concluded that the angle between the planes of the two phenyl rings was about  $45^{\circ}$ . Bastiansen suggested that this represented the normal configuration of the molecule and that in a crystal, as used for the X-ray work, crystalline forces made the molecule planar. This would mean that only electron diffraction results will be applicable when dealing with molecules in the vapour, and presumably in solution (the case of rigid glasses is still open and requires further experiment). However, Lonsdale (1937) by using X-ray and diamagnetic anisotropy data, has found that even in the crystal the phenyls of 1,3,5 triphenylbenzene are twisted relative to the benzene nucleus by about  $25^{\circ}$  and in 1,2 diphenylbenzene by about  $50^{\circ}$  (Clews and Lonsdale, 1937). Almenningen et al (1958), using electron diffraction, have found  $\theta = 90^{\circ}$  for hexaphenylbenzene in the vapour state. Thus the complete range of  $\theta$  is possible.

A further means of investigating the planarity of molecules is the study of the optical absorption spectra. Following earlier work by Pickett et al (1936) and Merkel and Wiegand (1948), Suzuki (1959) has made a detailed study of the effects of non-planarity on the absorption spectrum, and obtains angles of twist with about the same accuracy as for the electron diffraction work. This is a more

involved technique and a number of corrections are necessary, but the results for vapours agree with the electron diffraction data. The most important conclusion however, is that the angle of twist is different in the vapour and in solution. As the X-ray and electron diffraction techniques are applicable to crystals and vapours respectively, the absorption spectrum method is the only one applicable to solutions.

As the  $\pi$  electron distribution depends on the planarity of a molecule, the overlap integral for a twisted bond varying as  $\cos\theta$ , it appeared that an investigation of the ESR spectrum from the ion of 9,10 DPA would be an alternative means of investigating the amount of twist. Cherkasov's suggestion concerning the increased planarity of the molecule in the excited state somewhat complicates the matter. The positive ion represents the molecule in a rather higher excited state, but the difference should not be great. In alternant hydrocarbons the ESR spectra of positive and negative ions are effectively the same. In the case of 9,10 DPA it would be expected that in the two ions any change in  $\theta$  would be in opposite directions. It would be of interest to examine the ESR spectra of both ions to check this: if the change in  $\theta$  is not small, this could provide

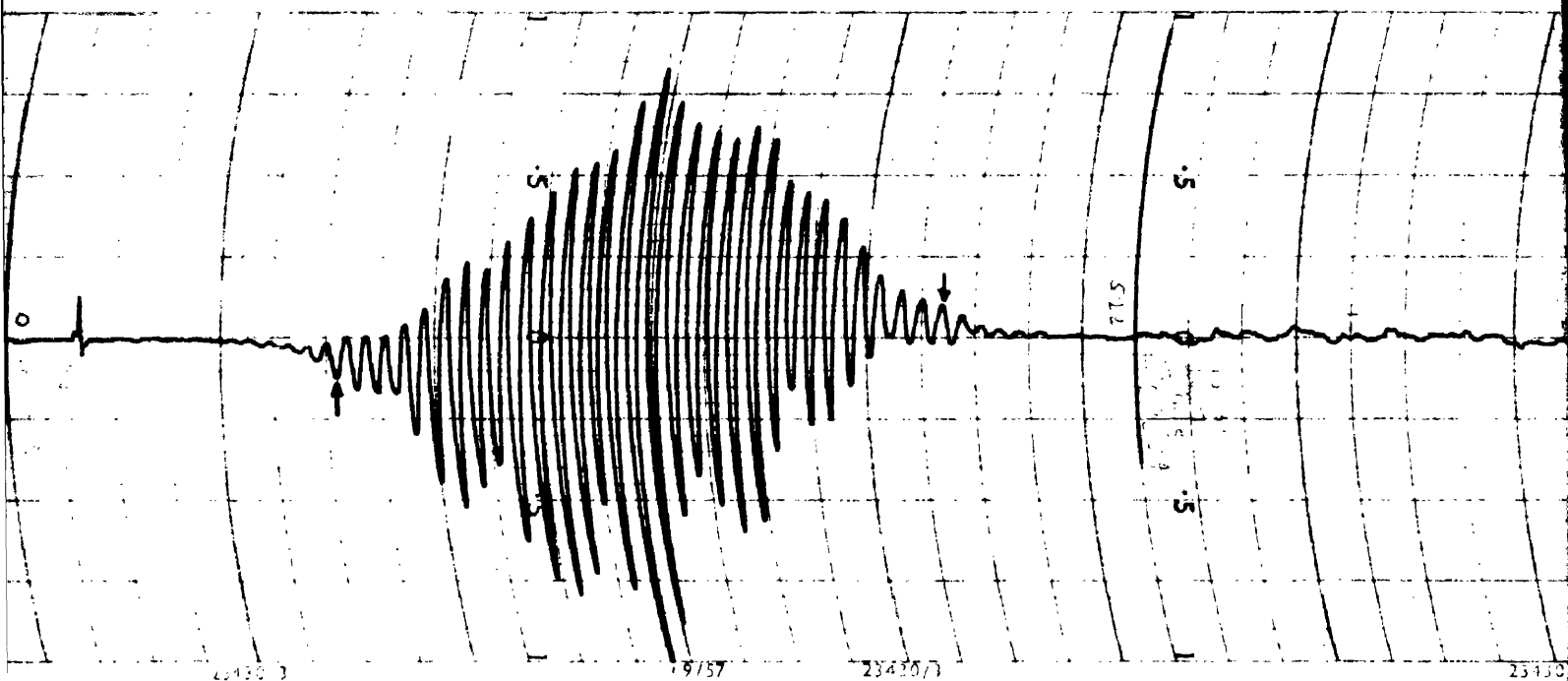


Figure 6i: ESR Spectrum of 9,10 Diphenylanthracene.

Field sweep: 47.4gauss/50min

Chart scale: 1" = 4.74gauss

Modulation : 0.25gauss

Gain : 5

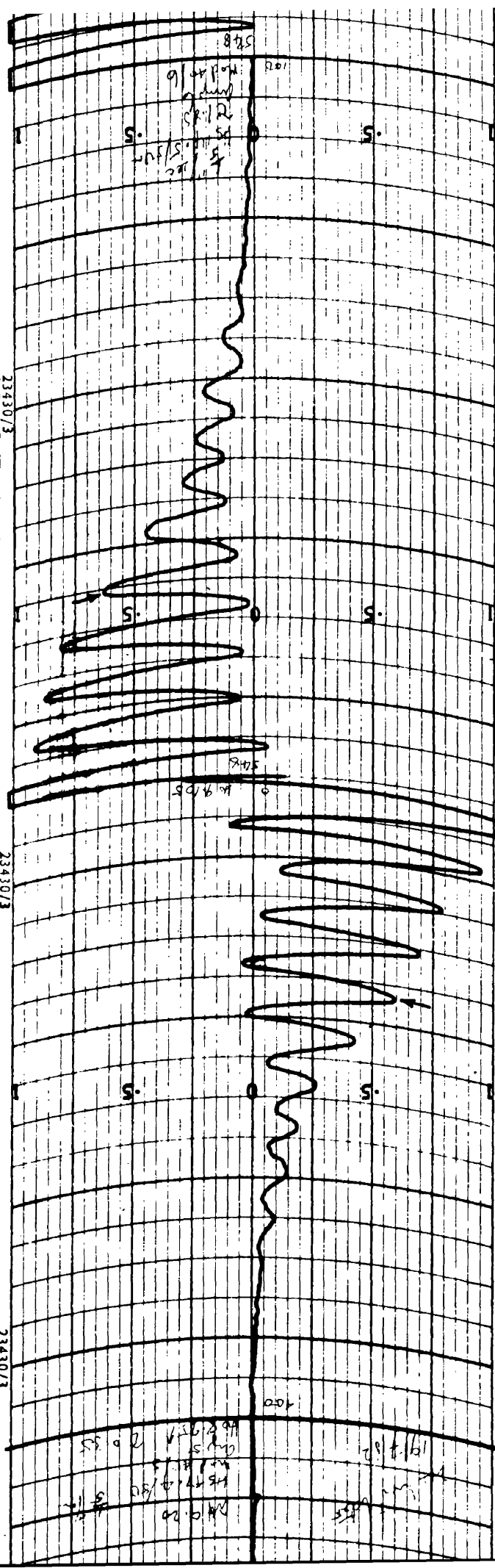
Bandwidth : 0.4c/s

Sample : Approx. 0.02ml at 0.01M

Source : Nuclear Enterprises

Colour : Blue

Lifetime : 24 to 36hr



23430/3

23430/3

23430/3

Figure 6j: ESR Spectrum of 9,10 Diphenylanthracene;

Ends of Spectrum.

Field sweep: 14.5gauss/50min

Chart scale: 1" = 1.45gauss

Modulation : 0.5gauss

Gain : 7

Bandwidth : 0.08c/s

Sample : Approx. 0.025ml at 0.01M

Source : Nuclear Enterprises

Colour : Blue

Corresponding peaks in this spectrum and fig.6i  
shown thus: ↓

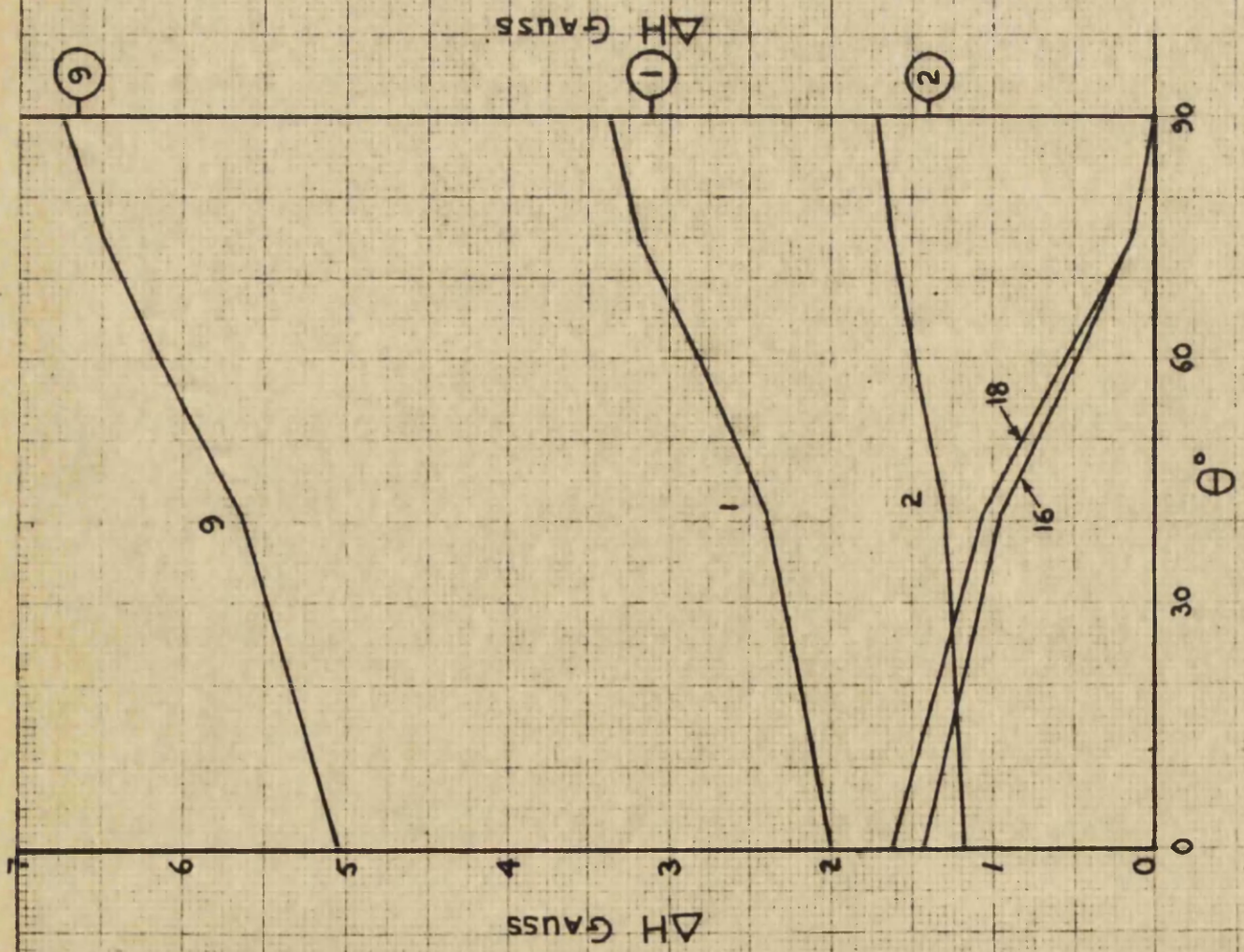
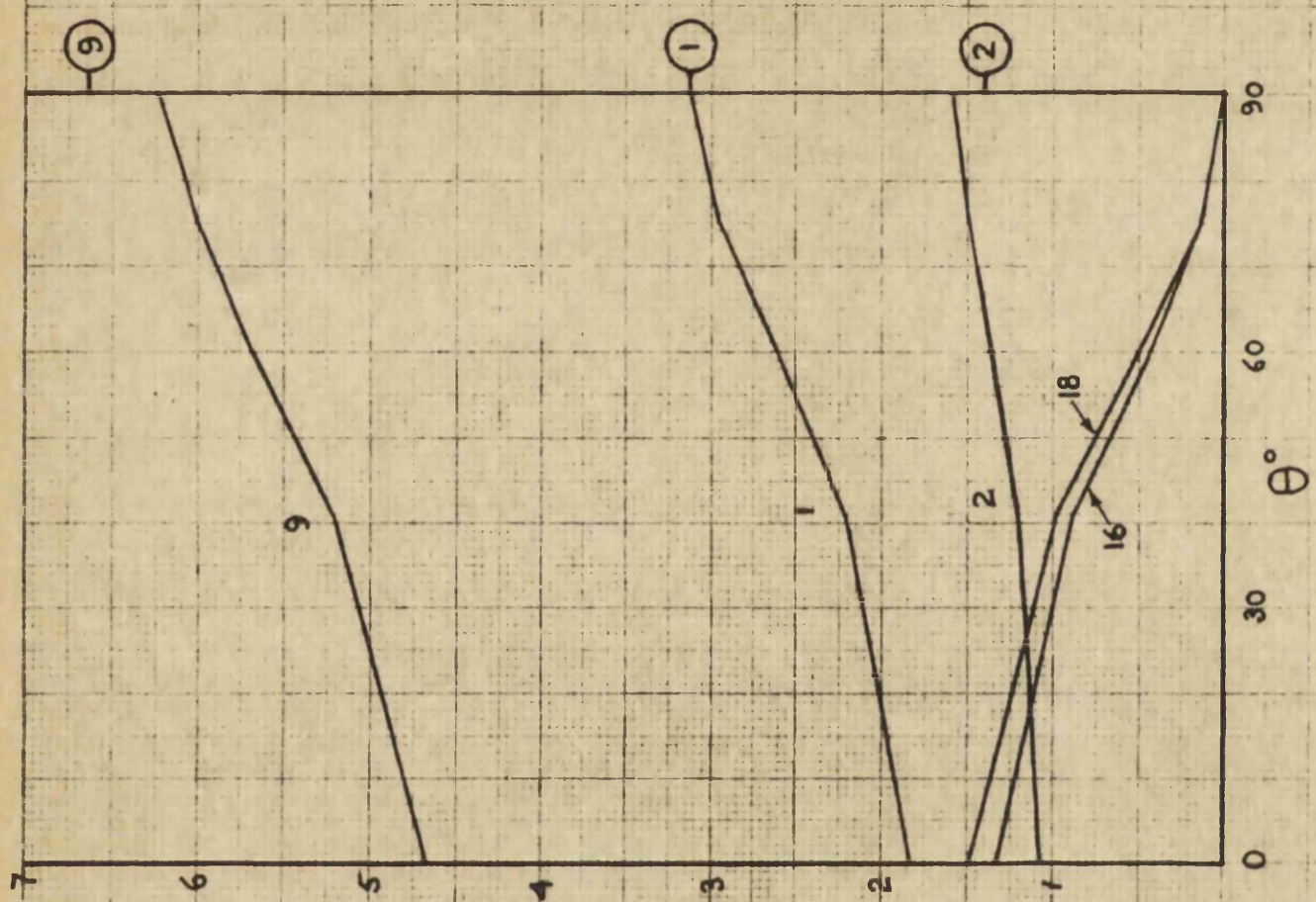




Table 6.5.1: HMO Electron Densities for 9,10 DPA.

Position	1	2	9	11	15	16	17	18
$\theta=0^\circ$ $C_i$	2410	1839	3838	1089	983	2072	339	2177
$C_i^2$	58	34	147	12	10	42	1	47
$\theta=41^\circ$ $C_i$	2645	1962	4048	1040	893	1673	310	1782
$C_i^2$	70	38	164	11	8	28	1	31
$\theta=60^\circ$ $C_i$	2871	2078	4227	982	699	1190	245	1284
$C_i^2$	82	43	179	10	5	14	0	16
$\theta=75^\circ$ $C_i$	3043	2165	4352	931	390	623	138	679
$C_i^2$	93	47	189	8	1	4	0	4
$\theta=90^\circ$ $C_i^2$	98	50	196	4	-	-	-	-
$\Delta H_{\text{exp}}$	3.11	1.40	6.65	0	-	-	-	-

$C_i$  is the computed orbital coefficient times  $10^4$

$C_i^2$  is the computed electron density times  $10^3$

$\theta=90^\circ$  gives the values for anthracene

$\Delta H_{\text{exp}}$  gives the experimental splittings for anthracene

Figure 6k: Variation of  $\Delta H$  with  $\theta$ .

Top:  $Q = 31.8$

Bottom:  $Q = 34.4$

a case of different spectra for an alternant molecule. In any case, if the result turns out to be that the ion is still highly twisted, then it seems unlikely that a molecule excited to the first excited state would be much more planar. It was found later that a similar attempt to determine  $\theta$  for diphenyl had been made by McLachlan (1960), but the best fit of theoretical to experimental spectrum was found for  $\theta = 0^\circ$ . This may be due to nearly free rotation of the phenyls about the central bond as suggested by Adrian (1958). A similar experiment by Reitz (1961) has shown that in the free radical pentaphenylcyclopentadienyl the phenyls are twisted by about  $30^\circ$  relative to the cyclopentadienyl nucleus.

No molecular orbital calculations were available for 9,10 DPA. The calculation for a planar configuration was therefore carried out and further calculation for several values of  $\theta$  were kindly carried out by Dr. H.O. Pritchard on the Manchester University Mercury computer. The results are shown in table 6.5.1., which includes the values for anthracene, to which the 9,10 DPA values converge as  $\theta$  goes to  $90^\circ$ . The resulting splitting values  $\Delta H$  are shown in fig.6k for two values of  $Q$ . The value  $Q = 34.4$  is the average value used previously and

$Q = 31.8$  is the average for the known experimental splittings of anthracene (Carrington et al 1959) which are indicated on the right hand axes.

The solution of 9,10 DPA in sulphuric acid is a strong blue colour and the ions have a lifetime of about two days. The ESR spectrum obtained is shown in fig.6i, and the two ends at higher gain in fig.6j. There are 43 lines with equal splitting between lines of 0.43gauss and overall width 18.1gauss. The two groups of four equivalent protons on the anthracene nucleus can give rise to only 25 lines, so it is evident that the phenyl protons must be involved. Even omitting any possible splitting at the 17 position (i.e. from any possible negative density), a maximum of 225 is possible, so that there is considerable overlapping in the recorded spectrum. From the equal splitting between the lines it would appear that, to the accuracy imposed by the resolution, the various splittings have integral ratios.

The total splitting density (638 to 585 for  $\theta = 0^\circ$  to  $\theta = 75^\circ$ ) gives an overall spectrum of about 22 to 18.6 gauss for  $Q = 34.4$  to 31.8. Comparing this with the measured width of 18.1 gauss, it is evident that the splitting due to position 17 must be very small even



EXPT.

$\theta = 0^\circ$

$\theta = 20^\circ$

$\theta = 45^\circ$

$\theta = 60^\circ$





Figure 6m: Calculated Spectra for 9,10 DPA for Q=34.4.

- (i) Experimental spectrum. Amplitude of lines  
proportional to derivative and interval = 0.43gauss.  
Spectrum has 43 lines and half-width = 9.03gauss.

- (ii) Spectrum for  $\theta = 0^\circ$ :

Position	1	16/18	2
Splitting	2.15	1.72	1.29
Multiplicity	5	7	5
Spectrum half-width = 12.04			

- (iii) Spectrum for  $\theta = 20^\circ$ :

Position	1	2	16/18
Splitting	2.15	1.29	1.29
Multiplicity	5	5	7
Spectrum half-width = 10.75			

- (iv) Spectrum for  $\theta = 45^\circ$ :

Position	1	2	16/18
Splitting	2.58	1.29	0.86
Multiplicity	5	5	7
Spectrum half-width = 10.32			

- (v) Spectrum for  $\theta = 60^\circ$ :

Position	1	2	16/18
Splitting	2.58	1.29	0.43
Multiplicity	5	5	7
Spectrum half-width = 9.03			

Outer ends of spectra shown times 20.

EXPT.

$\theta = 0^\circ$

$\theta = 20^\circ$

$\theta = 45^\circ$

$\theta = 60^\circ$





Figure 6n: Calculated Spectra for 9,10 DPA for Q=31.8.

(i) Experimental spectrum. Amplitude of lines  
proportional to derivative and interval = 0.43gauss.  
Spectrum has 43 lines and half-width = 9.03gauss.

(ii) Spectrum for  $\theta = 0^\circ$ :

Position	1	16/18	2
Splitting	1.72	1.29	0.86
Multiplicity	5	7	5

Spectrum half-width = 9.03

(iii) Spectrum for  $\theta = 20^\circ$ :

Position	1	2	16/18
Splitting	2.15	1.29	1.29
Multiplicity	5	5	7

Spectrum half-width = 10.75

(iv) Spectrum for  $\theta = 45^\circ$ :

Position	1	2	16/18
Splitting	2.15	1.29	0.86
Multiplicity	5	5	7

Spectrum half-width = 9.46

(v) Spectrum for  $\theta = 60^\circ$ :

Position	1	2	16/18
Splitting	2.58	1.29	0.43
Multiplicity	5	5	7

Spectrum half-width = 9.03

Outer ends of spectra shown times 20.

if it is negative, and it has been assumed to be negligible in all the computed spectra. The computed spectra shown in fig.6m and 6n are based on integral multiples of a basic splitting of 0.43gauss using the nearest values of  $\Delta H$  from fig.6k, and taking the splittings of positions 16 and 18 to be equal. In the experimental spectrum shown in fig.6m and 6n the amplitude of the lines is proportional to the derivative line amplitude of fig.6i. However, because of the incomplete resolution, too great a significance should not be placed on these amplitudes. Because of this and the lack of any further features in the spectrum, there is some difficulty in fitting the theoretical to the experimental spectrum.

From the trace shown in fig.6j it appears unlikely that any lines have not been recorded that may have been expected from any of the theoretical spectra. It is therefore considered that agreement of overall length and lack of missing lines are the main criteria on which to judge the correspondence of the spectra. On this basis only the spectrum for  $\theta = 60^\circ$  (it is the same for both values of  $Q$ ) agrees with the experimental spectrum. Values of  $\theta$  greater than  $60^\circ$  have not been considered as a minimum value of about 0.4gauss is required for the 16/18 position splitting to give anything like the observed spectrum.



The results give an angle of twist about equal to that suggested by Jones (1947), so that if there is to be any significant flattening of the molecule in the excited state it must be twisted by more than  $60^\circ$  in the ground state. It may be noted here that some of the work on which Cherkasov's suggestion was based (due to Braude and others: see Cherkasov (1959) for references), has been criticised by Suzuki (1959). It is difficult to determine the change in  $\theta$  required to produce the spectral shifts, but on the basis of Suzuki's calculations a change of about  $10^\circ$  (for  $\theta$  around 60 to  $70^\circ$ ) would be required for the shift of about  $1400\text{cm}^{-1}$  between anthracene and 9,10 DPA.

There is a further factor, suggested by Cherkasov's results, which may influence the spectra. He has shown that when cooled to liquid air temperatures the fluorescence spectrum of 9,10 DPA in the rigid solvent glass is very similar to that of anthracene. He claims that this is not due to the effect of the rigid glass, as this effect is not found for a solution in polystyrene at room temperature. It has been shown by Almenningen et al (1958) that in the considerably more hindered hexaphenylbenzene ( $\theta = 90^\circ$ ), the phenyls oscillate by about  $\pm 10^\circ$  around the single bond. For 9,10 DPA it may

be assumed that the phenyls could oscillate by at least this much. At low temperatures this oscillation will be reduced due to the rigid glass as well as the lower temperature. The results for the solution in polystyrene are not convincing because of lack of knowledge of the 'local' rigidity of the polymer (see e.g. Basile, 1962): it is safer to go to low temperatures. Thus the coupling between the phenyl and anthracene  $\pi$  electron systems will be modulated, and this can affect the spectrum. This would agree with the ideas of Kortüm and Dreesen (1951), who suggest that fine structures(i.e. vibrational structure) depends on the rigidity of the molecule. The difference in vibrational structure could then be due to a greater interaction between the excited state and the oscillation than between ground state and oscillation, since the excited state wave function will be expanded compared with the ground state.

It has been suggested by Jones (1947) that rubicene (fig.6a-11) may provide an intermediate case, similar to 9,10 DPA but more planar due to the extra bonding. This molecule was tried, as was rubrene (or tetraphenyltetracene, fig.6a-12) and 9,9' dianthryl (fig.6a-13), both very similar cases to 9,10 DPA, but

unfortunately none formed positive ions in sulphuric acid.

On the basis of the large angle of twist in 9,10 DPA, the absence of photo-dimers can now be explained by a steric effect, in which the twisted phenyl groups prevent molecules approaching close enough to form dimers (in anthracene the dimers form by bonding at the 9 and 10 positions). The reduction of quantum yield in solutions in general is probably due to collisions with solvent molecules. In 9,10 DPA the action of the phenyl groups could be to act as a buffer against collisions, and, because their  $\pi$  electron systems are only weakly coupled to that of the anthracene nucleus, reduce the effect of the collisions and maintain the high quantum yield. If these suggestions concerning dimer formation and quantum yield have any validity, they should also hold for rubrene and tetracene. In fact rubrene does not form dimers (Bowen and Tanner, 1939) whereas tetracene probably does. The quantum yield of rubrene (in benzene) is 1.0 and for tetracene (in m-xylene) is 0.06 (Bowen and Williams, 1939). Thus the ideas appear to have some basis, but further cases will have to be investigated.

There are few conclusions that can be drawn

with certainty, but a number of further experiments have been suggested which should resolve some of the uncertainties. The ESR spectrum of 9,10 DPA will have to be investigated at rather higher resolution before definite assignments can be made and so give a more reliable value for  $\theta$ . A study of such properties as structure (by X-ray or electron diffraction), absorption and fluorescence spectra and quantum yield, in the crystalline and vapour state would give useful information for comparison with the solution results and for checking many of the previous suggestions. It may also be necessary to consider more sophisticated types of molecular orbital calculation (see e.g. McLachlan, 1960), particularly to check the spin density at the 17 position.

#### 6.7 Rigid Glasses.

As a possible means of investigating the positive ions of some of the compounds that do not form these ions in sulphuric acid, an attempt has been made to detect the ESR signal from molecules in boric acid glass after irradiation with ultra-violet light. The glass was made up according to the directions of Kasha (1948) and irradiated with light from a small mercury arc. With triphenylene (fig.6a-14) the glass acquired a permanent blue colour as found by Evans (1955), and a

good ESR signal was obtained, but no fine structure was detected. The resonance is shown in fig.6p. As discussed in section 5.4, the lack of fine structure is probably due to the random orientation of the molecules in the glass, so that the dipole-dipole interaction is in random directions.

There appears to be a method of obtaining aligned molecules without the use of a solid crystal solution (McClure, 1954, Huthison and Mangum, 1961). It has been found by Lewis and Bigeleisen (1943)(see also Albrecht and Simpson, 1955), that irradiation of molecules in a glass with polarized light ionises those molecules aligned in a particular direction referred to the plane of polarization. The alignment can be demonstrated by measurement of the absorption spectrum using polarized light, and the polarization of transitions have been measured using this technique (Hoijsink and Zandstra, 1960).

The resonance from triphenylene in boric acid glass irradiated with polarized ultra-violet light has been measured, but no difference in line width or shape was found. This does not necessarily invalidate the idea, as the means used to polarize the light was not very satisfactory. The only means available was polarization

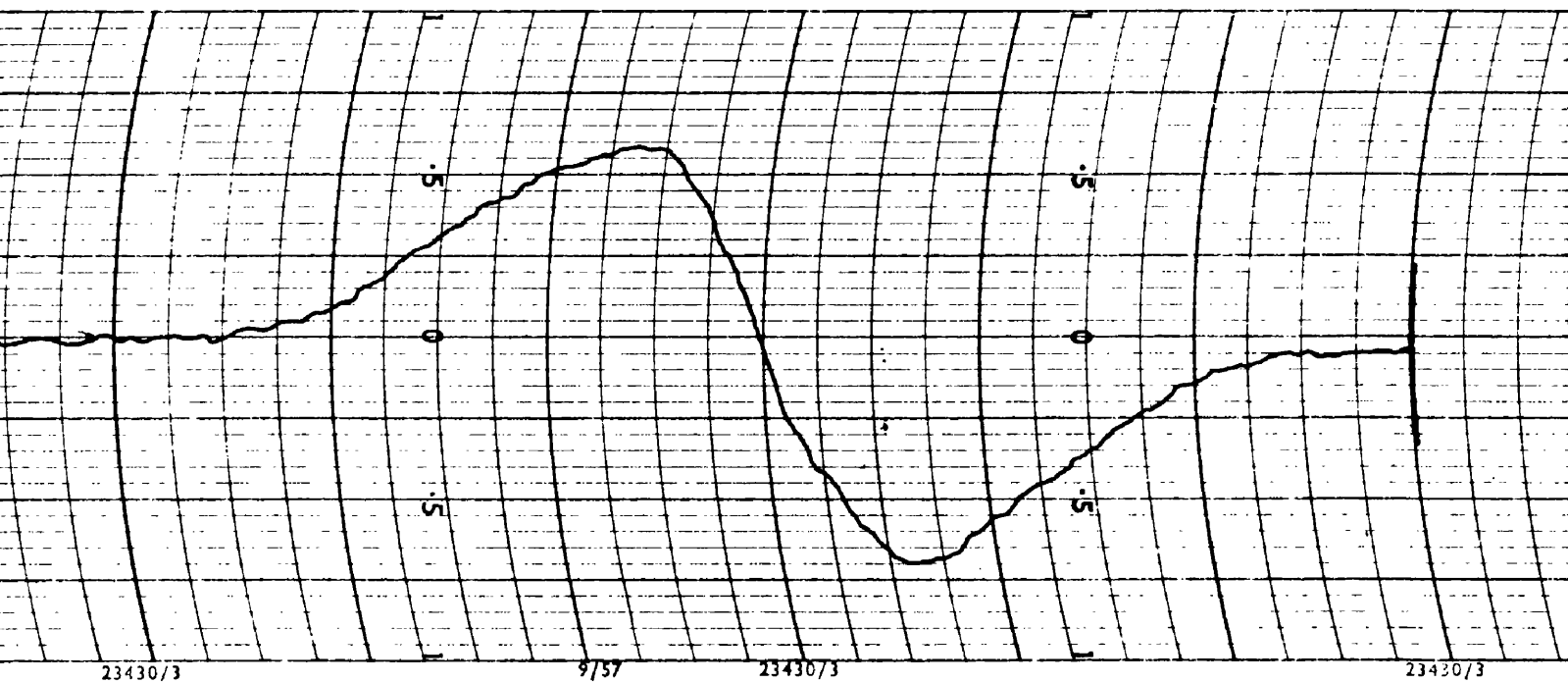


Figure 6p: ESR Spectrum of Triphenylene in  
Boric Acid Glass.

Field sweep: 47.4gauss/50min

Chart scale: 1" = 4.74gauss

Modulation : 0.5gauss

Gain : 7

Bandwidth : 0.04c/s

Sample :  $5 \times 10^{15}$  spins if all molecules ionised.

Colour : Blue

Source : L.Light & Co.

by reflection from a quartz plate, but since the refractive index of quartz varies rapidly in the ultra-violet region the light was only partly polarized. Also, since the reflected intensity was small, very long irradiation times were required. The use of a monochromator reduced the intensity so much that no visible colouring was produced in the glass after several days irradiation. More suitable ultra-violet polarizers, such as those described by McDermott and Novick (1961), will be required to make a satisfactory test.

Ionization potentials are of importance in theories of photoconductivity, photo-oxidation, fluorescence quenching and other phenomena. An interesting point brought out by the ionization of molecules in a glass is the considerably lower ionization potential than in the gas phase (see e.g. Hoyland and Goodman, 1962, Smith, 1961). The difference is due to polarization forces in the solid (Lyons, 1957). The value for triphenylene is about 5-6ev (2500-2100Å) compared with a value of about 7.8-8.1ev for the free molecule (Briegleb and Czekalla, 1959). Some measurements on surface ionization potentials have been made by Kearns and Calvin (1961), who estimated the bulk



value for the crystal of similar type molecules to be about 4.7ev. Provided some correction can be determined for the probably small difference between glass and crystal, the ions in glass technique would appear to be a very suitable way of measuring the bulk ionization potential. A possible experiment to detect the formation of ions in a crystal by examination of the fluorescence is described in section 6.8.

Preliminary experiments on the ionization of 3,4 benzpyrene in boric acid glass have indicated the possibility of a two quantum ionization process. (Hamilton and Ray, 1962). At a wavelength of about 2100A (6ev) the molecule is ionized rapidly. Between this wavelength and about 3000A (4.1ev) it is ionized slowly, and above the latter not at all. This upper wavelength energy corresponds to the difference between the ionization potential and the energy of the lowest triplet state (1.8ev)(Muel and Hubart-Habart, 1958). The suggestion is that molecules excited to the triplet state, which has a relatively long lifetime, have a reasonable chance of absorbing a further quantum and so reach the ionization level. The two quantum requirement will account for the slow formation of the ions in the intermediate region. If this process is confirmed,

it will have important consequences, for example in the field of biophysics.

#### 6.8 Fluorescence of Ionized Molecules.

The solutions of positive ions in sulphuric acid have been examined for visible fluorescence, but none has been observed. A similar result has been obtained by Hoijsink, Velthorst and Zandstra (1960) for solutions of negative ions in 2-methyltetrahydrofuran. The first absorption bands of the ions are at considerably longer wavelengths than for the normal molecules. For example, in anthracene the shift is from 4000Å to 7700Å and in pyrene from 3300Å to 10,000Å. Thus any fluorescence emission, which is at longer wavelengths than the absorption, will be in the red or infra-red region, which was outside the range of the detector used. The longer wavelength absorption also indicates that the excited state is much closer to the ground state than in the normal molecule, so that there is a greater possibility of internal conversion to the ground state.

The absorption and fluorescence of ions is of importance in explaining some of the processes of scintillations in organic materials (see e.g. Birks, 1962). The ionizing particle produces a column of ionized and highly excited molecules. If the ionized molecules

are non-fluorescent or only fluoresce in the infra-red region, any energy will be lost as any that may be emitted will be outside the range of the normal photomultiplier detector. The spectral overlap of ion absorption and normal molecule fluorescence is very much greater than for two normal molecules, so that the ions can reabsorb much of the excited molecule fluorescence and dissipate the energy as described above.

It has been found by a number of workers (Bennema et al, 1959, Linschitz et al, 1954), that when the positive ions recombine with an electron the light emitted is primarily phosphorescence i.e. the ions recombine to the triplet state preferentially. For scintillation purposes, any light emitted as phosphorescence is effectively lost because of the time delay before emission and possibly partly due to the shift to longer wavelengths, which may take it outside the spectral response of the detector. The excited but not ionized molecules can also be affected by the high concentration of paramagnetic centres present, which can cause transitions from the first excited singlet state to the triplet state to give the same effect as described above (see e.g. Hoiijtink, 1960, Murrell, 1960).

A phosphor in a rigid glass forms a convenient system for investigating some of the scintillation processes in slow motion as it were, as the recombination of the ions can be controlled at will by changing the temperature. The strong phosphorescence and negligible fluorescence from rigid glass systems provides a useful means of investigating phosphorescence processes. There is a drawback in that the system requires repeated alternate irradiation and heating. The heating can, however, be replaced by infra-red irradiation (Dolan and Albrecht, 1962) to give a much simpler arrangement. This would constitute a type of phosphoroscope, except that there is no need to use high chopping speeds for short lifetime triplet states.

A possible way of investigating the formation of ions in a crystal would be to measure the ratio of fluorescence to phosphorescence with decreasing exciting wavelength (i.e. increasing energy). When the ionization potential is reached the ratio will decrease as the ions should recombine to the triplet state, thus increasing the phosphorescence emission.

#### 6.9 Conclusion.

The application of ESR to the detection and investigation of ions of aromatic hydrocarbons in a

number of systems has been considered. The results have been combined with optical measurements to provide possible explanations of a number of luminescence phenomena. Several further experiments have been suggested, the results of which should lead to further clarification of some important questions. Although the original work on the detection of ESR in triplet states was unsuccessful, the technique has proved to be of great use in other hands. The correlation of spin density with ESR splitting in ions has been somewhat frustrated by the limited resolution obtained in the experimental spectra, but this should be improved by a new magnet with 9" dia. pole faces. With the improved resolution it is expected that further useful results will be obtained.

The application of ESR to aromatic hydrocarbons has been shown to be a technique of considerable use, even though a number of other applications, such as to charge transfer compounds and photo-oxides have not been discussed.

References.

- Aalbersberg, W.Ij., Hoijtink, G.J., Mackor, E.L.,  
Weijland, W.P., 1959a, J.Chem.Soc., 3049.
- Aalbersberg, W.Ij., Hoijtink, G.J., Mackor, E.L.,  
Weijland, W.P., 1959b, J.Chem.Soc., 3055.
- Abragam, A., Pryce, M.H.L., 1951, Proc.Roy.Soc.A, 205, 135.
- Adrian, F.J., 1958, J.Chem.Phys., 28, 608.
- Albrecht, A.C., Simpson, W.T., 1955, J.Amer.Chem.Soc.,  
77, 4454.
- Almenningen, A., Bastiansen, O., Skancke, P.N., 1958, Acta  
Chem.Scand., 12, 1215.
- Basile, L.J., 1962, J.Chem.Phys., 36, 2204.
- Bastiansen, O., 1949, Acta Chem.Scand., 3, 408.
- Bennema, P., Hoijtink, G.J., Lupinski, J.H., Oosterhof, L.J.,  
Selier, P., van Voorst, J.D.W., 1959, Mol.Phys., 2, 431.
- Birks, J.B., 1962, Nuclear Electronics, I, 17.
- Bloch, F., Hansen, W.W., Packard, M.E., 1946, Phys.Rev.,  
69, 37.
- Blume, R.J., 1958, Rev.Sci.Instr., 29, 574.
- Bolton, J.R., Carrington, A., 1961, Mol.Phys., 4, 271.
- Bowen, E.J., Williams, A.H., 1939, Trans.Faraday Soc.,  
35, 765.

Bowen,E.J., Tanner,D.W., 1955, Trans.Faraday Soc.,  
51, 475.

Briegleb,G., Czekalla,J., 1959, Z.Elektrochem., 63, 6.

Brovetto,P., Ferroni,S., 1957, Nuovo.Cim., 5, 142.

Buckerfield,P.S.T., 1952, Proc.Instn.Elect.Engrs.,  
99, Part II, 497.

Carrington,A., Dravnieks,F., Symons,F.C.R., 1959,  
 J.Chem.Soc., 947.

Cherkasov,A.S., 1959, Optics & Spect., 7, 211.

Clews,C.J.B., Lonsdale,K., 1937, Proc.Roy.Soc.A, 161, 493.

Coulson,C.A., 1958, Steric Effects in Conjugated Systems,  
 Editor G.W.Gray, (London: Butterworths), p.8.

Cummerow,R.L., Halliday,D., 1946, Phys.Rev., 70, 433.

Daudel,R., Lefebvre,R., Moser,C., 1959, Quantum Chemistry  
 (New York: Interscience).

DeBoer,E., 1956, J.Chem.Phys., 25, 190.

DeBoer,E., Weissman,S.I., 1958, J.Amer.Chem.Soc., 80, 4549.

DeGroot,M.S., van der Waals,J.H., 1960, Mol.Phys., 3, 190.

Dhar,J., 1932, Ind.J.Phys., 7, 43.

Dhar,J., 1949, Proc.Nat.Inst.Sci.India, 15, 11.

Dolan,E., Albrecht,A.C., 1962, J.Chem.Phys., 37, 1149.

Evans,D.F., 1955, Nature, 176, 777.

Farmer,J.B., Gardner,C.L., McDowell,C.A., 1961,  
J.Chem.Phys., 34, 1058.

Feher,G., 1957, Bell Syst.Tech.J., 36, 449.

Fermi,E., 1930, Z.Phys., 60, 320.

Garwin,R.L., Hutchinson,D., Penman,S., Shapiro,G.,  
1959, Rev.Sci.Instr., 30, 105.

G.E.C. Valve Department: 1957, An Approach to Audio  
Frequency Amplifier Design (London: Chapman & Hall)  
pp40-43.

G.E.C. Valve Service: Low Noise Amplifier Design  
(M-0 Valve Co. Brook Green, London, W6).

Gorter,C.J., 1936, Physica, 3, 995.

Hamilton,T.D.S., Ray,J.P., 1962, Work in progress.

Henning,J.C.M., 1961, Rev.Sci.Instr., 32, 35.

Hirshon,J.M., Fraenkel,G.K., 1955, Rev.Sci.Instr., 26, 34.

Hoijtink,G.J., 1958, Rec.Trav.Chim., 77, 555.

Hoijtink,G.J., 1960, Mol.Phys., 3, 67.

Hoijtink,G.J., Velthorst,N.H., Zandstra,P.J., 1960,  
Mol.Phys., 3, 533.

Hoijtink,G.J., Zandstra,P.J., 1960, Mol.Phys., 3, 371.



Hoiijtink, G.J., Townsend, J., Weissman, S.I., 1961,

J.Chem.Phys., 34, 507.

Hoyland, J.R., Goodman, L., 1962, J.Chem.Phys., 36, 12.

Hückel, E., 1931, Z.Phys., 70, 204.

Hutchison, C.A., Mangum, B.W., 1958, J.Chem.Phys., 29, 952.

Hutchison, C.A., Mangum, B.W., 1961, J.Chem.Phys., 34, 908.

Ingram, D.J.E., 1955, Spectroscopy at Radio and Microwave  
Frequencies, (London: Butterworths).

Ingram, D.J.E., 1958, Free Radicals as Studied by ESR,  
(London: Butterworths).

Jarrett, H.S., 1956, J.Chem.Phys., 25, 1289.

Jervis, M.W., 1955, Proc.Instn.Elect.Engrs., 102B, 274.

Jones, R.N., 1945, J.Amer.Chem.Soc., 67, 2127.

Jones, R.N., 1947, Chem.Revs., 41, 353.

Karle, I.L., Brockway, L.O., 1944, J.Amer.Chem.Soc., 66, 1974.

Kasha, M., 1948, J.Opt.Soc.Amer., 38, 1068.

Kasha, M., McGlynn, S., 1956, Ann.Rev.Phys.Chem., 7, 403.

Kearns, D.R., Calvin, M., 1961, J.Chem.Phys., 34, 2026.

Kon, H., Blois, M.S., 1958, J.Chem.Phys., 28, 743.

Kortüm, G., Dreesen, G., 1951, Chem.Ber., 84, 182.

- Laserew, B.G., Schubnikow, L.W., 1937, Phys.Z.Sowjet.,  
11, 445.
- Lewis, G.N., Bigeleisen, J., 1943, J.Amer.Chem.Soc., 65, 520.
- Lewis, G.N., Kasha, M.J., 1944, J.Amer.Chem.Soc., 66, 2100.
- Lewis, G.N., Calvin, M., 1945, J.Amer.Chem.Soc., 67, 1232.
- Lewis, G.N., Calvin, M., Kasha, M., 1949, J.Chem.Phys.,  
17, 804.
- Linschitz, H., Berry, M.G., Schweitzer, D., 1954,  
J.Amer.Chem.Soc., 76, 5833.
- Lipkin, D., Paul, D.E., Townsend, J., Weissman, S.I., 1953,  
Science, 117, 534.
- Lonsdale, K., 1937, Z.Krist., A97, 91.
- Lund, H., 1957, Acta Chem.Scand., 11, 1323.
- Lyons, L.E., 1959, J.Chem.Soc., 5001.
- Mays, J.M., Moore, H.R., Schulman, R.G., 1958, Rev.Sci.Instr.,  
29, 300.
- McClure, D.S., 1954, J.Chem.Phys., 22, 1668.
- McConnell, H.M., 1956, J.Chem.Phys., 24, 764.
- McConnell, H.M., Chesnut, D.B., 1957, J.Chem.Phys., 27, 984.
- McDermott, M.N., Novick, R., 1961, J.Opt.Soc.Amer., 51, 1008.
- McLachlan, A.D., 1959, Mol.Phys., 2, 271.
- McLachlan, A.D., 1960, Mol.Phys., 3, 233.
- McLachlan, A.D., 1961, Mol.Phys., 4, 49.

Merkel,E., Wiegand,C., 1948, Z.Naturforsch. 3b, 93.

Muel,B., Hubart-Habart,M., 1958, J.Chim.Phys., 55, 377.

Murrell,J.N., 1960, Mol.Phys., 3, 319.

Pake,G.E., Townsend,J., Weissman,S.I., 1952, Phys.Rev.,  
85, 683.

Pauli,W., 1924, Naturwissenschaften, 12, 741.

Pickett,L.W., Walter,G.F., France,H., 1936,  
J.Amer.Chem.Soc., 58, 2296.

Pound,R.V., 1948, Microwave Mixers, M.I.T. Radiation  
Laboratory, Vol.16, Chap 6 (New York: McGraw-Hill).

Pringsheim,P., 1949, Fluorescence and Phosphorescence,  
(New York: Interscience), p.453.

Purcell,E.M., 1946, Phys.Rev., 69, 681.

Purcell,E.M., Torrey,H.C., Pound,R.V., 1946, Phys.Rev.,  
69, 37.

Rabi,I.I., Millman,S., Kusch,P., Zacharias,J.R., 1939,  
Phys.Rev., 55, 526.

Reitz,D.C., 1961, J.Chem.Phys., 34, 701.

Roberts,J.D., 1961, Notes of Molecular Orbital Calculations,  
(New York: W.A. Benjamin).

Robinson,G.B., Geiger,F.E., 1958, Rev.Sci.Instr., 29, 730.

Rogers,D.W.W., 1957, Electronic Radio Engr., 34, 320.

Scott,N.D., Walker,J.F., Hansley,V.L., 1936,

J.Amer.Chem.Soc., 58, 2442.

Smith,F.T., 1961, J.Chem.Phys., 34, 793.

Stern,O., 1921, Z.Phys., 7, 249.

Streitweiser,A., 1962, Private Communication, to be

published in Streitweiser,A., Brauman,J.I., Tables  
of Molecular Orbital Calculations, (Oxford: Pergamon).

Strum,P.D., 1953, Proc.Inst.Radio Engrs., 41, 875.

Suzuki,H., 1959, Bull.Chem.Soc.Japan, 32, 1340.

Terman,F.E., 1950, Radio Engineers' Handbook,

(London: McGraw-Hill), p.147.

Townsend,J., Weissman,S.I., Pake,G.E., 1953, Phys.Rev.,

89, 606.

Townsend,M.G., Weissman,S.I., 1960, J.Chem.Phys., 32, 309.

Uhlenbeck,G.E., Goudsmit,S.A., 1925, Naturwissenschaften,

13, 953.

Valley,G.E., Wallman,H., 1948, Vacuum Tube Amplifiers,

M.I.T. Radiation Laboratory, Vol.18, p.657,

(New York: McGraw-Hill).

Van der Meij,P.H., 1958, Thesis, Free University,

Amsterdam, p.15.

Van der Waals, J.H., de Groot, M.S., 1959, Mol.Phys., 2, 333.

Varian Associates, 1960, NMR and EPR Spectroscopy,

(Oxford: Pergamon).

Venkataraman, B., Fraenkel, G.K., 1956, J.Chem.Phys., 24, 737.

Weijland, W.P., 1958, Thesis, Free University, Amsterdam, p.91.

Weissman, S.I., Townsend, J., Paul, D.E., Pake, G.E., 1953,

J.Chem.Phys., 21, 2227.

Weissman, S.I., 1956, J.Chem.Phys., 25, 890.

Weissman, S.I., de Boer, E., Conradi, J.J., 1957,

J.Chem.Phys., 26, 963.

Weissman, S.I., Tuttle, T.R., de Boer, E., 1957,

J.Phys.Chem., 61, 28.

Yokozawa, Y., Miyashita, I., 1956, J.Chem.Phys., 25, 796.

Zavoisky, E., 1945, J.Phys.USSR, 9, 211.